MODELING REFERENCE EVAPOTRANSPIRATION USING HYBRID ARTIFICIAL INTELLIGENCE TECHNIQUES IN ARID AND SEMI-ARID REGIONS OF INDIA

Thesis

Submitted in partial fulfilment of the requirements for the degree of

DOCTOR OF PHILOSOPHY

by

PATIL AMIT PRAKASH

DEPARTMENT OF APPLIED MECHANICS AND HYDRAULICS

NATIONAL INSTITUTE OF TECHNOLOGY KARNATAKA,

SURATHKAL, MANGALORE - 575025

JANUARY, 2017

MODELING REFERENCE EVAPOTRANSPIRATION USING HYBRID ARTIFICIAL INTELLIGENCE TECHNIQUES IN ARID AND SEMI-ARID REGIONS OF INDIA

Thesis

Submitted in partial fulfilment of the requirements for the degree of

DOCTOR OF PHILOSOPHY

by

PATIL AMIT PRAKASH
(AM13F04)

DEPARTMENT OF APPLIED MECHANICS AND HYDRAULICS
NATIONAL INSTITUTE OF TECHNOLOGY KARNATAKA,
SURATHKAL, MANGALORE - 575025

JANUARY, 2017

D E C L A R A T I O N

I hereby *declare* that the Research Thesis entitled **Modeling reference evapotranspiration using hybrid artificial intelligence techniques in arid and semi-arid regions of India** which is being submitted to the National Institute of Technology Karnataka, Surathkal in partial fulfilment of the requirements for the award of the Degree of Doctor of Philosophy in the Department of Applied Mechanics and Hydraulics is a *bonafide report of the research work carried out by me*. The material contained in this Research Thesis has not been submitted to any University or Institution for the award of any degree.

Register Number :- AM13F04

Name :- PATIL AMIT PRAKASH

(Signature)

Department of Applied Mechanics and Hydraulic

National Institute of Technology Karnataka, Surathkal

Place: NITK-Surathkal

Date:

C E R T I F I C A T E

This is to *certify* that the Research Thesis entitled **Modeling reference evapotranspiration using hybrid artificial intelligence techniques in arid and semi-arid regions of India** submitted by PATIL AMIT PRAKASH (Register Number: AM13F04) as the record of the research work carried out by him, is *accepted as the Research Thesis submission* in partial fulfilment of the requirements for the award of degree of Doctor of Philosophy.

Dr. Paresh Chandra Deka
(Research Guide)
Department of Applied Mechanics and Hydraulics
National Institute of Technology Karnataka, Surathkal

Prof. G.S. Dwarakish
(Chairman - DRPC)
Department of Applied Mechanics and Hydraulics
National Institute of Technology Karnataka, Surathkal

ACKNOWLDGEMENT

In my journey towards the completion of my doctoral thesis, I was assisted and shown the path by numerous people.

Things are definitely a lot easier when there is a person who gives you ideas, who goes through each and every word written by you over and over, correcting it, impoving it, a person whom you turn to each time you have a doubt or some problem. Words are insufficient to express my sincere gratitude and thanks towards my research supervisor **Dr. Paresh Chandra Deka**, for his continued inspiration, motivation, support, discussions and great patience. I admire among his other qualities, kindness and balanced approach towards success and failure. His scientific foresight and excellent knowledge have been crucial for the accomplishment of this work. I have learnt a lot and still have plenty to learn from him. I consider myself privileged for having had the opportunity to study under his able supervision.

I am greatly thankful to Reseach Progress Appraisal Committee members, Dr. Ramesh H and Dr. M N Satyanarayan for their critical evaluation during the progress of the work. I humbly thank **Subramanya sir** who inspired me to join this course. This would have not been possible without his belif and confidence in me.

I also extend my heartfelt thanks to Prof. G.S. Dwarakish, Head, Department of Applied Mechanics and Hydraulics, and Chairman DRPC for for providing me all the necessary facilities during my research period.

I gratefully acknowledge all the faculty members of Applied Mechanics and Hydraulics Department, for their continuous support, care and good wishes during the course of my work. I sincerely acknowledge the help of Mr. Jagadish, Mr. Anil, Mr. Balakrishna and Mrs. Pratima and all the non teaching staff of Applied Mechanics and Hydraulics department.

I am very much thankful to all my friends and fellow research scholars Santosh, More sir, Mahajan sir, Kahandekar sir, Rahul sir Kartik, Sanjeev, Sujay, Leeladhar, Amrut, Syuls, Jagalingam, Diwan, Beena, Amogh, Sinan, Arun, Chaitanya, Abhishekh, Usha, Bhojaraja, Geeta, Shridhar, Ganasri, Suman, Harish, Kiros, Arega, Arun, Abhishekh, Anup, Palankar and Rishi for their excellent company. I would like to thank Sachin, Pravin, Madhu, Anil, Vinoth and Sujata for their support and encouragement during my stay in the NITK.

A special thanks to my beloved friends Pritam, Faizum, Dhairyasheel, Shantanu, Anup, Amit, Yuvraj, Santaji and Kasture who have been a pillar of support since my schooling days. A special thanks to Dr. Amol Patil, Mr. Vinayak Yadav, Mr. Prashant Jagtap and Mr. Gajanan Kanade for their support and encouragement.

Whatever I am today, is because of the life long support of my father **Mr. Prakash Patil** and my mother **Mrs. Nanda Patil**. This thesis would not have been possible without the amazing support, patience, constant encouragement, care, unfettered belief and prayers of my parents. No words can express my gratitude for them.

I dedicate the successful completion of my doctoral thesis to the fond memories of my grandfather Late **Mr. Pandurang Patil.** My younger sister **Neha** has provided me a lot of support during my research work. Finally, I wish to express my love and affection to my family members Mr. Anna Patil, Ms. Nirmala Patil, Mr. Janardan Patil, Mr. Vilas Patil, Mr. Satish Salokhe, Mrs. Pragati Salokhe, Mr. Vikas Patil, Mrs. Jyoti Patil, Mr Dayanand Jadhav, Mrs. Jagruthi Jadhav and Mr. Aadarsh Pandit for being with me during good and bad times.

Last but not the least, my deepest gratitude towards the Almighty for making this thesis possible.

Amit Prakash Patil

ABSTRACT

Evapotranspiration (ET) plays an important role in efficient crop water management. Accurate estimation of ET is a challenging task in developing countries like India, where the availability of meteorological data is often minimal. This study makes an attempt to evaluate the potential and applicability of hybrid Wavelet-Artificial Intelligence (AI) models for estimating reference crop evapotranspiration (ETo) in arid and semi-arid regions of India. The hybrid models were developed by using wavelet decomposed subseries of meteorological variables as inputs to the ANN, ANFIS and LS-SVM models. Performance of the proposed hybrid models was then compared to the classical AI models.

The study used forty year weekly dataset from Jodhpur and Pali (arid region) weather station. Also, daily data for six years were obtained from Hyderabad and Kurnool weather station (semi-arid region). In absence of lysimeter data, ETo values are calculated by FAO-56PM equation. Prior to the development of models, factor analysis test was employed to identify the input combination that may yield more efficient model under limited data scenario. Additionally, the effectiveness of using ETo data from another station in the same climatic region (extrinsic data) was also evaluated. It is expected that the proposed hybrid models together with extrinsic input variables would provide efficient ETo estimation models.

The performance of hybrid and classical AI models were compared using RMSE, NSE and threshold statistics. Scatter plots were used to evaluate the accuracies of the models and box plots were used to analyze the spread of the data points estimated by the models. The results show that the proposed AI models worked better at estimating weekly ETo in arid regions compared to estimating daily ETo in semi-arid regions. The hybrid AI models displayed a better performance compared to the classical AI models at all the stations. It was found that hybrid W-LSSVM was the best model for estimating ETo in both arid and semi-arid region. Further, it was observed that the use of extrinsic inputs delivered good results only in arid regions. It was also observed that in semi-arid regions, use of wavelet decomposed extrinsic data deteriorated the performance of some hybrid models.

***Keywords* :** Evapotranspiration; Arid Region; Semi-arid Region; Factor Analysis; Wavelet Transform; ANN; ANFIS; LS-SVM

Table of contents

List of figures

List of tables

Nomenclature

Abbreviation	Description
ABC	Artificial bee colony optimization
ACF	Autocorrelation function
AI	Artificial intelligence
ANFIS	Adaptive neuro-fuzzy inference system
ANN	Artificial neural network
CWT	Continuous wavelet transform
DWT	Discrete wavelet transform
ERM	Empirical risk minimization
ET	Evapotranspiration
ETo	Reference crop evapotranspiration
FAO	The food and agricultural organization of united nations
FFBP	Feed-forward backpropagation network
FG	Fuzzy genetic approach
FT	Fourier transform
GA	Genetic algorithm
GRNN	Generalized regression neural network
LM	Levenberg-Marquet learning algorithm
LS-SVM	Least square support vector machine
MF	Membership function
MLP	Multilayer perceptron
MLR	Multiple linear regression
MNLR	Multiple nonlinear regression
RBF	Radial basis function
SBP	Standard back-propagation methodology
SRM	Structural risk minimization
STFT	Short term Fourier transform
SVM	Support vector machine
W-ANFIS	Hybrid wavelet-adaptive neuro-fuzzy inference system model
W-ANN	Hybrid wavelet-artificial neural network model
W-LSSVM	Hybrid wavelet-least square support vector machine model
WT	Wavelet transform

CHAPTER 1

INTRODUCTION

1.1 INTRODUCTION

In agriculture sector, evapotranspiration (ET) is closely related to crop water demand. ET is the process that returns water from the earth's surface to the atmosphere and therefore completes the hydrological cycle. ET is a combination of water evaporated from surfaces such as soil and water bodies, combined with the water transpired from the vegetation. ET is an important process in the water cycle and is responsible for 15% of the atmosphere’s water vapor. Without this input of water vapor, precipitation would never occur. ET is a highly complex phenomenon, depending on various factors and comprising different processes. A number of factors affect ET, including weather parameters (solar radiation, temperature, relative humidity and wind speed), crop factors (crop type, stage of growth, variety and plant density) and management and environmental factors (soil fertility, salinity, pest and disease control). Additionally, ET is heavily influenced by land use changes and climate variations regionally and globally. The currently well-evidenced global warming characterized by increasing temperature has the potential to alter the hydrological cycle. Generally, it can be easily and readily accepted that increasing temperature can cause increased evaporation (Oki and Kanae 2006). However, observations indicate decreasing trend in pan evaporation and ET (Zhang et al. 2007) leading to more complexity and ambiguity in modeling these processes. Accurate estimation of ET plays a key role in successful management of irrigation systems. Additionally, accurate estimation of ET plays a very vital role in hydrological modeling, conducting water balance studies and environmental assessment works.

Considering the significance of accuracy in estimating ET, hydrologists over the time have mainly focused on developing more reliable and accurate methods for ET estimation. ET can be directly measured by conducting a soil water balance with lysimeters. Lysimeters measure ET by isolating a soil-plant system from its environment and evaluating the components of the water balance by measuring incoming and outgoing water fluxes. Use of lysimeters is limited due to the fact that

this technique is very expensive and demanding in terms of accuracy in measurement. Owing to the difficulties in direct measurement, several equations were developed for ET estimating. A concept of 'reference crop evapotranspiration' (ETo*)* avoided the need to calibrate a separate ET equation for different vegetation and moisture availability. ETo refers to the rate of ET from a hypothetical grass reference crop with specific characteristics. The concept of the reference evapotranspiration was introduced to study the evaporative demand of the atmosphere independently of crop type, crop development and management practices. The Food and Agricultural Organization of United Nations (FAO) has accepted the FAO Penman-Monteith (FAO-56PM) as the standard equation for estimating evapotranspiration (Allen et al. 1998). However, large amounts of climatic variables, including solar radiation, wind speed, humidity and temperature has made the use of FAO-56PM equation difficult in developing countries like India where, availability of meteorological records has often been minimal.

In the nineteenth century, several empirical and semi-empirical equations needing fewer climatic variables were developed for estimating ET. The empirical equation that needed fewer data included, the radiation-based models include Turc equation (Turc 1961), Priestley-Taylor equation (Priestley and Taylor 1972) and the FAO-24 radiation equation (Doorenbos and Pruitt 1977). The temperature-based models include Thornthwaite equation (Thornthwaite 1948), FAO-24 Blaney-Criddle equation and FAO-56 Hargreaves model (Allen et al. 1998). The Pan Evaporation model given by Doorenbos and Pruitt (1977) used pan coefficient for converting pan evaporation to ET. Different methods for estimation of pan coefficient include Snyder Pan Coefficient (Snyder 1992) and FAO-56 Pan Coefficient method (Allen et al. 1998). The simple empirical equations requiring fewer data like temperature, radiation and pan evaporation can be used to estimate ET, but these models have reported to generate inconsistent results when tested under different climatic and data availability condition. Hargreaves equation is good in estimation of ET for the arid and semiarid regions, while the Turc equation is found to perform better in the humid region (Nandagiri and Kovoor 2006; Martinez and Thepadia 2010). This may be for the reason that these equations were developed for different data availability conditions and for a specific climatic region. Considering the limitations and disadvantages of

the conventionally applied modeling techniques, they need to be further refined by implementing new or different methods to achieve improved performance.

1.2 ARTIFICIAL INTELLIGENCE

In recent years, application of artificial intelligence (AI) techniques in modeling hydrological processes like evapotranspiration has received much attention from the researchers. AI algorithms provide explanation of an externally driven process without a need of complex physical models. Literature reports use of AI methodologies like artificial neural network (ANN), adaptive neuro-fuzzy inference system (ANFIS) and least square support vector machine (LS-SVM) for modeling the process of evapotranspiration.

1.2.1 Artificial neural network

ANN is an information system, stimulating the ability of human brain to sort out patterns and learn from trial and error. ANN has an ability to extract relationships that exist within the data with which it is presented. This approach is faster, robust in noisy environments, flexible in the range of problems it can solve and highly adaptive to the new environments. Due to these established advantages, currently the ANN has numerous real world applications such as image processing, speech processing, robotics and stock market predictions. There has been research on its implementation in the system engineering related fields such as time series prediction, rule based control, etc. In recent years, ANN methods have been successfully applied to many studies in the field of water resources engineering.

1.2.2 Adaptive Neuro-fuzzy inference system

Jang (1993) proposed a method that used neural network learning algorithm for constructing a set of fuzzy if-then rules, with appropriate membership functions from the stipulated input output pairs. An ANFIS model combines the transparent and linguistic representation of a fuzzy system with learning ability of ANN. This incorporates the generic advantages of artificial neural networks like massive parallelism, robustness and learning in data-rich environments. The modeling of imprecise and qualitative knowledge as well as the transmission of uncertainty is possible through the use of fuzzy logic. ANFIS comes with an additional benefit of being able to provide a set of rules on which the model is based.

1.2.3 Least square support vector machine

Vapnik (1995) developed the foundation of support vector machines (SVM). SVM gained popularity due to many promising features like better empirical performance and providing globally optimal solutions. The formulation embodies structural risk minimization (SRM) principle, which has shown better performances than the empirical risk minimization principle (ERM), employed by conventional neural networks. SRM minimizes an upper bound on the expected risk, as opposed to ERM that minimizes the error on the training data. It is this difference, which equips SVM with a greater ability to generalize and achieve the goal of statistical learning. LS-SVM is a reformulation of the principles of SVM, which involves equality instead of inequality constraints.

1.2.4 Hybrid Wavelet-AI models

Performance of any AI model largely depends on the user's understanding of the model, along with the quantity and quality of inputs presented to it. Evapotranspiration, like many other hydrological processes operate under a large range of scales varying from one hour to several months leading to a non-linear and non-stationary behavior of the dataset. AI models alone may not be able to cope with these characteristics of the dataset if, input and/or output data is not preprocessed. Furthermore, there is also a need for working towards enhancing the performance of these models. Use of hybrid models may help in increasing the accuracy of ANN, ANFIS and LS-SVM models.

Wavelet theory (Mallat 1989) first developed at the end of 1980s is being widely applied in many engineering fields, such as signal processing, image compression, pattern recognition, hydrology, earthquake investigation, etc. Since the last decade, wavelet transform has become a popular technique for analyzing variations, periodicities, and trends in time series. Wavelet Transform decomposes original time series into wavelet subseries of different resolution in the time domain. Wavelet pre-processed data may increase the efficiency of an AI model by providing useful information about original data set at various resolution levels (Wang and Luo 2008; Deka and Prahlada 2012).

1.3 PLANNING THE PRESENT STUDY

This study proposes a hybrid Wavelet-AI model to model the process of ETo. Hybrid Wavelet-ANN (W-ANN), Wavelet-ANFIS (W-ANFIS) and Wavelet- least square support vector machine (W-LSSVM) models are developed for estimating ETo at daily and weekly time step. Further, performance of the classical and hybrid AI models are compared to select the best model for estimating ETo.

India's arid and semiarid lands constitute more than 50 percent of the country's geographic area and are home to 60 percent of the rural population where agriculture is the primary occupation. The arid and semiarid region in India is spread over six States, viz., Rajasthan, Gujrat, Haryana, Maharashtra, Karnataka and Andhra Pradesh. Arid and semi-arid regions are the regions where the precipitation is highly variable, sporadic and unpredictable (Jhajharia et al. 2015). This makes it necessary to focus on developing efficient models for estimating ETo in arid and semi-arid region. This study makes an attempt to model ETo at Jodhpur and Pali stations in arid regions. Additionally, data from Hyderabad and Kurnool weather stations were used to model ETo of the semi-arid region. Further, an attempt is made in this study to evaluate the effectiveness of using ETo values from a particular place to model the ETo of another place in the same climatic region. Use of such extrinsic inputs may help in improving the efficiency of AI models for accurate estimation of ETo in limited data scenario.

1.4 ORGANIZATION OF THE THESIS

This thesis comprises of five chapters as follows:

- Chapter 1 (Introduction) presents the relevant information pertaining to ETo and further deals with an overview of the conceptual basis for the research.
- Chapter 2 (Literature Review) deals with a brief discussion about the work carried out by researchers for estimating evapotranspiration and other hydrological parameters.
- Chapter 3 (Methodology and Model Development) describes the basics of wavelet transform, ANN, ANFIS and LS-SVM. This also deals with the procedure for developing classical and hybrid AI models. The procedure used for selecting relevant inputs is discussed in this chapter. Further, a brief discussion about the study area is also included.

- Chapter 4 (Results and Discussion) describes the method of evaluation and goes on to present the analysis of the results obtained from the developed models.
- Chapter 5 (Conclusions) presents a summary and conclusions of the research work. Limitations and future scope of the study are included towards the end.

CHAPTER 2

LITERATURE REVIEW

2.1 INTRODUCTION

Considering the significance of accuracy in estimating ET, hydrologists over the time have mainly focused on developing more reliable and accurate methods. In the following sections, various techniques employed by researchers for estimating ET under different climatic and data availability conditions are discussed. Application of physical based and empirical equations is presented in the first section. In the subsequent sections recent reviews of AI applications in modeling ETo and other hydrological processes are presented.

2.2 PHYSICAL AND EMPIRICAL MODELS

Until recent years empirical and semi empirical equations were the most widely used models for estimating ET. These models are used to estimate ET under limited data scenario. Nandagiri and Kovoor (2006) evaluated the performance of various empirical methods for estimating ET in different climatic regions of India. The study aimed at quantifying differences in ETo estimates influenced by climatic conditions and identify methods that yield results closest to the FAO-56PM method. In the study different ETo estimating methods, representing temperature based, radiation-based, pan evaporation-based and combination-type equations were compared with the FAO-56PM method using daily and monthly climate data from four stations located one each in arid, semiarid, subhumid and humid climates of India. The study concluded that, among all the ETo models evaluated, the Hargreaves (temperature-based) method yielded ETo estimates closer to the FAO-56PM ETo values in all the climates except the humid climate. In the humid region, Turc (radiation- based) method was found to be performing better.

In a similar study, Lopez-Urrea et al. (2006) evaluated the performance of different methods for calculating daily ETo values. The study found that FAO-56PM was the best method to estimate lysimeters readings. The Hargreaves equation showed good performance in estimating ETo at semiarid regions. Good performance of the Hargreaves equation in both high and low evaporative demand periods affirmed the

importance of temperature related variables in estimating ETo at semi-arid climates. In contrast to the earlier results Xystrakis and Matzarakis (2011) found that in dry climates, the radiation based equations performed better than the temperature based equations. Kostinakis et al. (2011) developed Visual Basic software that was used for estimating daily ETo by the means of FAO-56PM equation and thirteen additional empirical equations. The developed software had an additional feature of calculating goodness of fit for comparing and detecting the empirical equations that has a minimum bias of estimation against the FAO-56PM equation.

Rojas and Sheffield (2013) found that in case of missing wind data, using wind speed data from a nearby station provided better results compared to the method of using global default wind speed, as proposed by Allen et al. (1998). This study emphasized on the use of data from nearby stations in case of data unavailability. It was also observed that in humid climates, Turc and Priestley-Taylor equations underestimated ETo values, whereas the Hargreaves equation overestimated them.

2.3 ARTIFICIAL NEURAL NETWORK

In recent years, the AI models are being widely used for estimating various hydrological parameters (Gocić et al. 2015; Kisi et al. 2015; Shiri et al. 2015). Some studies related to the use of neural networks in estimating ET are discussed below.

Sudheer et al. (2003) employed a radial-basis function (RBF) type ANN for computing daily values of evapotranspiration. The study was carried out to estimate ET under limited data scenario. Various ANN models with different input (weather parameters) combination were developed to estimate evapotranspiration measured by lysimeter. The study revealed that, as the number of input variables reduced, the performance of the model deteriorated. This demonstrated the impact of individual climatic variable in estimating ET. Further, it was found that the ANN model with temperature data alone could satisfactorily estimate ET. The study concluded that crop evapotranspiration can be successfully estimated using limited data by employing the ANN approach.

Kisi (2006) used generalized regression neural network to model ETo. The study compared four combinations of input variables to estimate ETo. Starting from a single input model of solar radiation, four different models were tested by adding one

variable to the earlier model. The degree of effect of each of the variables (solar radiation, air temperature, relative humidity and wind speed) on estimation of ETo was evaluated in respect of the reduction or increment in error statistics. However, as discussed by Aksoy et al. (2007) sensitivity of variables were not studied before adding a variable to the model. The study concluded that the four input model performed better than the Hargreaves and Turc methods in estimation of FAO-56PM ETo.

Rahimikhoob (2007) compared the performance of temperature based Hargreaves and ANN method to estimate ETo. The data used for training of ANN models were used for calibration of Hargreaves model while the calibrated Hargreaves estimates were compared to the ANN estimates. The ANN model used backpropagation algorithm with Levenberg-Marquardt optimization technique. A trial and error procedure was used to determine optimum number of nodes in the hidden layer. The results of the study concluded that temperature based ANN models can be successfully used to estimate ETo values in semi-arid regions when radiation, relative humidity and wind data are not available. In a similar study, Rahimikhoob (2010) examined the potential of ANN model to estimate ETo in subtropical climate based only on air temperature data.

Zanetti et al. (2007) showed that an ANN model using maximum and minimum air temperatures, extraterrestrial radiation and daylight hours as inputs can be successfully used to estimate ETo. Out of all the inputs used, extraterrestrial radiation and daylight hours inputs were calculated as a function of either the local latitude or the Julian date. In a similar study, Kumar et al. (2008) found that the learning performance of ANN models does not improve with increased nodes in hidden layers, but depends on the number of inputs used and the climatic variables corresponding to the nodes.

Kim and Kim (2008) developed a genetic algorithm (GA) embedded generalized regression neural network (GRNN) model to estimate pan evaporation and ETo. In this study GA was employed to optimize centers, widths and connection weights of the GRNN model. Uncertainty analysis of the input layer variables for developing an optimum GRNN-GA model was also carried out using a simulation-based step-by-step method. This analysis helped in eliminating the input variables that are not

significant in modeling the process of ET. Results of the uncertainty analysis revealed that maximum temperature and sunshine hours are the most important climatic parameters for development of GRNN-GA model. The study also attempted to derive a linear regression model between pan evaporation and ETo values. Further, pan evaporation and evapotranspiration maps were also constructed to provide reference data for drought analysis.

Aytek et al. (2008) derived explicit neural network formulation for estimating ETo by multiplying each input and output variable with the corresponding model weights obtained from trained neural network. The results revealed that ENNF model has good generalization capabilities and can be used over a larger area without changing formulations. The study concludes that the proposed models performed marginally better than the multiple linear regression model and can be successfully used to estimate ETo.

Chauhan and Shrivastava (2009) attempted to find the best method for estimating ETo under limited data scenario. They compared the performance of various empirical equations to estimate ETo for the Mahanadi Reservoir Project command area. The study also compared the performance of ANN models to the empirical equations. Analysis of the results suggested that ANN models performed better than the climatic based methods and temperature based ANN models can effectively model ETo values.

Abudu et al. (2010) used ANN for infilling missing daily ET measured by eddy-covariance method. Several ANN models were evaluated for infilling different combinations of missing data percentages and different gap sizes. The results from this study suggest that infilling of daily ET using ANN and readily available weather data where the ET observations exist before and after the gap is a reliable and convenient method for infilling missing ET data.

Marti et al. (2010) tried to generalize a four inputs ANN model. In the training model proposed by Zanetti et al. (2007), two more exogenous inputs of RH and ETo from location having same indexes of continentality (k) were added. The continentality indexes proposed in this study tried to quantify the scale of thermal oscillation that takes place in a yearly data set. Models were developed by supplanting the missing climatic variables for one location, with those from a secondary

continentally similar location. The results showed that the supplanted models performed better than the original four inputs ANN model.

Ozkan et al. (2011) used artificial bee colony optimization algorithm to train ANN models (ANN-ABC). The performance of this model was compared with empirical and semi-empirical equations to predict daily ETo under limited data condition. Artificial bee colony (ABC) is an optimization algorithm that mimics the foraging behavior of honey bees. ABC tries to find the position of the most profitable food source (solution in the space) by searching the food source space. The results showed that the ANN-ABC models performed better than other ANN and empirical equations. Additionally, the results of the cross-station applications indicated that the ANN-ABC models are more accurate than the ANN models in estimation of daily ETo using nearby station data.

Tabari and Talaee (2012) employed multilayer perceptron (MLP) to model ETo under a limited data scenario in semiarid regions of Iran. They tested various input combinations with different learning algorithms and activation functions. It was found that different learning algorithms worked well for different models and the 'tanh' activation function performed better than the 'sigmoid' and 'linear' activation functions. This study demonstrated the potential of MLP modeling for estimating ETo.

Wang et al. (2013) developed a generalized artificial neural network model for ETo estimation using weather data from four locations representing different climatic patterns. The proposed model exhibited high accuracy under both arid and humid conditions when compared to multivariate linear regression model and empirical equations. The analysis showed that ANN model resulted in slightly larger errors in arid and semi-arid climate. It was concluded that longer time series data from more stations located in different climatic zones can develop a better neural networks for modeling ETo.

2.4 ADAPTIVE NEURO-FUZZY INFERENCE SYSTEM

An ANFIS model combines the transparent and linguistic representation of a fuzzy system with learning ability of ANN. This allows them to be trained to perform input/output mapping as an ANN model (Petković et al. 2015; Shiri et al. 2014a). ANFIS comes with an additional benefit of being able to provide a set of rules on

which the model is based. Many studies have concluded that the ANFIS model exhibit better performance than the ANN model. However, many contradictory results can also be found in the literature wherein the performance of ANN model was found to be better than the ANFIS model. Some recent studies that employed ANFIS models to estimate ET are discussed below.

Kisi and Ozturk (2007) compared the ETo estimation capabilities of ANFIS models to the empirical and ANN models. Two models, with two and four inputs were compared and cross-validated at two different stations. The results showed that the ANFIS models outperformed the conventional and ANN models in terms of performance criteria. The calibrated Hargreaves and Ritchie model performed better than the two input ANN model. It was seen that, in coastal areas relative humidity and wind speed are important in estimating ETo.

Cobaner (2011) investigated the potential of grid partition based fuzzy inference system (G-ANFIS) and subtractive clustering based fuzzy inference system (S-ANFIS) in modeling ETo. Based on the comparisons, it was found that the S-ANFIS model performed slightly better than G-ANFIS and MLP models in modeling the ETo process. Aytek (2009) proposed co-active neuro-fuzzy inference system (C-ANFIS) for daily ETo modeling. The C-ANFIS model was trained and tested using three station data from different geographical locations in California. Based on the statistical performance measurements the study concluded that C-ANFIS could be used as an alternative to existing conventional models for ETo modeling.

Abyaneh et al. (2011) compared ANN and ANFIS models with lysimeter data for computing garlic crop ET in semiarid region of Iran. Several ANN models were tested, but the feed forward back-propagation type ANN model with Levenberg-Marquet (LM) learning algorithm was found to be the best. ANFIS model using the standard back-propagation (SBP) methodology and three membership functions was also used to estimate ET. It was seen that ANN model performed slightly better than ANFIS model. This was because LM is more powerful and faster than the SBP algorithm and has less chance of getting trapped in local minima when compared to SBP. It was also seen that on comparing with the lysimeter data ANN and ANFIS models performed better than the crop coefficient method for estimating actual evapotranspiration from garlic crop.

Shiri et al. (2013) studied the capabilities of generalized neuro-fuzzy models for cross-station assessment of ETo values using weather data from Spain and Iran. The data from these humid (Spain) and non-humid (Iran) regions were pooled to evaluate the generalization capability of ANFIS model using grid partitioning identification method. Accordingly, different ANFIS models were trained using data from Spanish stations and subsequently tested in Iranian stations. From the observed results, it was concluded that the proposed methodology would allow for more accurate estimations of ETo than conventional approaches without the need to train ANFIS model in the test region.

Karimaldini and Shui (2012) investigated the potential of modeling daily ETo using ANFIS under arid conditions. Techniques like Gamma-test, *M*-test and *K*-fold cross-validation method were used to overcome the major drawback in soft computing of not having the ability to preprocess data before modeling. The gamma test technique initially introduced by Stefansson et al. (1997) was used to find the best combination of inputs and sufficient size of data. The M-test technique was used to decide how many data points are sufficient for training a model. A *K*-fold cross-validation method was used to address the problem of choosing a proper training dataset. It was found that the trend of the results from the ANFIS models for different input combinations was the same as that of the gamma test results. Hence, it was concluded that using gamma test helps to save a great amount of time for choosing proper input combinations and appropriate number of data points that are required for calibration of a model. It was also found that ANFIS models performed better than the corresponding empirical ETo equations.

Kisi (2010) used fuzzy genetic (FG) approach to model ETo. GA was used to adjust the membership functions. Fuzzy Genetic model performed well in estimating ETo when compared to the Penman model. Also, it outperformed two-parameter Hargreaves and Turc equations in estimating ETo (FAO-56PM) values. Moreover, on comparing with the best feed-forward ANN (sigmoid activation function) model, the FG models perform better. This may be because ANN model can very easily be trapped in a local minimum when using the backpropagation methodology for adjusting the weights. GA combines elements of directed and stochastic search, providing global optimum without being trapped in local optima. In a similar study by

Kisi and Cengiz (2013) for the Mediterranean region of Turkey, FG approach worked better than the ANN model for estimating ETo.

2.5 SUPPORT VECTOR MACHINES

SVM achieves an optimum network structure by minimizing the upper bound to generalization error instead of minimizing the training error. In addition, SVM is equivalent to solving a linear constrained quadratic programming problem, which always generates a unique and globally optimal solution (Raghavendra and Deka 2014). Recently, many studies have used SVM models to estimate ET.

Khan and Coulibaly (2006) used SVM for three to twelve months ahead lake water level predictions. The results were compared to ANN model and multiplicative seasonal autoregressive model. They found that SVM training consists of solving a uniquely solvable quadratic optimization problem, which is much more attractive because it guarantees to find a global minimum of the error surface. Wherein, the error referred to the difference between the desired response and the output of the SVM. In the study, it was found that radial basis kernel function was the most appropriate kernel function for SVM model. The proposed method showed some promising results and proved to be competitive with the widely used MLP model.

Kisi and Cimen (2009) found that the SVM model with four inputs performed better than the empirical and ANN models. Whereas, the two inputs (solar radiation and temperature) SVM model performed better than the Hargreaves, Ritchie and Turc model. The results also brought to notice that the comparison of AI models and uncalibrated empirical methods is not fair as the empirical methods are independent. This study also recommended the use of SVM models as a module for estimating ET in hydrological modeling studies.

Sungwon and Hung (2011) introduced εSVM-NNM (Neural network model) regression model to estimate FAO-56PM ETo. The accuracy of εSVM-NNM regression was largely dependent on the selection of model parameters such as cost function (C) and Gamma function (γ). A grid search and pattern search approach were used for finding optimal parameter values. Additionally, a cross-validation method was used to overcome the over-fitting problems in the models. From the results, it was found that climatic parameters like temperature, sunshine duration and relative

humidity were more effective than wind speed in the modeling of ETo. In this study, the performance of proposed models were found to be better than those of MLP-NNM models.

Tabari et al. (2012) studied the potential of SVM, ANFIS, multiple linear regression (MLR) and multiple nonlinear regression (MNLR) models for estimating ETo in a semi-arid highland environment. In addition to this, four temperature-based and eight radiation-based ETo equations were also tested against the FAO-56PM model. The SVM and ANFIS models yielded better results than the regression and climate based models. Furthermore, it was also seen that the SVM training process always searched a global optimized solution and tried to prevent over-fitting that eventually led to better generalization performance than the ANN model. SVM was able to select the support vectors in the training process and remove the non-support vectors automatically from the model. This helped the model to cope with noisy conditions.

Tabari et al. (2013) studied the applicability of SVM and ANFIS models to estimate potato crop ET. This study was undertaken to test the performance of empirical equations, ANFIS models and SVM models for estimating crop ET when lysimeter measurements or the complete weather data for applying the FAO method are not available. The results indicated that, the ANFIS models with two membership functions performed better. Also, the radial basis function was found to be the best kernel for all SVM models. In this study, the SVM models were found to be performing better than the ANFIS models.

Wen et al. (2015) employed SVM models to estimate ETo in extremely arid regions using limited climatic data. The performance of the SVM model was compared to the ANN model and three different empirical models. From the results, it was found that the performance of SVM model with limited climatic data was similar to the conventional FAO-56PM equation employing the full complement of meteorological data. Further, it was also found that temperature and extraterrestrial radiation were enough to estimate daily ETo values satisfactorily. The study concluded that SVM models were best among all the other tested models.

Kisi (2012) examined the accuracy of LS-SVM in modeling ETo. LS-SVM proposed by Suykens and Vandewalle (1999) is originated from SVM. LS-SVM

changes the inequality constraints of a SVM into a set of equality constraints and forces the sum of squared error loss function to become an experience loss function of the training set. This allows the problem to be solved as a linear programming problem. When compared to the empirical equations and conventional feed-forward ANN, LS-SVM was found to be superior.

Mellit et al. (2013) proposed LS-SVM model for short-term prediction of meteorological time series like solar radiation, air temperature, relative humidity, wind speed and wind direction. The authors employed K-fold cross-validation and Kolmogorov–Smirnov test for checking the generalization capability of LS-SVM model. The results showed that the LS-SVM model produced significantly better results than different ANN architectures.

Goyal et al. (2014) investigated the abilities of LS-SVM, fuzzy logic, ANN and ANFIS models to improve the accuracy of daily pan evaporation estimation in sub-tropical climates of India. Prior to model development, Gamma-test was used to derive estimates of the noise variance for each input–output set in order to identify the most useful predictors for use in the AI approaches. This study found that Gamma-test can be successfully used for input selection while developing an AI model. It was also found that LS-SVM and Fuzzy logic performed better than the other models.

2.6 HYBRID ARTIFICIAL INTELLIGENCE MODELS

Conventional AI models are found to be weak in dealing with nonlinear and non-stationarity datasets resulting due to the climate change effect, anthropogenic influences and seasonal changes. Various hybrid models tested have yielded good results (Feng et al. 2016; Shamshirband et al. 2016). Recently, wavelet transform has become a popular time series analysis tool due to its ability to simultaneously present both spectral and temporal information within the signal (Daubechies 1990). Some recent literature on development of hybrid Wavelet-AI models are included below.

Wang and Luo (2008) proposed a neural network based wavelet network model (W-ANN) for forecasting ETo time series. In this study, delay parameters of average ETo data were calculated according to correlation analysis. Then Db3 wavelet from Daubechies mother wavelet was applied to transform ETo into wavelet subseries. These decomposed wavelet subseries were then used as inputs to the ANN models.

This study concluded that the use of wavelet transform in conjunction with ANN model can produce fine results for forecasting ETo.

Partal and Cigizoglu (2008) estimated daily-suspended sediment yield in rivers by combining wavelet transform and ANN method. The measured data were decomposed into wavelet components using discrete wavelet transform, and the new wavelet series, consisting of the sum of selected wavelet components, was used as input for the ANN model. It was found that the W-ANN model provided a good fit to observed data for both training and testing period. It was observed that the number of inaccurate sediment estimations decreased significantly and the cumulative sediment sum was closely approximated with the W-ANN method. Their proposed model was also found to be more efficient in predicting peak sediment values when compared to the conventional ANN model.

Izadifar (2010) used cross wavelet analysis to explore correlation between evapotranspiration and meteorological variables. Wavelet analysis was used to differentiate between predictive abilities of various models from a new time-scale variations perspective. Results of the cross wavelet analysis indicated that, the cause and effect relationship between ET and meteorological variables vary based on the time-scale variation under consideration. At smaller time-scales (hourly), significant linear correlations were observed between ET and climatic variables like net radiation, relative humidity, and wind speed. While at larger time-scales, significant linear correlations were observed between ET and climatic variables like net radiation, relative humidity, ground temperature and air temperature.

Kisi and Cimen (2011) investigated the accuracy of wavelet and SVM conjunction model for monthly streamflow forecasting. They proposed the conjunction model by combining discrete wavelet transform with SVM, and then compared the performance of this model to single SVM model. The results revealed that conjunction model could increase the forecasting accuracy of the SVM in monthly streamflow. It was also found that the presence of only a small number of training patterns in peak flow was the reason behind underestimation of the peak values.

Adamowski et al. (2012) proposed a method based on coupling discrete wavelet transforms and ANN for urban water demand forecasting. The proposed model was used for modeling urban water demand forecasting at lead times of one day. The

performance of the model was compared to multiple linear regression, multiple nonlinear regression, autoregressive integrated moving average and ANN models. From the results it was determined that the use of wavelet decomposed subseries as inputs to ANN models helps in providing accurate forecasts of daily urban water demand. The results of this study indicated that coupled W-ANN model was a promising new method of short-term water demand forecasting.

Campisi-Pinto et al. (2012) used ANN coupled with wavelet-denoising for forecasting urban water demand. The study measured the impact of using five different wavelet filter-banks (Haar and Daubechies of type Db2, Db3, Db4, and Db5) on the performance of neural network. In this study wavelet analysis was used to decompose water demand into a few selected component series that carried most of the information. The data were then selectively used in forecasting the water demand. This allowed most of the noisy data to be removed and facilitated the extraction of quasi-periodic and periodic signals in the water demand time series. Results showed that the W-ANN models provided more accurate results than the ANN models. This may be because the wavelet transforms provided useful decompositions of the original time series and the wavelet-transformed data improved the ANN forecasting performance by capturing detail information on various wavelet resolution levels.

Deka and Prahlada (2012) developed hybrid W-ANN models for ocean wave height forecasting. Firstly, main time series of significant wave height data was decomposed to multiresolution time series using discrete wavelet transformations. Then, the multiresolution time series data were used as input to the ANN for forecasting the significant wave height at different multistep lead times. The results showed that the wavelet-ANN model made use of multiresolution time series as inputs allowed for more accurate and consistent predictions compared to the classical ANN models.

Kisi and Cimen (2012) proposed a new wavelet-support vector machine conjunction model for daily precipitation forecasting. This study investigated the performance of wavelet and support vector machine conjunction model for one-day ahead precipitation forecasting. The performance of proposed model was compared to single SVM and ANN model. From the study it was found that SVM performed better

than the ANN model. Additionally, it was also found that combining discrete wavelet transform and SVM improved the performance of the single SVM model.

Moosavi et al. (2013) evaluated the performance of ANN, ANFIS, W-ANN and W-ANFIS for forecasting monthly ground water level. It was found that W-ANFIS models were more accurate than other models. The W-ANFIS model was found to be more accurate for 1 and 2 months ahead forecasting than for 3 and 4 months. Further, it was found that decomposition level in wavelet transform should be determined according to the periodicity and seasonality of the data series. This study confirmed that the optimum number of neurons in the hidden layer cannot be always determined by using a specific formula.

Shirmohammadi et al. (2013) carried out a study to evaluate the ability of W-ANN and W-ANFIS techniques for meteorological drought forecasting in Iran. The study demonstrated that wavelet transform improved meteorological drought modeling. In the first step, the original SPI data were decomposed into a series of details using discrete wavelet transform. The decomposition process was iterated with successive approximation signals being decomposed in turn. In this way, the original time series was broken down into many lower resolution components. From the study it was observed that W-ANFIS models provided more accurate predictions than W-ANN models

Nayak et al. (2013) investigated the potential of using Wavelet-neural network model to simulate river flow of the Malaprabha river basin for a period of 20 years. The input data was decomposed into details and approximations and they were then used as input to ANN model. The results were compared with the standard ANN model. The study concluded that the proposed model performed better at estimating the hydrograph characteristics. Wei et al. (2013) utilized W-ANN modeling method to predict monthly river flow in the Wei River basin, China. The performance of the W-ANN model was compared with that of the ANN model. They noted that decomposing the input data with wavelets increased the accuracy of the ANN model.

Falamarzi et al. (2014) proposed wavelet neural network model for forecasting daily ETo values from temperature and wind speed data. The proposed ANN model used one hidden layer and wavelet function as an activation function. The study

concluded that the use of wavelet function as activation function enhanced the performance of ANN models.

The ability of W-SVM model for predicting ground water level was studied by Suryanarayana et al. (2014). They employed discrete wavelet transform with two coefficients (Db2 wavelet) for decomposing the input into wavelet series. The performance of the hybrid model was compared with SVM, ANN and the traditional auto regressive integrated moving average models. The results indicated that W-SVM model was more accurate in predicting groundwater levels compared to other models.

2.7 SUMMARY OF LITERATURE

The literature review suggests that AI models can be successfully used for modeling various hydrological processes like evapotranspiration. Various studies undertaken found that for estimating evapotranspiration, AI models have performed better than the empirical equations. The hybrid models combining the advantages of different AI techniques have performed well. However, there is a need for further investigation on the behavior of these models under different climatic and data availability condition.

AI models are data driven models and limited availability of datasets has been always a concern while using these models. There is a need to address this issue by testing different input combinations.

2.8 RESEARCH QUESTIONS

- Can hybrid wavelet-AI models be developed which are able to better handle the complex statistical behaviour of the hydrological processes like evapotranspiration?
- What will be the strategy to address the difficulty of limited data availability scenario in developing countries like India?

2.9 PROBLEM FORMULATION

- Accurate estimation of evapotranspiration is of a great importance in arid and semi-arid regions where the evaporation losses often exceed the amount of precipitation, leading to exploitation of ground water resources and further degradation of the ecosystem. As India’s arid and semiarid lands constitute more

than 50 percent of the country's geographic area, modeling ET in arid and semi-arid regions becomes imperative.

- ET is affected by a number of factors including; weather parameters, crop factors and environmental factors. Additionally, evapotranspiration is also heavily influenced by human interventions, which further increases the complexity of the process.
- As ET is a complex and nonlinear phenomenon depending on many interdependent factors which exhibits significant variability in both space and time, developing models for this extremely complex process is a difficult task.
- Owing to the difficulties associated with nonlinear model structure identification and parameter estimation of the complex evapotranspiration process, most of the models that have been developed are empirical in nature. These empirical methods which use fewer inputs are not found to be performing well when tested under different data availability and climatic conditions.
- Recently, significant progress in the fields of AI has made possible to use models like ANN, ANFIS, SVM and ELM to be widely used in various engineering fields.
- ET, like many other hydrological processes operate under a large range of scales varying from one hour to several months leading to a non-linear and non-stationary behavior of the dataset. Classical AI techniques may not be able to cope with these characteristics of the dataset if, input and/or output data is not pre-processed. Data preprocessing techniques which facilitate stabilization of mean and variance, and seasonality removal, are often applied to remove non stationarity in data used to deal with AI models.
- Recently, wavelet transform analysis has become a popular analysis tool due to its ability to elucidate simultaneously both spectral and temporal information within the signal. Wavelet transforms provide useful decompositions of original time series, so wavelet-transformed data improve the ability of a forecasting model by capturing significant information on various resolution levels.
- In view of the above aspects, there is a need to take up a study on utilization of hybrid wavelet-AI models for modeling the process of evapotranspiration. A

comparative study on performance evaluation of different hybrid AI models also needs to be undertaken.

2.10 HYPOTHESIS OF THE STUDY

- Use of hybrid Wavelet-AI models can help in better estimation of ETo values.
- Use of meteorological data from nearby weather stations (within similar climatic zone) to estimate ETo at weather stations of our interest (having limited data) can help in obtaining better estimates of ETo values.

2.11 OBJECTIVES OF THE STUDY

The objective of this study is to study the applicability of hybrid AI models in hydrological modeling. The objectives of this study are

- Development of hybrid models combining wavelet transform and AI model (W-ANN, W-ANFIS and W-LSSVM) to estimate daily and weekly ETo in arid and semi-arid regions of India.
- Performance evaluation of developed hybrid models to select the best model with reference to FAO-56PM for estimating ETo.
- Assessing the impact of using extrinsic ETo values for modeling the process of ETo.

CHAPTER 3

METHODOLOGY AND MODEL DEVELOPMENT

As this study is based on developing hybrid AI models for estimating ET in arid and semiarid regions, the basics of various modeling paradigms like artificial neural network, adaptive neuro-fuzzy inference system, least-square support vector machines and wavelet transform are discussed in this chapter. Further, the study area, input selection and input combinations used for development of various models are also discussed in this chapter.

3.1 ARTIFICIAL NEURAL NETWORK

Neural network is a group of interconnected artificial neurons that can be used as a computational model for information processing. These are non–linear statistical data modeling tools used to develop a relationship between input and output. Mathematically, an ANN can be treated as universal approximators having ability to learn from examples without the need of explicit physics.

3.1.1 Feed-forward backpropagation (FFBP)

A FFBP network has an input layer an output layer and one or more hidden layers between the input and output layer. Information in a neural network passes from the input to the output side (figure 3.1). Hidden layers enhance the network's ability to model complex functions. The data passing through the connections from one neuron to another are manipulated by weights that control the strength of a passing signal. The neurons in one layer are connected to those in the next, but not to those in the same layer. Thus, the output of a node in a layer is only dependent on the inputs it receives from previous layers and the corresponding weights.

The strength of the signal passing from one neuron to the other depends on the weight of the interconnections. Each node multiplies every input by its weight, sums the product, and then passes the sum through a transfer function to produce its result (figure 3.1). This transfer function is generally a steadily increasing S-shaped curve, called a sigmoid function. The attenuation at the upper and lower limbs of the 'S'

constrains the raw sums smoothly within fixed limits. The transfer function also introduces a nonlinearity that further enhances the network's ability to model complex functions.

3.1.2 Training a neural network

The process of training ANN models involves optimization of various parameters and is similar to calibration of a hydrological model. Generally, ANN models do not have any prior knowledge about the problem. The data enters the network through the input layer. The nodes in the input layer are not computational nodes and simply broadcast the data over weighted connections to the hidden nodes. The ANNs are trained with a set of known input and output pairs called the training set.

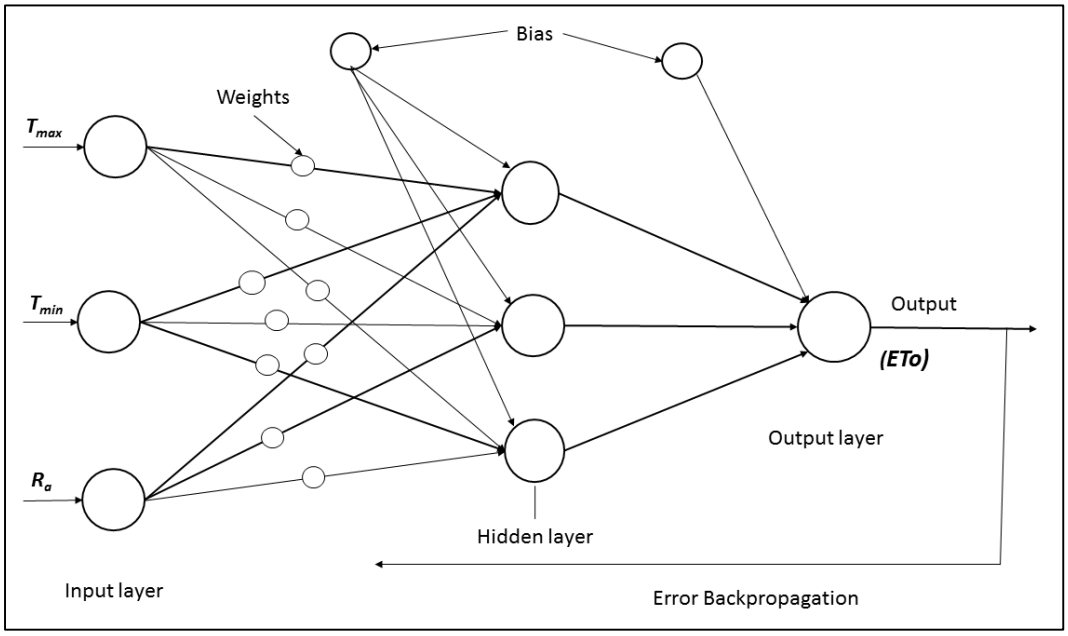

Figure 3.1 Architecture of feedforward backpropagation network used in the study

In the training process, the weights are optimized to get a specific response from ANN. The network weights are initialized based on some previous experience or with a set of random values. These initial values of weights are then corrected during a training (learning) process. The weights in the hidden and output layer neurons are calculated using Eqs. 3.1 and 3.2, respectively

$$w(N+1) = w(N) - \eta\delta\phi \quad (3.1)$$

$$w(N+1) = w(N) + \eta x \sum_{q=1}^{r} \delta_q \quad (3.2)$$

Where w is training weight, N is the number of iteration, x is input value, η is learning weight and ϕ is the output. δ is defined as $2\varepsilon_q \partial\phi/\partial I$, where I is the sum of the weighted inputs, q is neuron index of the output layer, and $\varepsilon_q$is error signal. The above training method is the standard backpropagation training method. The architecture of a typical FFBP network used in this study is also shown in figure 3.1. In the training process, estimated outputs are compared to the known outputs, then the errors occurred are back propagated to obtain the appropriate weight adjustments necessary in minimizing the errors. The neural network model stops iteration for training when the error becomes smaller than the target error. This error signal is propagated back and the weights are adjusted to reduce the difference between desired and computed outputs. The process of adjusting weights is continued until the required level of accuracy is obtained between target values and computed outputs. After learning, the weights are frozen. Then a dataset that the ANN has not encountered before is presented to validate its performance. Depending on the outcome, the ANN has to be either retrained or can be implemented for its designated use.

A number of training algorithms were developed for error back propagation learning. A three layered feed-forward backpropagation network with LM algorithm for weight optimization was used in this study. LM is a combination of steepest descent and Gaussian-Newton method. LM algorithm has fast convergence among other algorithms and it is able to obtain lowest mean square error in many cases (Kisi 2006). Referring to the recommendations given by researchers, all the ANN models in this study used only one hidden layer. Different ANN architectures for modeling daily ETo were tested by varying the number of neurons in the hidden layer. A trial and error procedure was adopted to find the optimum number neurons in the hidden layer. Performance of the sigmoid activation function in the hidden layer with linear activation function at the output layer was also studied.

3.2 ADAPTIVE NEURO-FUZZY INFERENCE SYSTEM

Jang (1993) proposed a method that used neural network learning algorithm for constructing a set of fuzzy if-then rules from stipulated input output pairs.

Fundamentally, ANFIS is a functional equivalent of fuzzy inference systems endowed with neural learning capabilities. An ANFIS model combines the transparent and linguistic representation of a fuzzy system with learning ability of ANN. This allows them to be trained in performing input/output mapping as an ANN model. ANFIS comes with an additional benefit of being able to provide a set of rules on which the model is based.

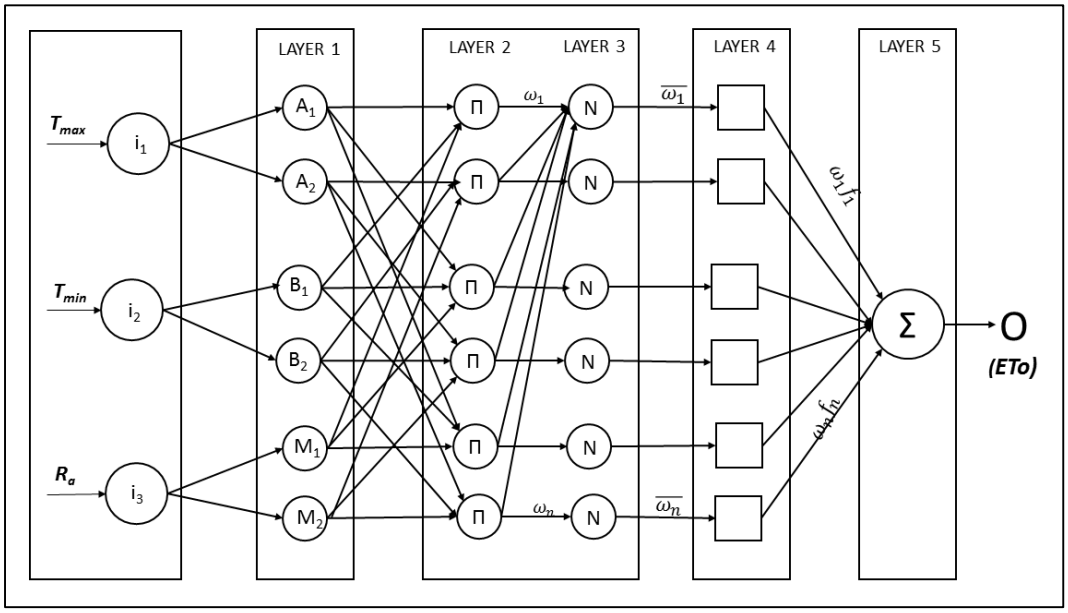

Figure 3.2 Architecture of ANFIS model used in the study

Typically, an ANFIS network architecture consists of five different layers (figure 3.2). Each layer contains several nodes described by the node function. Let O_i^j denote the output of the i^{th} node in layer j.

Each node in Layer 1 is an adaptive node with node output defined as

$$O_i^1 = \mu A_i(x), \text{ for i=1,2…} \quad (3.3)$$

$$O_i^1 = \mu B_i(y), \text{ for i=3,4…} \quad (3.4)$$

Where x (or y) is the input to the node; and A_i (or B_i) is a linguistic label associated with this node. The membership function for A_i and B_i can be represented by various functions.

In layer 2, each node Π multiplies incoming signal and output is the product of all the incoming signals.

$$O_i^2 = \omega_i = \mu A_i(x)\mu B_i(y), \text{ for i=1,2..} \quad (3.5)$$

Each node output represents the firing strength of a rule.

In layer 3, each node N calculates the ratio of the i^{th} rules firing strength to the sum of all rule's firing strengths.

$$O_i^3 = \overline{\omega_\iota} = \frac{\omega_i}{\omega_1+\omega_2}, \text{ for i=1,2…} \quad (3.6)$$

The normalized firing strengths are the output from this layer.

In layer 4, each node calculates the contribution of the i^{th} rule to the overall output

$$O_i^4 = \overline{\omega_\iota} f^i = \overline{\omega_\iota}(a_i x + b_i y + c_i), \text{ for i=1,2…} \quad (3.7)$$

Where $\overline{\omega_\iota}$ is the output of layer 3 and (a_i, b_i, c_i) is the parameter set. The parameter of this layer are known as consequent parameters.

In layer 5, the signal node calculates the final output as the summation of all input signals

$$O_i^5 = overalloutput = \sum \overline{\omega_\iota} f_i = \frac{\sum_i \omega_i f_i}{\sum_i \omega_2} \quad (3.8)$$

Thus, an adaptive network is functionally equivalent to a sugeno-type fuzzy inference system. In this study, a hybrid approach combining least square error and backpropagation methodology was adopted to develop all the ANFIS models. Based on the literature it was decided to evaluate the performance of three and five number of membership functions (MFs) with triangular, trapezoidal, Gaussian, generalized bell-and spline shapes to determine the most efficient ANFIS model.

3.3 LEAST SQUARE SUPPORT VECTOR MACHINE

The foundation of support vector machines (SVM) has been developed by Vapnik, (1995) and is gaining popularity due to many attractive features and promising empirical performances. The formulation embodies SRM principle, which has shown better performances than ERM which is employed by conventional neural networks. SRM minimizes an upper bound on the expected risk, as opposed to ERM that minimizes the error on the training data. It is this difference, which equips SVM with

a greater ability to generalize, thus, achieving the goal of statistical learning. SVM comes with an advantage of using kernel trick to minimize both model complexities and prediction errors simultaneously. SVMs were initially developed to solve the classification problems, but recently they have been extended to the domain of regression problems. LS-SVM provides fast implementation of the traditional SVM. Further details about the LS-SVM model are briefly discussed in the sections below.

3.3.1 SVM algorithm for nonlinear function estimation

Considering a training dataset

$$D = \{(x_1, y_1), \dots, (x_k, y_k), \dots, (x_n, y_n)\}, x_k \in R^n, y_k \in R \tag{3.9}$$

with a nonlinear function

$$f(x) = \langle \omega, \varphi(x) \rangle + b \tag{3.10}$$

where $\langle \cdot, \cdot \rangle$ denotes the dot product; $\omega \in R^{n_k}$ is the weight vector in primal weight space; $\varphi(\cdot): R^n \rightarrow R^{n_k}$ is the nonlinear function that maps the input space to a so-called high dimensional feature space where linear regression is performed; b is the bias term.

The optimization problem is given

$$\text{minimize} \quad \frac{1}{2}\|\omega\|^2 + C \sum_{k=1}^{N} (\xi_k + \xi_k^*) \tag{3.11}$$

$$\textit{Subjected to} \quad \begin{Bmatrix} y_k - \langle \omega, \varphi(x_k) \rangle - b \leq \varepsilon + \xi_k \\ \langle \omega, \varphi(x_k) \rangle + b - y_k \leq \varepsilon + \xi_k^* \\ \xi_k, \xi_k^* \geq 0 \end{Bmatrix} \tag{3.12}$$

With ε-insensitive loss function

$$|y - f(x, \omega)|_\varepsilon = \begin{cases} 0, & \text{if } |y - f(\mathrm{x}, \omega)| \leq \varepsilon \\ |y - f(\mathrm{x}, \omega)| - \varepsilon, & \text{otherwise} \end{cases} \tag{3.13}$$

where ε is the approximation accuracy that can be violated by means of the slack variables ξ, ξ^* for the non-feasible case. Constant C > 0 determines trade-off between flatness of f and the amount up to which deviations larger than ε are tolerated. A smaller value of C tolerates a larger deviation.

The Lagrangian function is given by equation (3.14), where $\alpha, \alpha^*, \eta, \eta^* \geq 0$ are Lagrange multipliers. To find the saddle point, one obtains the partial derivate of L_{SVM} with respect to the primal variable (ω, b, ξ, ξ^*) by equation (3.15).

$$L_{SVM} = \frac{1}{2}\|\omega\|^2 + C\ \sum_{k=1}^{N}(\xi_k + \xi_k^*) - \sum_{k=1}^{N} a_k\ (\varepsilon + \xi_k - y_k + \langle \omega, \varphi(x_k)\rangle + b) - \sum_{k=1}^{N} a_k^*\ (\varepsilon + \xi_k^* + y_k - \langle \omega, \varphi(x_k)\rangle - b) - \sum_{k=1}^{N}(\eta_k \xi_k + \eta_k^* \xi_k^* \quad (3.14)$$

$$\begin{cases} \frac{\delta L_{SVM}}{\delta \omega} = 0 \longrightarrow \omega = \sum_{k=1}^{N}(\alpha_k - \alpha_k^*)\varphi(x_k) \\ \frac{\delta L_{SVM}}{\delta b} = 0 \longrightarrow \sum_{k=1}^{N}(\alpha_k^* - \alpha_k) = 0 \\ \frac{\delta L_{SVM}}{\delta \xi_k} = 0 \longrightarrow C - \alpha_k - \eta_k) = 0 \\ \frac{\delta L_{SVM}}{\delta \xi_k^*} = 0 \longrightarrow C - \alpha_k^* - \eta_k^*) = 0 \end{cases} \quad (3.15)$$

The condition for optimality yield the following dual problem

$$max_{\alpha,\alpha^*} Q = -\frac{1}{2}\sum_{k,l=1}^{N}(\alpha_k - \alpha_k^*)(\alpha_l - \alpha_l^*)\,\langle \varphi(x_k), \varphi(x_l)\rangle - \varepsilon \sum_{k=1}^{N}(\alpha_k - \alpha_k^*) + \sum_{k=1}^{N} y_k(\alpha_k - \alpha_k^*) \quad (3.16)$$

Subject to $\begin{cases} \sum_{k=1}^{N}(\alpha_k - \alpha_k^*) = 0 \\ \alpha_k, \alpha_k^* \in [0, C] \end{cases}$

The parameter b can be computed by exploiting the so-called KKT conditions which states that, at the optimal solution, the product between dual variables and constrains has to vanish.

$$\begin{cases} \alpha_k[\varepsilon + \xi_k - y_k + \langle \omega, \varphi(x_k)\rangle + b] = 0 \\ \alpha_k^*[\varepsilon + \xi_k^* + y_k - \langle \omega, \varphi(x_k)\rangle - b] = 0 \end{cases} \quad (3.17)$$

$$\begin{cases} \eta_k \xi_k = (C - \alpha_k)\xi_k = 0 \\ \xi_k^* \xi_k^* = (C - \alpha_k^*)\xi_k^* = 0 \end{cases} \quad (3.18)$$

From (3.17) it follows that only for $|f(x_k) - y_k| \geq \varepsilon$ the Lagrange multipliers may be nonzero, or in other words, all samples inside ε-tube the α_k, α_k^* vanish. So one gets a sparse expansion of ω, and samples that come with non-vanishing coefficients are called support vectors.

In the end, the resulting SVM for nonlinear function estimation take form:

$$f(x) = \sum_{k=1}^{N}(\alpha_k - \alpha_k^*)\langle\varphi(x), \varphi(x_k)\rangle + b \quad (3.19)$$

According to Mercer's condition, the inner product $\langle\varphi(x), \varphi(x_k)\rangle$ can be defined through a kernel $K(x, x_k)$ so the equation (3.19) can be expressed as

$$f(x) = \sum_{k=1}^{N}(\alpha_k - \alpha_k^*)K(x, x_k) + b \quad (3.20)$$

3.3.2 LS-SVM for nonlinear function estimation

In least square support vector machine for function estimation, the optimization problem is formulated as,

$$\min J(\omega, e) = \frac{1}{2}\|\omega\|^2 + \frac{1}{2}\gamma\sum_{k=1}^{N} e_k^2 \quad (3.21)$$

Subject to $y_k = \langle\omega, \varphi(x_k)\rangle + b + e_k$, k=1,…N

where $e_k \epsilon R$ are error variables; $\gamma \geq 0$ is regularization constant. Smaller γ can avoid overfitting in case of noisy data. The Lagrangian is given by

$$L_{LS-SVM} = \frac{1}{2}\|\omega\|^2 + \frac{1}{2}\gamma\sum_{k=1}^{N} e_k^2 - \sum_{k=1}^{N} a_k\{\langle\omega, \varphi(x_k)\rangle + b + e_k - y_k\} \quad (3.22)$$

with Lagrange multipliers $\alpha_k \epsilon R$. The conditions for optimality are given by

$$\begin{cases} \frac{\delta L_{LS-SVM}}{\delta\omega} = 0 \longrightarrow \omega = \sum_{k=1}^{N}\alpha_k\,\varphi(x_k) \\ \frac{\delta L_{LS-SVM}}{\delta b} = 0 \longrightarrow \sum_{k=1}^{N}\alpha_k = 0 \\ \frac{\delta L_{LS-SVM}}{\delta e_k} = 0 \longrightarrow \alpha_k = \gamma e_k), (k = 1, \dots N) \\ \frac{\delta L_{LS-SVM}}{\delta \alpha_k} = 0 \longrightarrow \langle\omega, \varphi(x_k)\rangle + b + e_k - y_k \end{cases} \quad (3.23)$$

These conditions are similar to standard SVM optimality conditions (3.15), except for the condition $\alpha_k = \gamma e_k$. After elimination of ω, e one obtains the following linear equation

$$\begin{bmatrix} 0 & 1_V^T \\ 1_v & \Omega + I/\gamma \end{bmatrix}\begin{bmatrix} b \\ \alpha \end{bmatrix} = \begin{bmatrix} 0 \\ y \end{bmatrix} \quad (3.24)$$

where $y = [y_1, \dots, y_n], 1_v = [1, \dots, 1], \alpha = [\alpha_1, \dots, \alpha_N]$ and on applying the Mercer's condition again

$$\Omega_{kl} = \langle \varphi(x_k), \varphi(x_l) \rangle = K(x_k, x_l)\ k, l = 1, \ldots, N \quad (3.25)$$

Although the choices of the kernel function in LS-SVM are the same as those in SVM, more emphasis has been put on the powerful Gaussian radial basis function kernel which is given as

$$K(x, x_k) = \exp(-\|x - x_k\|^2 / 2\sigma^2 \quad (3.26)$$

The resulting LS-SVM model for function estimation becomes

$$f(x) = \sum_{k=1}^{N} \alpha_k K(x, x_k) + b \quad (3.27)$$

where α, b are solution to (3.24).

On comparing (3.11) to (3.21) we can see that LS-SVM is a reformulation of the principles of SVM, which involves equality instead of inequality constraints. Furthermore, LS-SVM uses the least squares loss function instead of the e-insensitive loss function. In this way, the solution follows a linear KKT system instead of a computationally hard quadratic programming problem. Therefore, it is easier to optimize with shorter computational time. Also, the dual problem of LS-SVM corresponds to solving a linear KKT system, which is a square system with a global and possibly unique solution if the matrix has full rank.

Choice of kernel functions and hyper-parameters are some critical issues needed to be addressed before the application of LS-SVM. Radial basis function (RBF) a more compactly supported kernel function is able to reduce the computational complexity of the training process and provides a good performance. Hence, the RBF kernel function was employed in this study. Different techniques for tuning of the hyper-parameters related to the regularization constant are available in the literature. In this study the regularization parameter gamma (γ) and kernel function parameter (σ^2) were obtained by grid search technique based on leave-one-out cross validation.

3.4 WAVELET TRANSFORM

The existing literature reveals that ETo, like many other hydrological processes operate under a large range of scales varying from one hour to several months leading to non-linear and non-stationary behavior of the dataset. Classical AI models alone may not be able to cope with these characteristics of the dataset if input and/or output

data are not preprocessed. Wavelet is a time series analysis tool, which provides simultaneous time and frequency information about the time series. Use of wavelet per-processed data provides useful decompositions of the original time series and may enhance the performance of AI models by capturing detail information on various wavelet resolution levels

Signals whose frequency content changes with time are called non-stationary signals. In other words, the frequency content of non-stationary signal changes in time. Hence, it becomes important to know which frequency component exists at what time. Wavelet transform is widely used for the analysis of non-stationary time series. In wavelet transform, the original time series is broken down into its 'wavelets' which is a scaled and shifted version of the mother wavelet. The main advantage of using wavelet transform is that it provides both time and frequency information simultaneously. This time-frequency representation of wavelet transform is not available in traditional Fourier transform (FT) and Short Term Fourier Transform (STFT). FT of a signal in time domain gives information about how much of each frequency exists in the raw signal without giving the information about time. Therefore, FT is not suitable for analysis of non-stationary data. On the other hand, STFT provides a measure of time and frequency resolutions, but the use of a fixed window size at all times and for all frequencies is a limitation of this method.

3.4.1 Discrete wavelet transform

Wavelet transform (WT) addresses the above limitation by partitioning the time-frequency plane using a range of window sizes. At high frequencies, the wavelet transform gives up some frequency resolution compared to the Fourier transform. Figure 3.3 shows a representation of FT, STFT and WT. Wavelet transform provides multi resolution analysis of a time signal. At low scales (high frequency) it gives a better time resolution (represented by compact width of time window) and poor frequency resolution (represented by wider width of scale window) while, at high scales (low frequency) it gives a better frequency resolution and poor time resolution. In actual practice, this information is important for analysis of the time series signals. The lower scales (compressed wavelet) traces the abrupt change or high frequency component of a signal while the higher scales (stretched wavelet) traces slowly

progressing occurrences or low-frequency component of the signal. Using this method, wavelet transform breaks the signal into wavelets (small wave) which are scaled and shifted versions of the original wavelet (mother wavelet). The wavelet transformation can be divided into following two types:

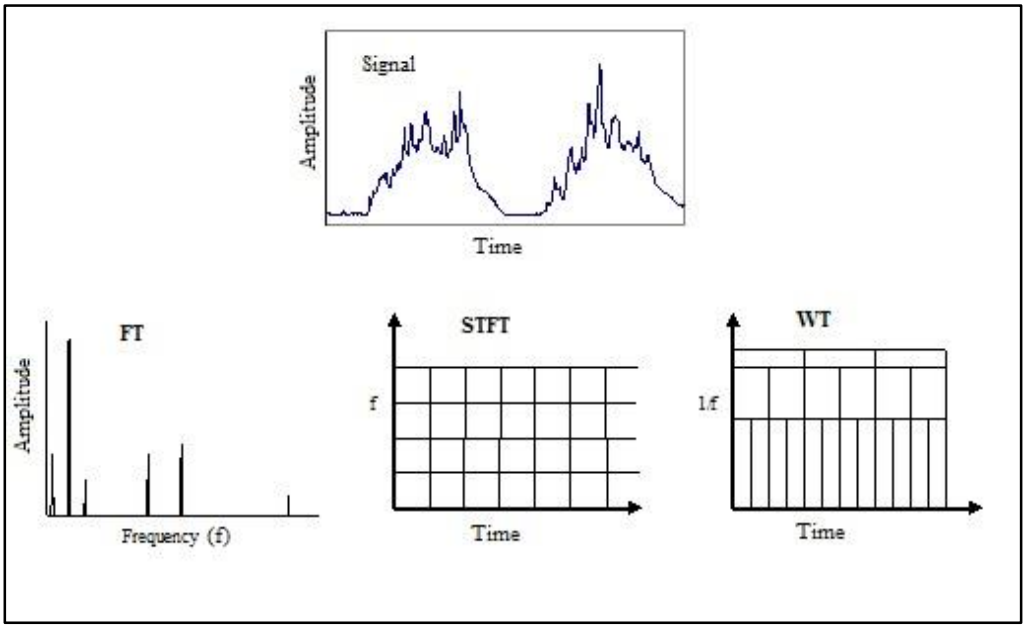

Figure 3.3 Fourier transform, short time Fourier transform and wavelet transform

3.4.1.1 Continuous wavelet transform (CWT)

The basic objective of the CWT is to achieve a complete time-scale representation of localized and transient phenomenon occurring at different time scales. The CWT of a signal is given by the equation

$$CWT(a,b) = \frac{1}{\sqrt{a}} \int_{-\infty}^{\infty} x(t)\, \psi^* \left(\frac{t-b}{a}\right) dt \qquad (3.28)$$

In the equation above, the transformed signal is a function of two variables, *a*, the scale factor and *b*, the translation function of the function $\psi(t)$. While, * corresponds to the complex conjugate, $\psi(t)$ the transforming function called mother wavelet is defined as

$$\int_{-\infty}^{\infty} \psi(t)dt = 0 \qquad (3.29)$$

The term translation is related to the location of the window, as the window is shifted through the signal. This term, obviously, corresponds to time information in

the transform domain. The scale parameter is defined as the reciprocal of frequency. Low frequencies (high scales) correspond to the global information of a signal (that usually spans the entire signals) whereas, high frequencies (low scales) correspond to a detailed information of a hidden pattern in the signal (that usually lasts a relatively short time).

The CWT is computed by changing the scale of the analysis window, shifting the window in time, multiplying by the signal, and integrating over all times. The original signal is reconstructed using the inverse wavelet transform which is given as

$$x(t) = \frac{1}{c_\psi} \int_{-\infty}^{\infty} \int_{0}^{\infty} \frac{1}{\sqrt{a}} \psi\left(\frac{t-b}{a}\right) CWT(a,b) \frac{da.db}{a^2} \tag{3.30}$$

where c_ψ is the admissibility constant.

3.4.1.2 Discrete wavelet transform (DWT)

Calculating the CWT coefficients at every possible scale is a fair amount of work, and generates a large amount of data. CWT produces N^2 coefficients from a dataset of length *N*. If one chooses scales and positions based on the powers of two (dyadic scales and positions) then the analysis becomes more efficient and accurate. Also, it provides *N* transform coefficients. This transform is called discrete wavelet, and has the form

$$\psi_{m,n}(t) = \frac{1}{\sqrt{a_o^m}} \psi\left(\frac{t - n b_o a_o^m}{a_o^m}\right) \tag{3.31}$$

where m and n are integers that control the wavelet dilation and translation, respectively; b_o is the location parameter and must be greater than zero; a_o is a specified fixed dilation step greater than 1. The most common and simplest choice of parameters a_o and b_o are 2 and 1 (time steps), respectively. This power of two logarithmic scaling of the translations and dilations is known as the dyadic grid arrangement (Mallat, 1989) and is defined as

$$\psi_{m,n}(t) = 2^{-m/2} \psi(2^{-m} t - n) \tag{3.32}$$

For discrete time series, x_t, where x_t occurs at discrete time *t*, the discrete wavelet transform becomes

$$W_{m,n} = 2^{-m/2} \sum_{i=0}^{N-1} \psi\,(2^{-m}t - n)x_t \qquad (3.33)$$

Where $W_{m,n}$ is wavelet coefficient for the discrete wavelet of scale $a = 2^m$ and location $b = 2^m n$. Eq.(3.33) considers a finite time series x_t (t=0,1,2,…,N-1), and N is an integer power of 2: $N = 2^M$; n is time translation parameter. This gives the range of m and n as, respectively, $0 < n < 2^{M-m} - 1$ and $1 < m < M$. At the largest wavelet scale (i.e. 2^m where $m = M$) only one wavelet is required to cover the time interval, and only one coefficient is produced. At the next scale (2^{m-1}), two wavelets cover the time interval, hence two coefficients are produced, and so on down to $m = 1$. At $m = 1$, the a scale is 2^1, i.e. 2^{M-1} or $N/2$ coefficients are required to describe the signal at this scale. The total number of wavelet coefficients for a discrete time series of length $N = 2^M$ is then $1 + 2 + 4 + 8 + \ldots + 2^{M-1} = N-1$.

In addition to this, a signal smoothed component, $\bar{W}$, is left, which is the signal mean. Thus, a time series of length N is broken into N components, i.e. with zero redundancy. (Mallat, 1998) gives the inverse discrete transform as

$$x_t = \bar{W} + \sum_{m=1}^{m} \sum_{n=0}^{2^{M-m}-1} W_{m,n}\, 2^{-m/2} \psi(2^{-m}t - n) \qquad (3.34)$$

which can be written as,

$$x_t = \bar{W}(t) + \sum_{m=1}^{M} W_m(t) \qquad (3.35)$$

where $\bar{W}(t)$ is the approximation sub-signal at level M and $W_m(t)$ are detail sub-signals at level m = 1,2,….,M. The detail wavelet coefficients $W_m(t)$ can capture small features of interpretational value in the data. The residual term $\bar{W}(t)$ represents background information of data.

DWT operates two sets of function; high-pass filter (wavelet function) and low-pass filters (scaling function). The original time series are passed through high-pass and low-pass filters (as shown in figure 3.4) and down sampled by two (Deka and Prahalada, 2012). After passing the signal through high pass and low pass filters, detailed (D1, D2,…., Dn, which are high frequency components of the original signal) and approximation coefficients (A1, A2,….An, which are low frequency components of the original signal) are obtained. At any n^{th} decomposition level, there will be one series of approximation coefficients at n^{th} level (i.e. An) and n series of detailed

coefficients (i.e. D1, D2,….,Dn). Therefore, there will be total n+1 coefficients and the sum of An + D1 + D2 + ……+ Dn is equal to the original signal x (t).

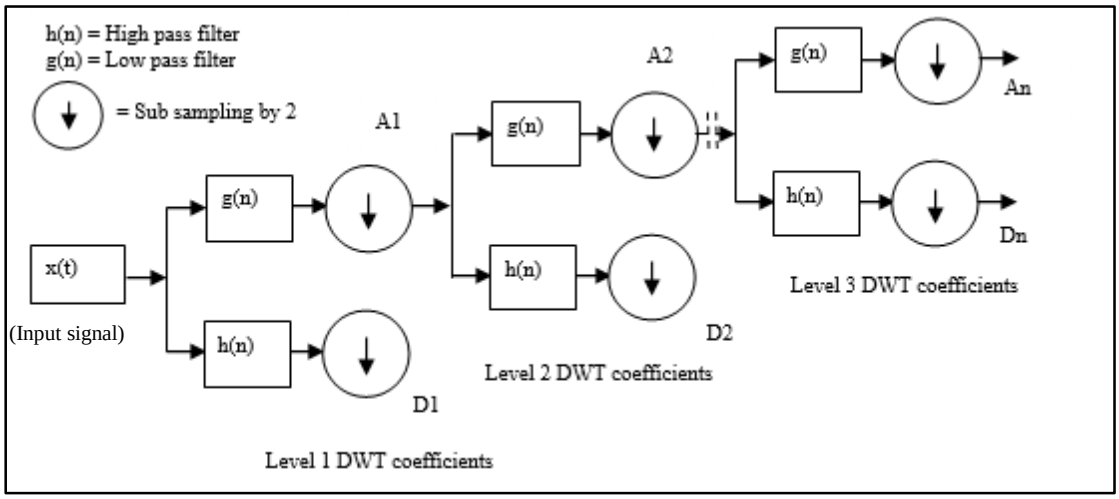

Figure 3.4 Discrete wavelet transform decomposition tree

3.4.1.3 Selection of mother wavelet

For developing hybrid W-ANN, W-ANFIS and W-LSSVM models input datasets were first decomposed into subseries using DWT. Then, these wavelet-decomposed subseries were used as inputs to improve the efficiency of ANN, ANFIS and LS-SVM models. During wavelet analysis, selection of appropriate mother wavelet functions becomes crucial. As dyadic wavelet transform was used in this study, orthogonal mother wavelets were employed for wavelet decomposition. The choice of mother wavelet depends on the data to be analyzed. In this study, the performance of various Db wavelets was evaluated. Daubechies wavelets are a family of orthogonal wavelets defining a discrete wavelet transform. They are further sub classified according to the number of vanishing moments they have. For Db family wavelets, the smoothness of scaling and wavelet function increases with the number of vanishing moments. Daubechies wavelets Db2, Db3, Db4 and Db5 are used in this study (refer figure 3.5). All Daubechies wavelets of order *N* (Db*N*) are asymmetric, orthogonal and biorthogonal. They are compactly supported wavelets with extremal phase and highest number of vanishing moments for a given support width. Daubechies wavelets have a compact support, which is suitable for local analysis of the signal.

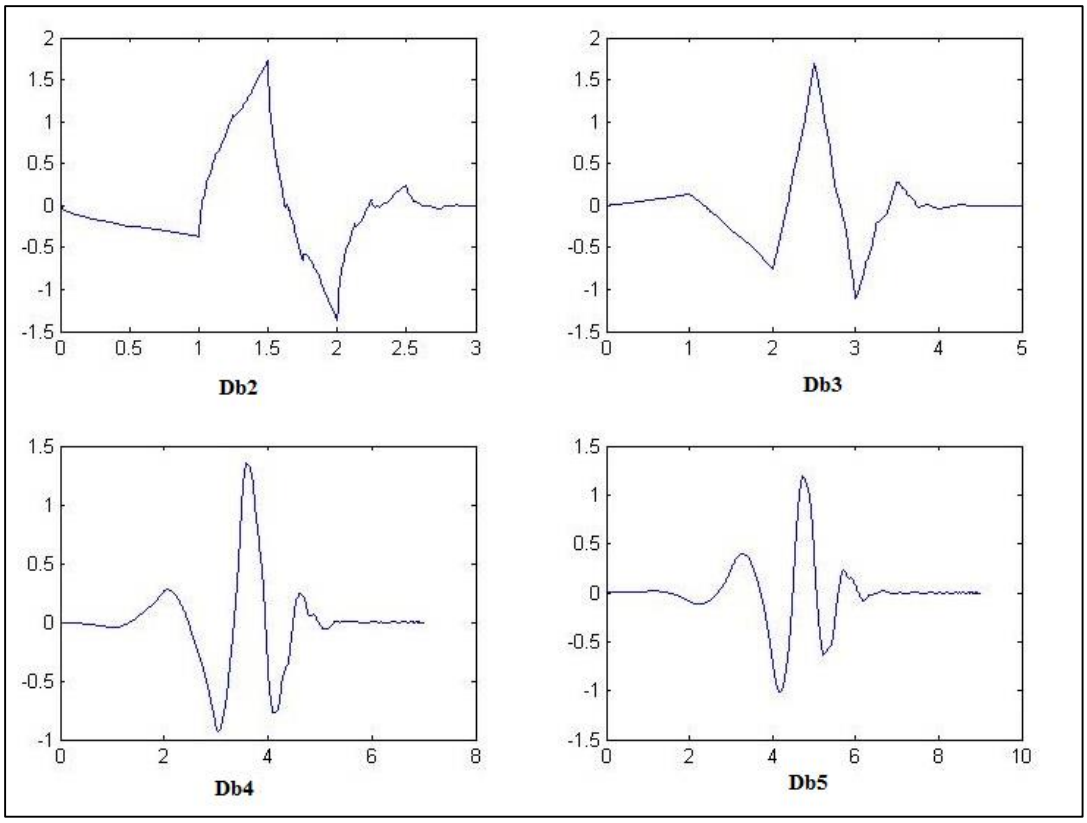

Figure 3.5 Wavelet from Daubechies family

Another important concern in the use of wavelet transform is the selection of optimum decomposition level. The effect of using various decomposition levels on the performance of W-ANN model was also investigated. The maximum level of decomposition was selected using the formula L = int [log (N)], where L and N are decomposition level and number of time series data respectively. In this study, the time series of various climatic variables were decomposed into one, two and three levels using the mother wavelets mentioned earlier. Figure 3.6 presents a second level decomposition of a time series using Db3 mother wavelet. In the figure 's' represents the raw signal (maximum temperature at the Jodhpur weather station), a_2 represents the approximation at level 2 while d_1 and d_2 represent the details at level 1 and 2 respectively. As mentioned earlier the sum of a_2, d_2 and d_1 is equal to the value of the original signal 's'.

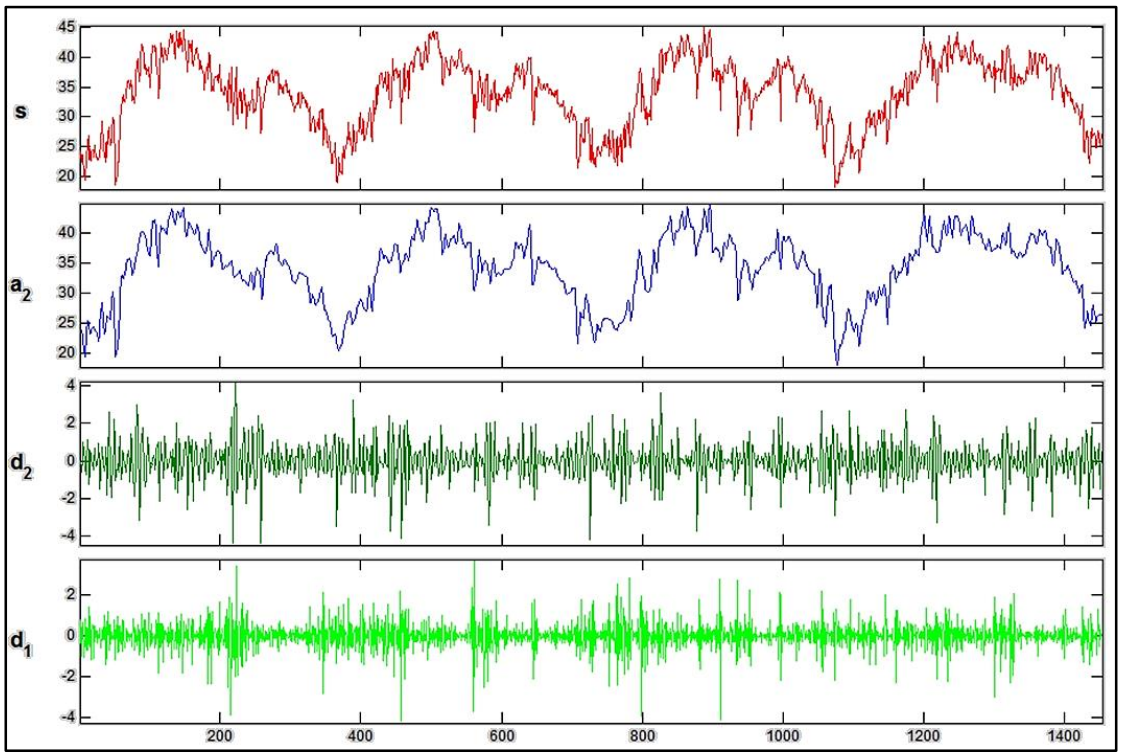

Figure 3.6 Wavelet decomposition of maximum temperature time series for Jodhpur weather station

3.5 FAO-56PM METHOD FOR ESTIMATING REFERENCE CROP EVAPOTRANSPIRATION

The procedure for estimation of ET rates from agricultural crops involves computation of ETo using regularly recorded climatological data. Several equations, broadly classified as temperature-based, radiation-based and combination-type have been proposed for ETo computations. Majority of the studies carried out to evaluate the performance of various ETo estimation equations have found the physically-based Penman-Monteith equation as the best estimator of ETo across a wide range of climates. The recent version of the internationally accepted FAO methodology for estimation of crop water requirements (Allen et al. 1998), recommends the sole use of the Penman-Monteith (hereafter referred as FAO-56PM) equation for ETo computations.

As per Allen et al. (1998), the recommended form of the FAO-56PM equation is

$$ETo = \frac{0.408\Delta(R_n - G) + \gamma \frac{900}{T_{mean} + 273} u_2 (e_s - e_a)}{\Delta + \gamma(1 + 0.34u_2)} \quad (3.36)$$

where ETo is reference crop ET (mm/day) defined as ' the evapotranspiration from a hypothetical reference crop with an assumed crop height of 0.12 m, a fixed surface resistance of 70 s/m and an albedo of 0.23', where R_n is net radiation at crop surface ($MJ/m^2/d$), G is soil heat flux density ($MJ/m^2/d$), T_{mean} is mean air temperature (°C) at two meter height, U_2 is wind speed (m/s) at two meter height, e_s is saturation vapor pressure (kPa), e_a is actual vapor pressure (kPa), (e_s-e_a) is saturation vapor pressure deficit (kPa), Δ is slope of vapor pressure versus temperature curve at temperature T (kpa/°C) and γ is the psychrometric constant (kPa/°C). Application of the FAO-56PM requires standard ground-based climatological data of solar radiation or sunshine, air temperature, humidity and wind speed and site details of latitude and altitude. The structure of the equation suggests that, except wind speed and air temperature none of the other inputs appears explicitly in computation of ETo. In other words, use of this equation involves conversion of measured parameters into a number of estimated parameters. FAO-56PM describes the procedures to be adopted to compute these parameters. Various alternative methods for estimating these parameters in missing data scenario are also mentioned in Allen et al. (1998).

3.6 STUDY AREA AND DATASETS

India's arid and semiarid lands constitute more than 50 percent of the country's geographic area and are home to 60 percent of the rural population where agriculture is the primary occupation. Aridity is usually expressed as a function of rainfall and temperature. A useful representation of aridity is the following climatic aridity index;

$$Aridity\ index = \frac{precipitation}{potential\ evapotranspiration} \tag{3.37}$$

where, potential evapotranspiration is calculated by FAO-56PM.

Arid regions (aridity index 0.03 to 0.2) and semi-arid regions (aridity index 0.2 to 0.5) are the regions where a combination of high temperature and low rainfall causes evaporation that exceeds precipitation. Also, the precipitation received is highly variable, sporadic and unpredictable, making it almost impossible to produce crops without irrigation. Considering these factors, it was intended to carry out the study for arid and semi-arid regions of India.

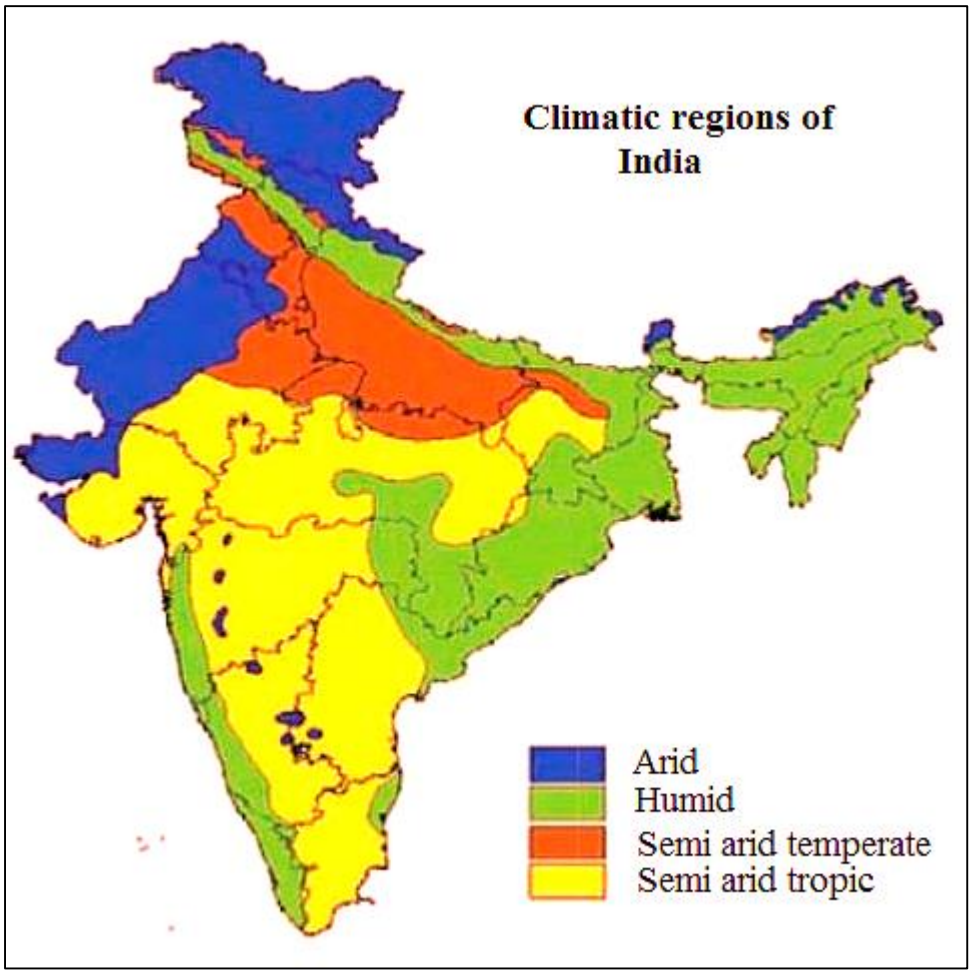

Figure 3.7 Arid and semi-arid zones of India

3.6.1 Datasets used for arid region

In this study, weekly climatic data from Jodhpur (26°28'N latitude and 73°02'E longitude) and Pali (25°77'N latitude and 73°33' E longitude) weather stations were used. The data were obtained from the Central Arid Zone Research Institute. Both these stations are located in The Thar Desert which is classified as Arid Region (BW) according to the Koppen climate classification. Extreme heat in summer and cold winters are the characteristics of the desert and the study area being no exception, the temperature may vary from a maximum of 49 ^{0}C in summer to a minimum of 1 ^{0}C in winter. The study area receives an annual average rainfall of about 326 mm and the rainy days are often limited to 30 days. The soil here can be classified mainly as sandy and loamy. The data samples covered forty years (1970-2009) of weekly records of climatic parameters. All the models were trained using first thirty years

(1970 to 1999) data while the remaining ten years (2000 to 2009) data were used for validation and testing the models.

The weekly weather data used in this study were maximum air temperature [T_{max} (^{0}C)], minimum air temperature [T_{min} (^{0}C)], maximum relative humidity [RH_{min} (%)], minimum relative humidity in percentage [RH_{min} (%)], sunshine duration (hours) and wind speed measured at 2 meters height above the ground level [U_2 (m/sec)]. Solar radiation [R_s (MJ/m/d)] is an important parameter for estimating ETo (Tabari et al. 2016). As solar radiation (Rs) measuring instruments such as pyranometer were not available, Rs was estimated using Angstrom formula, which relates solar radiation to extraterrestrial radiation and relative sunshine duration (n/N).

Table 3.1 Statistical properties of weekly dataset in arid region.

Station	Variable	X_{max}	X_{min}	X_{mean}	S_x	C_v	C_{sx}	Correlation with ETo
Jodhpur	T_{max}	46.20	19.60	33.91	05.5	0.16	-0.32	0.82
	T_{min}	32.40	05.30	20.37	06.41	0.31	-0.32	0.75
	RH_{max}	96.30	15.70	58.16	17.88	0.31	0.01	-0.15
	RH_{min}	85.90	03.90	28.54	16.87	0.59	1.02	-0.10
	U_2	07.31	00.00	01.83	01.04	0.57	1.02	0.77
	Rs	26.72	10.74	18.77	03.57	0.19	0.06	0.70
	ETo	12.83	01.24	05.23	02.15	0.41	0.61	1.00
Pali	T_{max}	47.00	19.50	34.22	05.42	0.16	-0.19	0.81
	T_{min}	32.80	2.80	19.11	07.51	0.39	-0.36	0.73
	RH_{max}	98.70	13.90	63.19	17.57	0.28	-0.22	-0.45
	RH_{min}	88.90	03.30	33.01	17.97	0.54	0.90	-0.29
	U_2	07.08	00.00	02.20	01.09	0.50	1.06	0.73
	Rs	29.79	10.41	19.80	04.08	0.21	0.31	0.72
	ETo	14.59	02.20	05.64	02.36	0.42	0.72	1.00

The statistical properties of each climatic variable for the entire dataset at Jodhpur and Pali weather stations are given in table 3.1. In the table the X_{max}, X_{min}, X_{mean}, S_x, C_v and C_{sx} denote the maximum, minimum, mean, standard deviation, variation coefficient and skewness, respectively. It can be observed in table 3.1 that the statistical properties of the Jodhpur and Pali station are quite similar. This may be due to the proximity (about 65 Km apart) of the weather stations. The wind speed and ETo show a skewed distribution. For both the stations, maximum temperature has the highest correlation with ETo followed by the wind speed and solar radiation.

Furthermore, a high correlation of 0.86 was also seen between the ETo values of both stations.

3.6.2 Datasets used for semi-arid region

Daily climatic data from Hyderabad (17°27'N latitude and 78°28'E longitude) and Kurnool (15°50'N latitude and 78°04' E longitude) weather station were used in this study. The Hyderabad weather station is located in the Deccan plateau and rises to an average height of 536 meters above sea level. The soil type in Hyderabad is mainly classified as red sandy soil. It also features rock formations which are amongst the oldest and hardest rocks in the world. Kurnool weather station is located on the banks of the Tungabhadra river at an altitude of 281 meters above sea level. Kurnool weather station is situated about 200 km away from the Hyderabad weather station. The soil here is mainly made of mixed red and black soil. The study area under consideration (Hyderabad and Kurnool) is classified as semi-arid region according to the Koppen climate classification and receives an annual rainfall of about 700 mm from the south-west monsoon winds.

Daily weather data for a period of six years (2004 to 2009) was obtained from the surface observatories operated and maintained by the India Meteorological Department, Government of India. Out of the six years data obtained, four years data (2004 to 2007) were used for training, while the remaining two years data (2008 to 2009) were used for validation and testing. Both the stations are equipped with standard ground based instruments; alcohol and wet-bulb thermometers, sunshine recorder, cup anemometer and mercury thermometers. The individual data records received from IMD were subjected to screening and integrity checks as per the procedures described in FAO-56PM.

The climatic data received from IMD included T_{max}, T_{min}, U_2, sunshine hours and dew point temperature [T_{min} (^{0}C)]. Unfortunately, good quality sunshine records were not available for the entire period considered; the solar radiation was calculated as a function of maximum and minimum temperature using the Hargreaves radiation formula. The statistical properties of daily datasets obtained from Hyderabad and Kurnool weather stations are given in table 3.2. It is clear from the table that the

statistical properties of the weather data at Hyderabad and Kurnool station are identical. The wind data at both the station show high positive skewness.

Table 3.2 Statistical properties of daily dataset in semi-arid region.

Station	Variable	X_{max}	X_{min}	X_{mean}	S_x	C_v	C_{sx}	Correlation with ETo
Hyderabad	T_{max}	43.98	22.60	33.01	3.93	15.42	0.46	0.77
	T_{min}	29.70	8.70	20.72	3.88	15.02	-0.51	0.56
	T_{dew}	27.60	1.60	16.46	4.78	22.82	-0.50	-0.12
	U_2	7.78	0.28	2.62	1.18	1.40	0.94	0.41
	Rs	27.65	6.93	18.60	4.56	20.82	-0.47	0.66
	ETo	13.25	2.12	5.67	1.65	2.71	0.83	1.00
Kurnool	T_{max}	45.30	23.60	34.34	3.75	14.06	0.42	0.72
	T_{min}	31.00	12.70	22.88	3.51	12.33	-0.33	0.72
	T_{dew}	27.60	1.60	16.45	4.77	22.73	-0.50	0.23
	U_2	5.94	0.00	1.18	0.91	0.82	1.12	0.69
	Rs	27.08	7.14	18.53	2.90	8.41	-0.17	0.65
	ETo	8.87	1.61	4.62	1.35	1.83	0.34	1.00

It can be observed from the table that T_{max} and T_{min} show very good correlation with the ETo data. Further, it can also be observed that R_s at both the weather station has a significant correlation with the ETo values. This high correlation between R_s and ETo in semi-arid region can be attributed to the fact that the R_s values are calculated using the temperature values. A high correlation of 0.73 was observed between the ETo values of Hyderabad and Kurnool weather station. This highlights the similarity of climatic conditions prevailing in the study area considered.

3.7 INPUT SELECTION USING FACTOR ANALYSIS

An essential task in developing any AI model is to determine the dependent (output) and independent variables (inputs). As this study focuses on developing AI models under limited data availability scenario, the most influential climatic parameters in the process of ETo (for the proposed site) were used as inputs to the AI models. Choosing influential input variables would provide a better predictive model under limited data availability scenario thus making data collection and processing easier. In this study, the input variables were selected based on factor analysis.

3.7.1 Factor analysis

When several variables are measured, the correlation between each pair of variables can be arranged in an R- matrix which is a table of correlation coefficients between the variables. The existence of clusters of large correlation coefficients between subsets of variables suggests that those variables could be measuring the aspects of the same underlying dimension. These underlying dimensions are known as factors. Factor analysis is a technique by which datasets of a group of interrelated variables are reduced into a smaller set of uncorrelated factors. It is a statistical technique that can be used to analyze the matrix of correlation coefficients of a set of variates and provide a better understanding and interpretability of the structure of the matrix. The method employs eigenvalue-eigenvector analysis to derive a smaller number of derived variables, from the matrix of correlation. The elements of the transformed eigenvector matrix are called factor loadings and are indicative of the amount by which each original variable contributes to the total variance. A factor can be described in terms of the variable measured and the relative importance fof them for that factor. As such

$$Factor_1 = \beta_1 variable_1 + \beta_2 variable_2 + \ldots . \beta_n variable_n \quad (3.38)$$

The β in the equation represents factor loading and indicates the relative importance of each variable to a particular factor.

It is possible to obtain as many factors as there are variables and each has an associated Eigenvalue. The Eigenvalue associated with a factor indicates the substantive importance of that factor. Therefore, factors only with large Eigenvalue can be retained as significant factors. In this study factors with Eigenvalue more than one were considered for further analysis. Once the factors are extracted it is possible to calculate the loading of the variable on each factor. Generally, it is found that most variables have high loadings on the most important factor and small loading on all other factors. This characteristic makes interpretation difficult and so a technique called factor rotation, by which factor axis are effectively rotated such that variables are loaded maximally to only one factor. In other words, the large elements in the factor loadings are made as large as possible and the small elements are made as small as possible. In this study varimax rotation was used in this study as it is a good general approach that simplifies the interpretation of factors. Independent variables

that have a high loading in a factor in which the dependent variables also has high loadings may then be identified as important variables in the underlying process.

3.7.2 Results of factor analysis

The analysis was performed separately for all the four weather stations considered. As lysimeter data from the weather station used as case study were not available, ETo estimated by the FAO-56PM method was used as dependent variable. The independent variables considered were the climatic variables used for computation of FAO-56PM ET. $T_{max,}$ $T_{min,}$ RH_{max} RH_{min}, Rs and U_2 were used as independent variables in arid regions, whereas $T_{max,}$ $T_{min,}$ T_{dew}, Rs and U_2 were used in semi-arid region.

Table 3.3 Results of factor analysis for the Jodhpur and Pali stations

Station	Variable	Rotated component matrix	
		Component	
		1	2
Jodhpur	T_{max}	0.91	-0.10
	T_{min}	0.89	0.34
	RH_{max}	-0.04	0.96
	RH_{min}	0.03	0.97
	U_2	0.78	0.17
	Rs	0.58	-0.68
	ETo	0.95	-0.10
Pali	T_{max}	0.85	-0.30
	T_{min}	0.92	0.22
	RH_{max}	-0.05	0.94
	RH_{min}	0.18	0.93
	U_2	0.83	0.10
	Rs	0.49	-0.75
	ETo	0.86	-0.47

For all the four stations considered, two-factor rotation (decided using scree plot) provided the best solution for interpreting the relative importance of independent variables on the dependent variable. The results for Jodhpur and Pali stations are shown in table 3.3.

Considering the rotated two-factor solution for Jodhpur and Pali site (arid region), it can be seen that ETo has the highest loading in the first factor in which T_{max} and T_{min} have high loading. Additionally, these two variables exhibit a high degree of correlation with the ETo values (Table 3.1). This implies that these two climatic

variables have the most dominant effect on ETo estimates of these sites. The variable having next highest loading on ETo is the wind speed and solar radiation. The second component has a very small loading on the dependent variable and may therefore be ignored. In summary, the result of factor analysis and correlation analysis for the arid Jodhpur and Pali site indicate that temperature (T_{max} and T_{min}) and to a lesser degree wind speed and solar radiation explain most of the variability associated with FAO-56PM estimated in arid regions.

Table 3.4 Results of factor analysis for the Hyderabad and Kurnool stations

Station	Variable	Rotated component matrix	
		Component	
		1	2
Hyderabad	T_{max}	0.90	0.07
	T_{min}	0.51	0.75
	T_{dew}	-0.24	0.84
	U_2	0.06	0.72
	Rs	0.81	-0.34
	ETo	0.92	0.24
Kurnool	T_{max}	0.98	0.02
	T_{min}	0.58	0.62
	T_{dew}	-0.20	0.82
	U_2	0.12	0.82
	Rs	0.94	-0.12
	ETo	0.75	0.60

Using a similar reasoning, the two-factor solution for Hyderabad and Kurnool station can be interpreted from table 3.4. The loading for ETo is quite high in the first factor. Variables T_{max}, R_s, and T_{min} exhibit high loading in the first factor. Use of an indirect method employing temperature values to estimate R_s values may be the reason behind high loading of solar radiation. Further, a high correlation was observed between temperature and ETo values of Hyderabad as well as Kurnool weather station. Considering this, it can be concluded that air temperature is an important component in estimating ETo of the semi-arid region also.

To the knowledge of the authors, in most of the studies undertaken earlier, the inputs to ET models are chosen according to the similarity between the empirical models and the defined AI model. However, different input combinations may work well for different sites. In this study, factor analysis and correlation analysis was employed to

identify the input combination that will yield a more efficient model under limited data condition. Results of factor analysis suggested that solar radiation is the second most influencing climatic variable in the process of ET at arid region. However, to limit the use of climatic variables and still develop a better model it was decided to use extra-terrestrial radiation (Ra) as an input instead of solar radiation (Rs). Ra which can be easily calculated by a formula and proves to be an important parameter in estimating ET under limited data condition. Use of Ra as input eliminates the need of measuring sunshine hours but still provides an idea about solar radiation to the model. From the results, it was decided to use maximum temperature, minimum temperature and extra-terrestrial radiation (Ra) values for modeling ETo in both regions.

Many researchers (Sudheer et al. 2003, Nayak et al. 2013) have used statistical properties like autocorrelation of the data to identify unique input vector that can best represent the process to be modeled. In this study, a high degree of autocorrelation was found between the ETo values of every station considered. The autocorrelation coefficient (ACF) for one week lag at both Jodhpur and Pali weather station was found to be 0.91. Similarly, for Hyderabad station the ACF was 0.80 and at Kurnool station the ACF observed was 0.91. The figure 3.8 presents a variation in the ACF for different lags at the Jodhpur station.

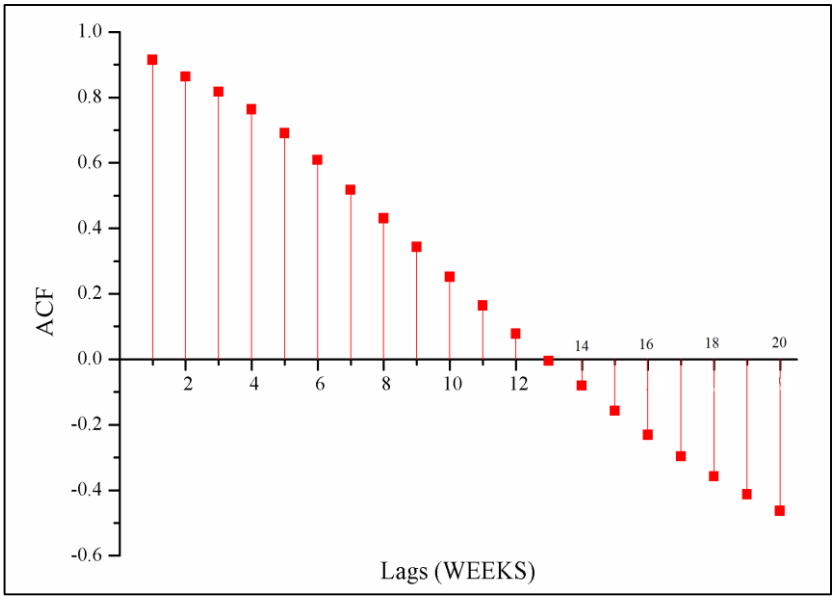

Figure 3.8 ACF for Jodhpur weather station

From the analysis of ACF at all the four weather stations, it was decided to use antecedent ETo values along with maximum and minimum temperature for modeling the process of ETo. In arid region one and two week antecedent values were used as inputs whereas, for semiarid region one and two day antecedent values were used as inputs. These inputs may help in improving the efficiency of only temperature based models.

In developing countries like India, the network of weather stations capable of measuring all the climatic variables necessary to estimate ETo by FAO-56PM equation is sparse. However, small weather stations capable of measuring only few parameters like air temperature are ample in number. This makes it necessary to develop a proficient ETo estimation system which can derive benefit from such set-up. As mentioned earlier a high degree of correlation was observed between the ETo values of stations in a particular climatic region (0.86 between Jodhpur and Pali, and 0.73 between Hyderabad and Kurnool). Also, using nearby weather station (within the same climatic region) data is most important because in some circumstances the weather data of one station may be missing (Shiri et al. 2014b). A model using locally available climatic data together with ETo values from a place situated in the same climatic region (extrinsic data) may help in improving the efficiency of ET estimation. Such a model may perform better as it can use data from weather stations capable of estimating ETo using FAO-56PM equation to model ETo of a place where only few climatic parameters can be recorded. In this study, an attempt was made to evaluate the effectiveness of using temperature data from a particular place in conjunction with extrinsic ETo values for modeling the process of ETo.

Table 3.5 presents the input combinations used for estimating ETo at all the four stations considered. In table 3.5, ETo represents the weekly evapotranspiration (calculated by FAO-56PM) value for Jodhpur and Pali weather station while, in Hyderabad and Pali weather station ETo represents daily values. ETo-1 and ETo-2 represent lagged ETo values (lag in weeks for arid region, whereas lag in days for semi-arid region). WT represents use of wavelet-decomposed inputs (using db2, db3, db4, and db5 at level 1, 2 and 3).

Table 3.5 Input combinations used in the study

Input combinations	Inputs	Models
Combination 1	T_{max}, T_{min} and R_a	Hargreaves, ANN1, ANFIS1 and LS-SVM1
Combination 2	T_{max}, T_{min}, R_a and ETo-1	ANN2, ANFIS2 and LS-SVM2
Combination 3	T_{max}, T_{min}, R_a, ETo-1 and ETo-2	ANN3, ANFIS3 and LS-SVM3
Combination 4	T_{max}, T_{min}, R_a and extrinsic ETo	ANN4, ANFIS4 and LS-SVM4
Combination 5	T_{max}, T_{min}, R_a, extrinsic ETo and extrinsic ETo-1	ANN5, ANFIS5 and LS-SVM5
Combination 6	T_{max}(WT), T_{min}(WT), R_a	W-ANN1, W-ANFIS1, and W-LSSVM1
Combination 7	T_{max} (WT), T_{min},(WT), ETo-1(WT), R_a	W-ANN2, W-ANFIS2, W-LSSVM2
Combination 8	T_{max} (WT), T_{min}, (WT),ETo-1(WT), ETo-2(WT), R_a	W-ANN3, W-ANFIS3, W-LSSVM3
Combination 9	T_{max}(WT), T_{min}(WT), R_a and extrinsic ETo(WT)	W-ANN4, W-ANFIS4 and W-LSSVM4
Combination 10	T_{max}(WT), T_{min}(WT), R_a, extrinsic ETo(WT) and extrinsic ETo-1(WT)	W-ANN5, W-ANFIS5 and W-LSSVM5

In this study, an attempt is made to evaluate the performance of different AI models for estimating ET in arid and semi-arid regions. The performance of ANN, ANFIS and LS-SVM were compared to the hybrid W-ANN, W-ANFIS and W-LSSVM models for studying the effectiveness of using wavelet transform as preprocessing technique. The study is carried out separately in arid (Jodhpur and Pali weather station) and semi-arid (Hyderabad and Kurnool weather station) regions. Flow chart for the process involved in the developing the models is presented in

figure 3.9. The results obtained from various models are discussed in subsequent chapters.

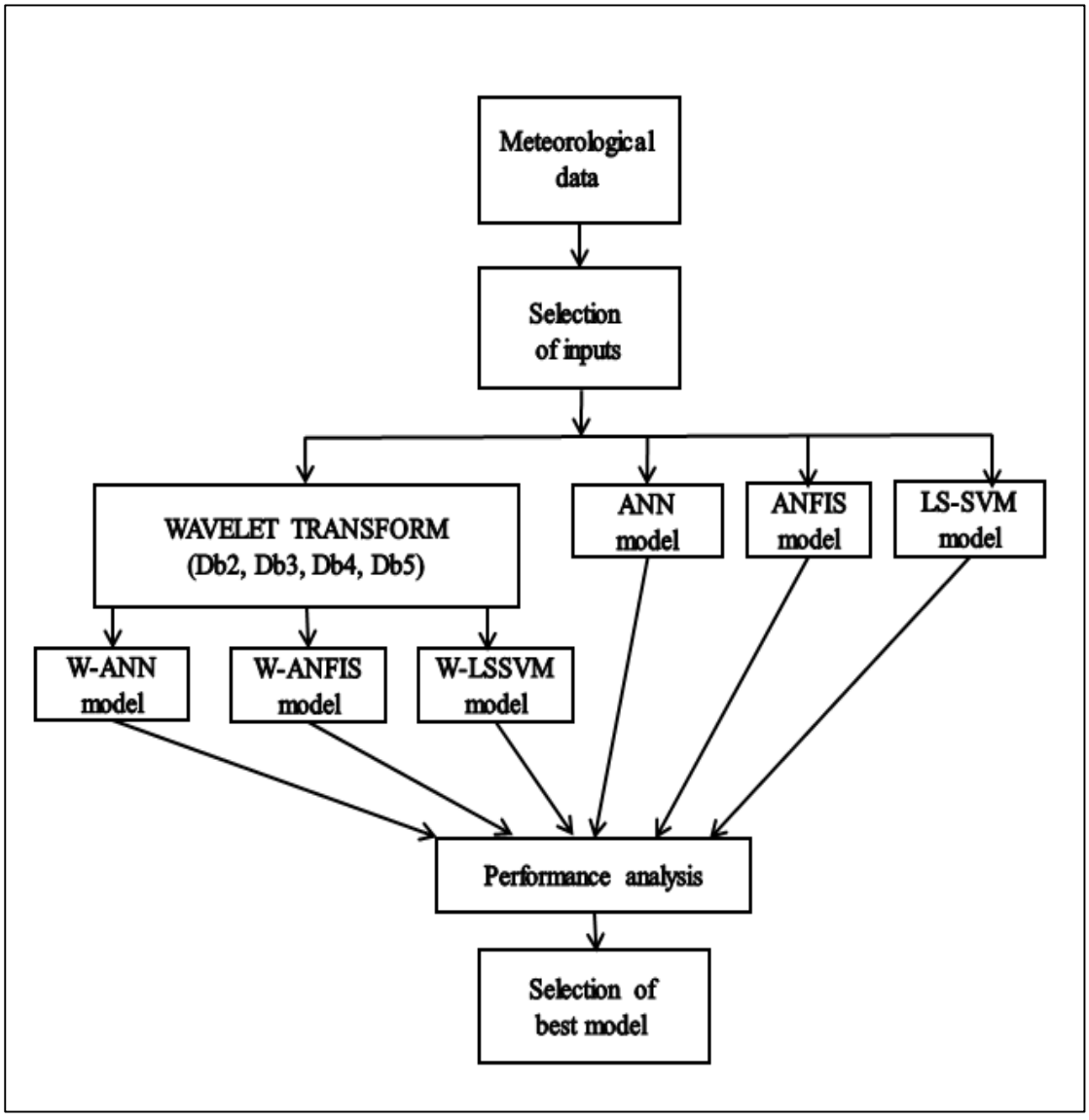

Figure 3.9 Flow chart of the methodology used in the study

3.8 MODEL PERFORMANCE CRITERIA

In this study root mean square error (RMSE) was used to evaluate the performance of the models. RMSE is frequently used to measure the difference between actual values and values predicted by the model.

$$RMSE = \sqrt{\frac{1}{N}\sum_{i=1}^{N}(X_i - Y_i)^2} \qquad (3.39)$$

where X = observed/actual values, Y = computed values and N = total number of data points. The lowest RMSE results in the best model.

In order to test the robustness of the developed model it is also necessary to test the model using some other performance evaluation indicators like Nash–Sutcliffe model efficiency coefficient (NSE) and threshold statistics (TS). The Nash–Sutcliffe coefficient was used to access efficiency of the models. NSE for a model can range from -1 to 1. An efficiency of 1 (NSE = 1) corresponds to a perfect match between estimate and observations.

$$NSE = 1 - \frac{\sum_{i=1}^{N}(X_i - Y_i)^2}{\sum_{i=1}^{N}(X_i - \bar{X})^2} \quad (3.40)$$

where $\bar{X}$ is the mean of actual data.

RMSE show the average of error in model and dosen't give any information about the error distribution. So to test the robustness of the output result, it is important to test the model using some other performance evaluation criterion such as threshold statistics (TS). The TS not only gives the performance index in terms of predicting ETo but also the distribution of errors. The TS for a level of x% is a measure of the consistency in estimating errors from a particular model. The TS is represented as TSx and expressed as a percentage. The threshold statistic for a level of absolute relative error (ARE) of x% (represented as TSx and expressed as a percent) is computed as follows:

$$TS_x = \frac{n_x}{N} \times 100 \quad (3.41)$$

where n_x = number of data points whose absolute relative error value is less than x%. In the present study, TS for absolute relative error of 5, 10 and 15 percent (TS5, TS10 and TS15) were used to measure the effectiveness of the models regarding their ability to accurately predict data from the calibrated model.

Scatter plots were also used to evaluate the accuracies of the models, while boxplots were used to analyze the spread of the data points estimated by the models.

CHAPTER 4

RESULTS AND DISCUSSION

In this part of the study, performance of the proposed models for estimating daily and weekly ETo at arid and semi-arid regions of India are analyzed and discussed. An attempt is made to identify efficient models for estimating ETo using different input combinations. The results for arid region are discussed first, followed by semi-arid region.

4.1 RESULTS FOR JODHPUR STATION (ARID REGION)

4.1.1 ANN results for Jodhpur station

The results for ANN models at Jodhpur weather station are presented in table 4.1. Table shows the optimum ANN structure, training and testing RMSE and testing NSE values.

Table 4.1 Results of ANN models at Jodhpur weather station.

Model	Optimum ANN structure	Training RMSE (mm/d)	Testing	
			RMSE (mm/d)	NSE
ANN1	3-5-1	0.80	0.76	0.85
ANN2	4-7-1	0.63	0.61	0.90
ANN3	5-6-1	0.63	0.60	0.91
ANN4	4-5-1	0.56	0.53	0.93
ANN5	5-8-1	0.53	0.50	0.94

The models presented in table 4.1 can be divided into three major groups, namely; the temperature based models (ANN1), the intrinsic data based models (ANN2 and ANN3) and the models using extrinsic data (ANN4 and ANN5). Out of all the ANN models tested for Jodhpur station the ANN1 model using Tmax, Tmin and Ra as inputs has yielded poor performance. The results show that the temperature data along with antecedent ETo values of the same station (intrinsic data) was successfully used for estimating ETo. On comparing the performance of ANN2 and ANN3 model, it is found that, despite having good autocorrelation, adding more inputs to the model does

not guarantee good performance. ANN2 and ANN3 models showed almost similar performance in terms of RMSE and NSE statistics. A similar trend was found in the results of models using ETo data from another station in the same climatic region (extrinsic inputs). Among these models, ANN4 model yielded an RMSE of 0.56 mm/day and the ANN5 model yielded an RMSE of 0.50 mm/day. Further, it was observed that the performance of models (ANN4 and ANN5) using extrinsic ETo data (ETo values from Pali station in this case) was better than the models using intrinsic antecedent ETo values. This may be because the dataset of both the weather stations exhibit similar statistical characteristics.

A time series plot for the proposed models in testing phase (year 2005) is presented in figure 4.1 below. The plot represents the time series plot for the best models (ANN1, ANN3 and ANN5) in the earlier mentioned three major input categories.

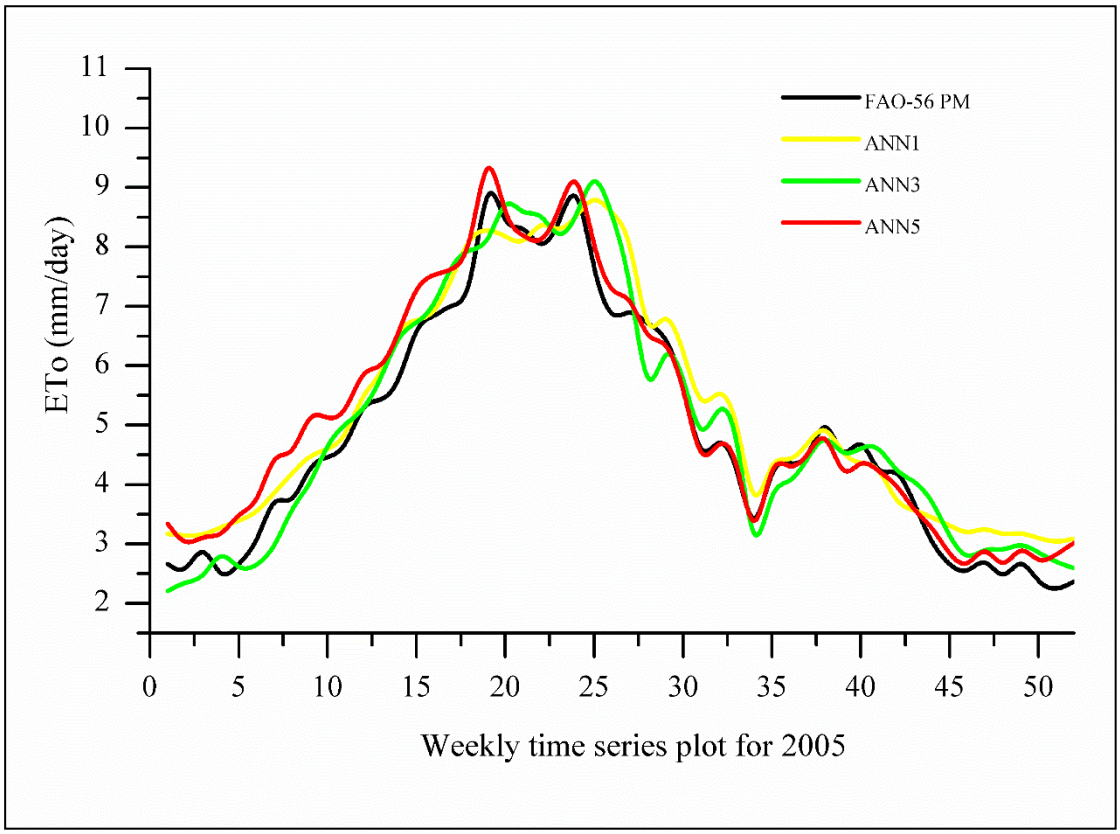

Figure 4.1 Time series plot of ANN models for testing period at Jodhpur station

The figure showed that ANN5 model overestimated the ETo values up to the twentieth week. It was also observed that the performance of this model was good

during the monsoon and post-monsoon period. On the other hand, performance of temperature based ANN1 model was not good during these periods. This may be because the components like humidity and wind speed significantly influence the process of ETo during these periods. The ANN1 and ANN3 models overestimated the smaller ETo values and underestimated the larger ETo values.

It is clear from table 4.1 that ANN5 is the best ANN model for estimating ETo in terms of RMSE and NSE statistics. This model used five inputs (refer table 3.5); eight nodes in the hidden layer and ETo calculated using FAO-56PM as the output. As mentioned in the methodology, a trial and error method is used for determining the optimum number of nodes in the hidden layer. The figure 4.2 below presents the variation in testing RMSE of ANN5 model on using different number of nodes in the hidden layers.

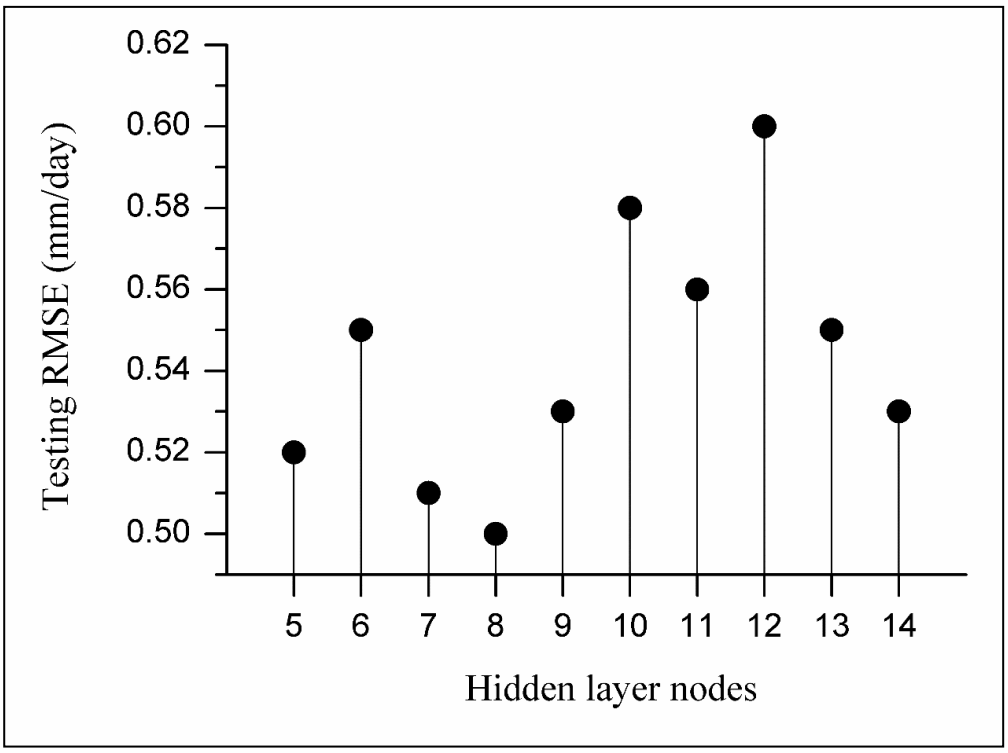

Figure 4.2 Variation in Testing RMSE of ANN5 model

The figure above does not depict a specific trend in model performance with the change in number of nodes in hidden layers. Similar behavior was observed in all the ANN models tested in this study. This result highlights the suitability of using trial and error method for finding the optimum number of nodes in the hidden layer.

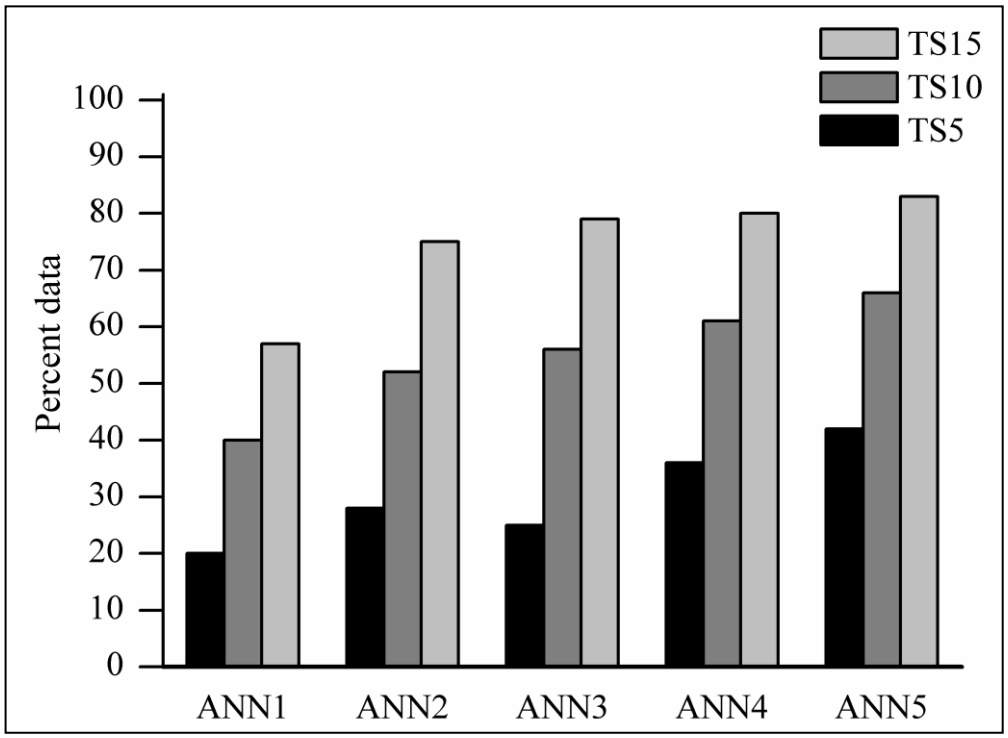

Figure 4.3 Threshold statistics for ANN models at Jodhpur weather station

Threshold statistics (TS) is an important parameter in evaluating the model performance. The bar diagram presented in figure 4.3 presents the TS statistics for the ANN models. Similar to the RMSE and NSE results presented in table 4.1, the TS statistics also reveal the superiority of ANN5 model. The ANN5 model performed slightly better than all the other ANN models tested for Jodhpur station. The performance of ANN1 model is inferior to all the other models tested. The TS15 values of ANN1 model observed was around sixty whereas, all the other models yielded TS15 value of more than seventy. The result shows that for Jodhpur weather station, the temperature based models displayed inferior performance, but use of antecedent ETo values with temperature data yielded good results.

The scatter plots and box plot for the ANN models presented in figure 4.4 makes it clear that the temperature based ANN1 model is not as good as other models in estimating ETo. ANN1 model overestimated the smaller ETo values and underestimated the larger ETo values.

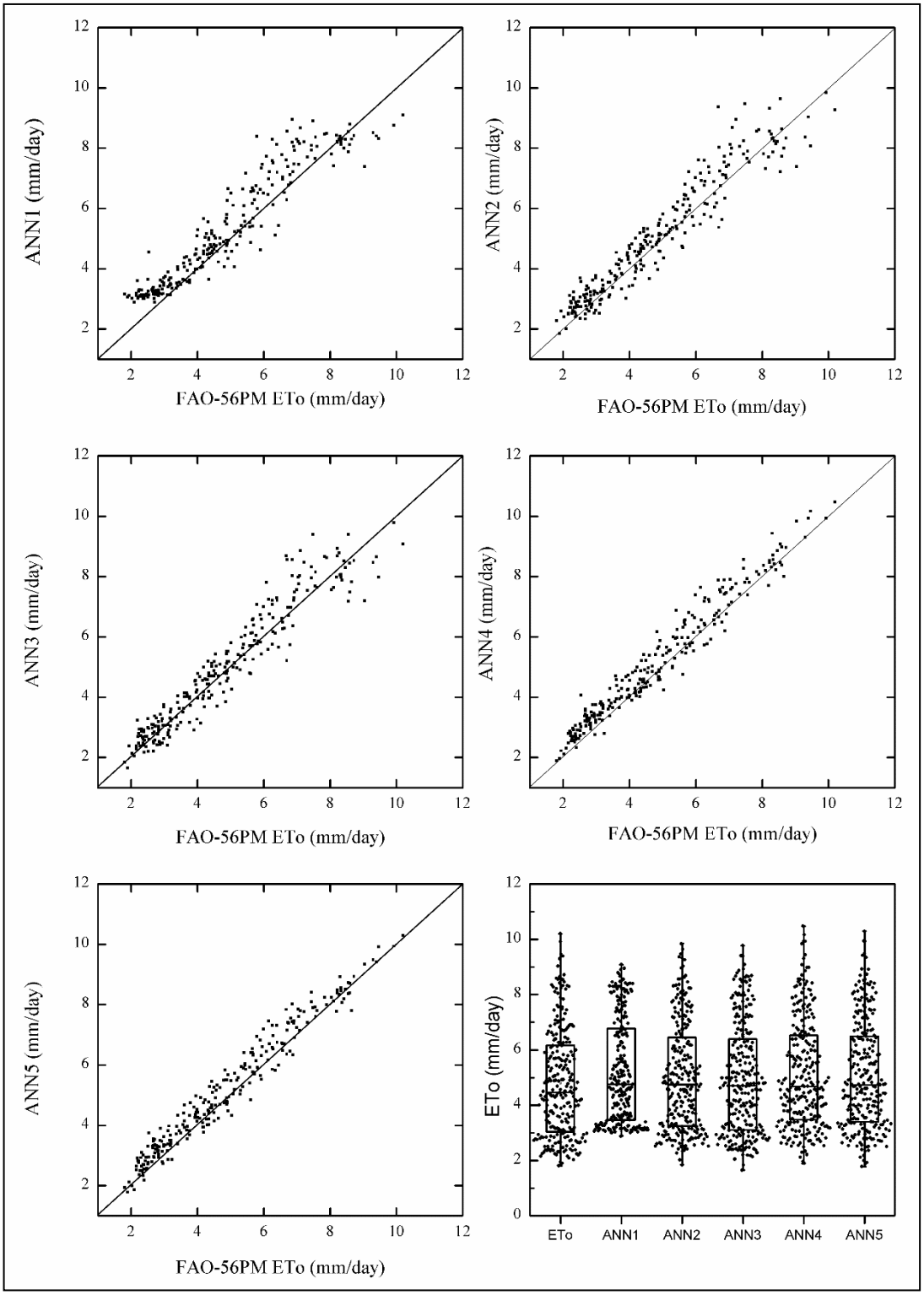

Figure 4.4 Scatter plots and box plot of ANN models for Jodhpur weather station.

The ANN2 and ANN3 model displayed similar performance. These models are good at estimating lower and average ETo values, but displayed a poor performance while estimating larger ETo values. The larger ETo values are both overestimated and

underestimated by these models and the data points are sparsely located from the 45° line. On comparing the box plots, it was observed that ANN3 model performed better than other models at estimating lower ETo values. The scatter plot and box plot results confirm that ANN4 and ANN5 are the best ANN models in estimating weekly ETo at Jodhpur station. The scatter plot shows that these models slightly overestimated the ETo models. The box plot for ANN5 model indicates overestimation of larger ETo values. Good performance of this model may be due to the use of ETo values from Pali weather station (extrinsic inputs).

4.1.2 W-ANN results for Jodhpur weather station

Table 4.2 presents the results of W-ANN models for Jodhpur station. Hybrid W-ANN models were developed by decomposing the input data using wavelet transform and then presenting it to ANN models as input. As discussed in the methodology, different mother wavelets were used to decompose the input variables. Table 4.2 presents the results for best performing W-ANN model with the mother wavelet used and the level of decomposition (e.g. Db3 L2 represents Db3 mother wavelet at second level of decomposition).

Table 4.2 Results of W-ANN models at Jodhpur weather station

Model	Mother wavelet	Optimum ANN structure	Training RMSE (mm/d)	Testing	
				RMSE (mm/d)	NSE
W-ANN1	Db3 L2	7-10-1	0.65	0.62	0.90
W-ANN2	Db3 L2	10-13-1	0.42	0.39	0.96
W-ANN3	Db3 L2	13-16-1	0.45	0.43	0.95
W-ANN4	Db5 L3	13-15-1	0.45	0.42	0.95
W-ANN5	Db3 L2	13-17-1	0.44	0.45	0.95

Results presented in table 4.2 revels that hybrid W-ANN models perform better than the conventional ANN models. A significant enhancement in the performance of ANN model is observed when the input variables are pre-processed by wavelet transform. The table makes it clear that the W-ANN2 model using Db3 mother wavelet with second level of decomposition is the best W-ANN model for estimating

weekly ETo at Jodhpur weather station. The architecture of W-ANN2 model used 10 input nodes and 13 nodes in the hidden layer.

On comparing the performance of ANN1 and W-ANN1 models at Jodhpur station, it is observed that the W-ANN1 model yielded an RMSE of 0.65 mm/day, which is about 19% lesser than the ANN1 model. Similar enhancement is also observed in other ANN models. However, the W-ANN2 and W-ANN3 have displayed better results compared to the W-ANN4 and W-ANN5 model. This result contrasts with the results obtained in table 4.1 where the ANN models using extrinsic ETo values perform better than the models using intrinsic inputs. This may be due to the use of wavelet decomposed intrinsic data used as inputs.

Table 4.3 Performance of W-ANN2 model using different mother wavelet at various decomposition levels

Mother wavelet	Optimum ANN structure	RMSE (mm/day)		Correlation coefficient (r)	
		Training	Testing	Training	Testing
Db2 L1	7-9-1	0.50	0.44	0.97	0.98
Db3 L1	7-10-1	0.49	0.40	0.97	0.98
Db4 L1	7-8-1	0.48	0.43	0.98	0.98
Db5 L1	7-10-1	0.46	0.45	0.98	0.97
Db2 L2	10-12-1	0.46	0.41	0.98	0.98
Db3 L2	10-13-1	0.42	0.39	0.98	0.98
Db4 L2	10-14-1	0.43	0.40	0.98	0.98
Db5 L2	10-12-1	0.41	0.41	0.98	0.98
Db2 L3	13-18-1	0.42	0.44	0.98	0.97
Db3 L3	13-14-1	0.44	0.39	0.98	0.98
Db4 L3	13-15-1	0.41	0.40	0.98	0.98
Db5 L3	13-13-1	0.43	0.41	0.98	0.98

The table 4.3 above represents the performance of various W-ANN2 models at different decomposition levels. The performance is examined using RMSE and correlation coefficient. Table 4.3 shows that Db3 L2 is the most efficient wavelet for

input pre-processing. The level of decomposition has shown a significant impact on the performance of models. The performance of the model enhanced with the increase in the decomposition level. It is observed that the performance of hybrid AI models at the second and third level of decomposition is better than the performance at the first level of decomposition. Further, the table shows that the testing performance of Db3 L2 wavelet is similar to the testing performance of Db3 L3. Nevertheless, Db3 L2 is considered as the best model because, the DB3 L2 model uses lesser inputs compared to the model using inputs decomposed by Db3 L3 wavelet. As the number of inputs plays an important role in model performance, generally lesser number of inputs are preferred. Further, it is observed that Db3 and Db5 wavelets display better overall performance in all the models tested.

A time series plot of the W-ANN models are presented in figure 4.5 below. Results for only the best models using temperature data (W-ANN1), intrinsic data (W-ANN2) and extrinsic data (W-ANN5) are displayed in this figure. This is because, the models using same kind of data set exhibited similar performance, making it apparent to compare only the best performing models.

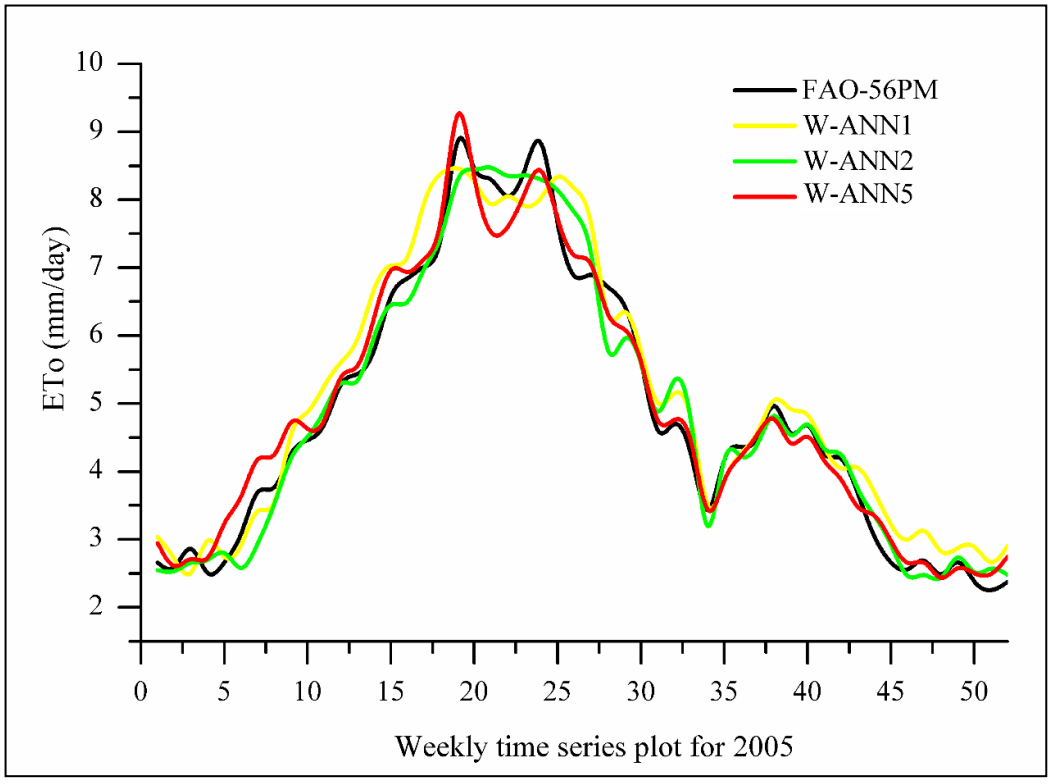

Figure 4.5 Time series plot of W-ANN models for testing period at Jodhpur station

On comparing the time series plot for ANN and W-ANN models, it is clear that wavelet preprocessing has helped in improving the performance of ANN models. It is further observed that the overall performance of W-ANN2 model is better than the other models. The W-ANN1 model overestimated the smaller values and underestimated the larger ETo values. Additionally, a similar trend was observed in the performance of W-ANN1 and W-ANN2 models. The W-ANN5 model initially overestimated the lower ETo values, but the amount of overestimation was lower when compared to the ANN5 model. On comparing the performance of W-ANN2 and W-ANN5 models, it is clear that the W-ANN2 model could not estimate the sudden spikes in the time series, whereas the W-ANN5 modeled the spikes but underestimated the ETo values.

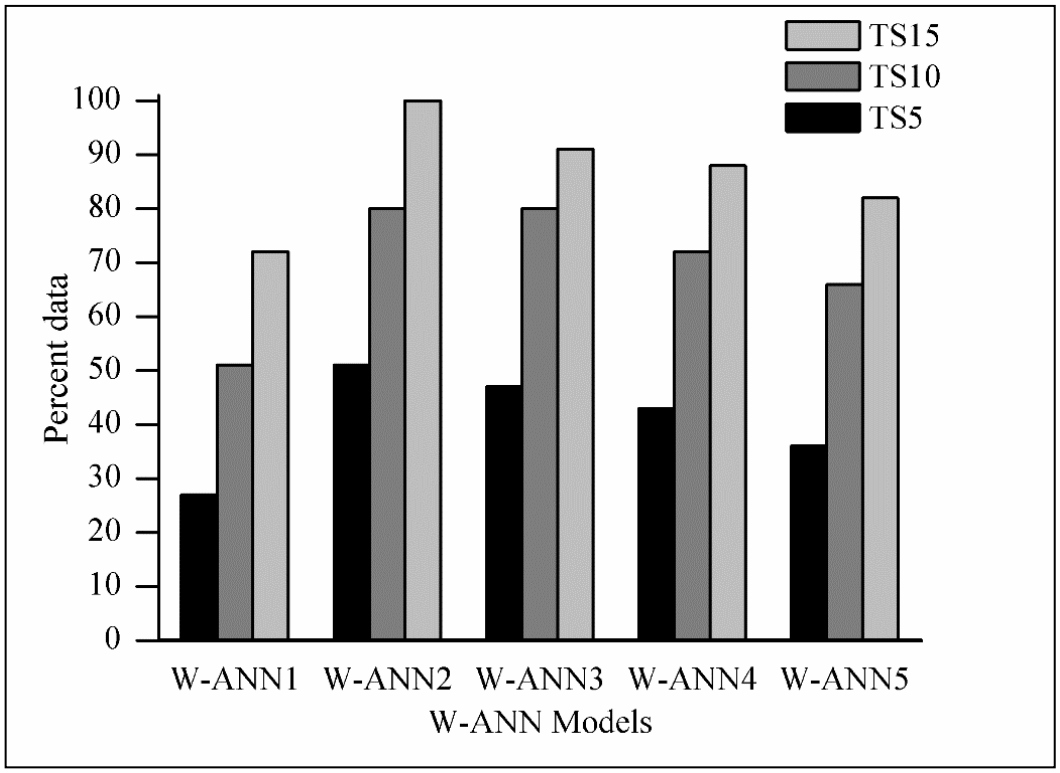

Figure 4.6 Threshold statistics for W-ANN models at Jodhpur weather station

The threshold statistics for the W-ANN models are presented in figure 4.6. The threshold statistics highlight the enhancement in performance of hybrid W-ANN models due to the use of wavelet preprocessed input datasets. The TS15 value of ANN2 model was about fifty, whereas the TS15 value for W-ANN2 model is hundred. This implies that all the estimated ETo values fall below 15% absolute

relative error. W-ANN models show a considerable increase in the TS5 values when compare to ANN models. Further, it is seen that increasing the number of inputs (in case of W-ANN3 and W-ANN5) deteriorated the performance of hybrid models.

The Scatter plot (Figure 4.7) reveals that the W-ANN1 model overestimated the smaller and average ETo values, whereas underestimated the larger ETo values. The W-ANN2 and W-ANN3 models accurately estimated the smaller ETo values, whereas the larger ETo values are both underestimated and overestimated. Additionally, most of the larger values are sparsely located around the 45° line. The W-ANN4 and W-ANN5 models are found to be good at estimating ETo values according to the scatter plots and box plots. The box plot for W-ANN1 represents poor performance of the model in estimating smaller as well as larger ETo values. The box plot for W-ANN5 model indicates presence of outliers. Presence of outliers may be due to the use of extrinsic inputs.

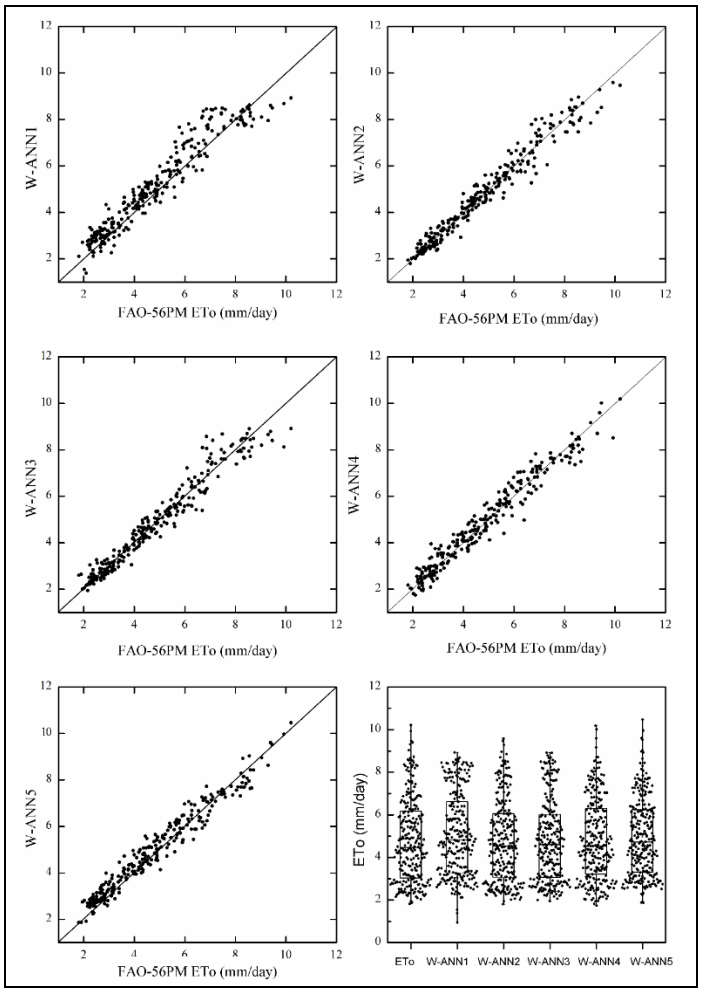

Figure 4.7 Scatter plots and box plot of W-ANN models for Jodhpur weather station.

4.1.3 ANFIS results for Jodhpur station

As mentioned earlier the performance of three and five membership functions (MFs) with triangular, trapezoidal, Gaussian and Spline shapes was evaluated to determine the most efficient ANFIS model. Table 4.4 presents the results for ANFIS models at the Jodhpur weather station.

Table 4.4 Results of ANFIS models at Jodhpur weather station.

Model	Membership function	Training RMSE (mm/d)	Testing	
			RMSE (mm/d)	NSE
ANFIS1	Gaussian	0.79	0.79	0.84
ANFIS2	Gaussian	0.63	0.61	0.90
ANFIS3	Gaussian	0.62	0.60	0.90
ANFIS4	Gaussian	0.54	0.52	0.93
ANFIS5	Gaussian	0.54	0.48	0.94

It is clear from table 4.4 that the Gaussian membership function works best for all the models. Further, it is observed that, all the ANFIS models worked slightly better than the ANN models except for the ANFIS1 models where the performance of ANN1 model was found to be slightly better than the ANFIS1 model. Inferior performance of ANFIS1 model may be due to the inability of ANFIS model to formulate sufficient rules using only the temperature data. The ANFIS5 model (0.48 mm/day testing RMSE and 0.94 NSE) was found to be the best ANFIS model for estimating ETo at Jodhpur weather station. In comparison to the ANN5 model, the ANFIS5 model delivered a lower RMSE during the testing period.

The performance of the ANFIS5 model using trimf, trapmf, gaussmf, gbellmf and pimf for three and five membership function is presented in table 4.5. The results of the models are compared using RMSE statistics for the testing period. From the results it is clear that, the models using three number of membership functions (3MF) yielded better results. This may be because use of five membership functions results in more number of rules thus increasing the complexity of the model.

Table 4.5 Results of ANFIS5 models for Jodhpur station using different MFs.

Membership function	Testing RMSE (mm/day)	
	3MF	5MF
Trimf	0.75	0.66
Trapmf	0.64	0.75
Gbellmf	0.61	0.68
Gaussmf	0.48	0.57
Pimf	0.66	0.72

Table 4.5 makes it clear that Gaussian shaped membership function performed better than all the other membership functions. The Gaussian function has performed well in all the ANFIS models tested at the Jodhpur station (table 4.4). The results also suggest that increasing the number of membership functions in ANFIS models does not necessarily enhance the ANFIS model performance. This may be because more number of membership functions generate many rules, thus resulting in a complex model.

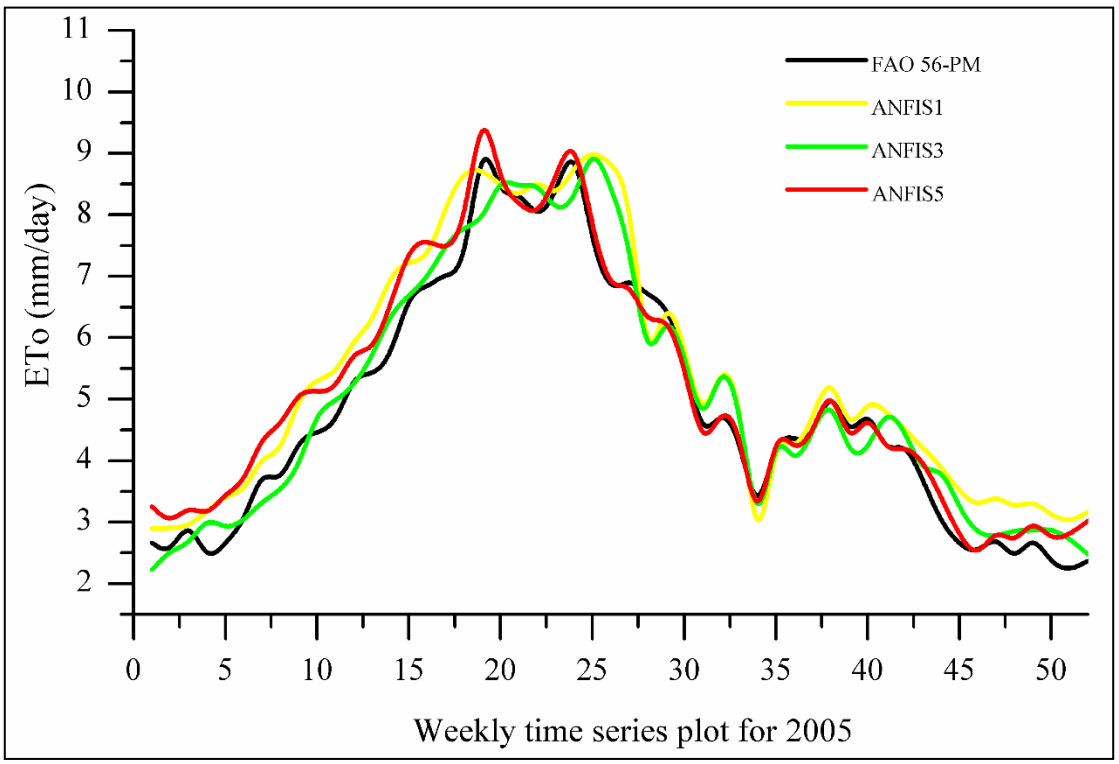

Figure 4.8 Time series plot of ANFIS models for testing period at Jodhpur station

Figure 4.8 represents the time series plot for the best ANFIS models at Jodhpur weather station. The performance of ANFIS models is similar to the ANN models. The figure shows that the ANFIS5 is the best ANFIS model to estimate ETo at Jodhpur weather station. ANFIS5 model initially overestimated the ETo values, but after the 25th week, this model almost accurately estimated all the ETo values. The ANFIS1 and ANFIS3 models also overestimated the ETo values, but the performance of ANFIS3 model is better than the ANFIS1 model. A slight shift towards left is observed in the time series of ETo estimates for the first half of the year, while for the rest of the year the shift is on the right side.

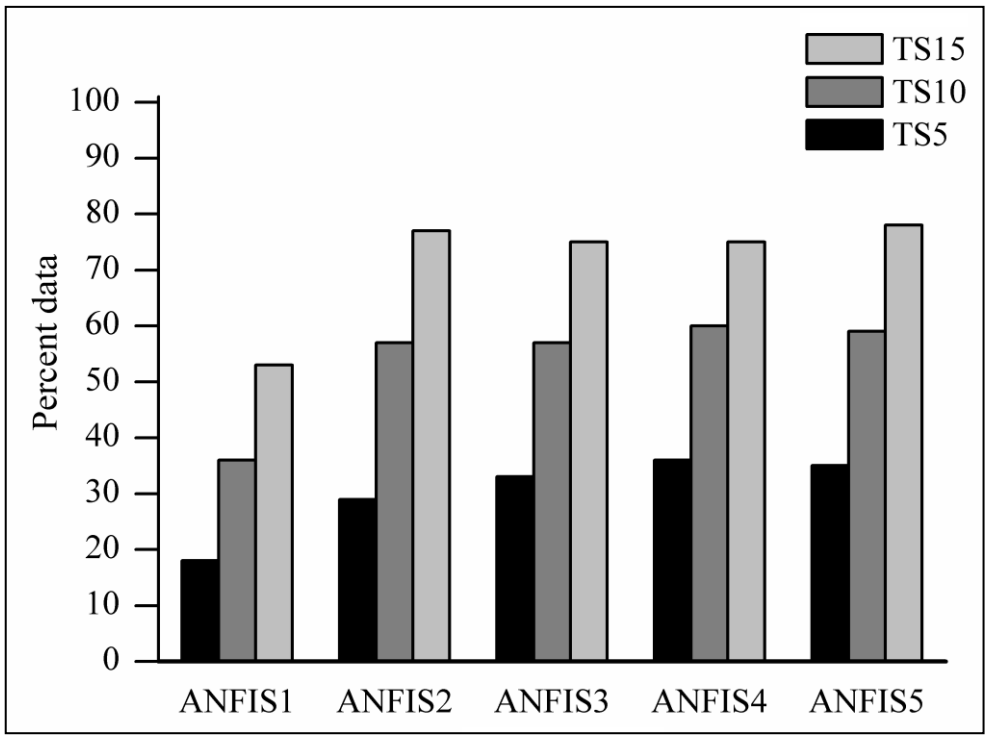

Figure 4.9 Threshold statistics for ANFIS models at Jodhpur weather station

The performance of ANFIS models in terms of threshold statistics is presented in figure 4.9. According to the threshold statistics, performance of ANN and ANFIS models tested at Jodhpur station is found to be similar. At Jodhpur station the ANN models using extrinsic data performed well however, in case of ANFIS models, both the intrinsic and extrinsic data based models displayed similar performance. Compared to the ANN5 model, the ANFIS5 model delivered a lower RMSE but the performance of ANFIS5 model was inferior to the ANN5 model when compared in terms of TS statistics.

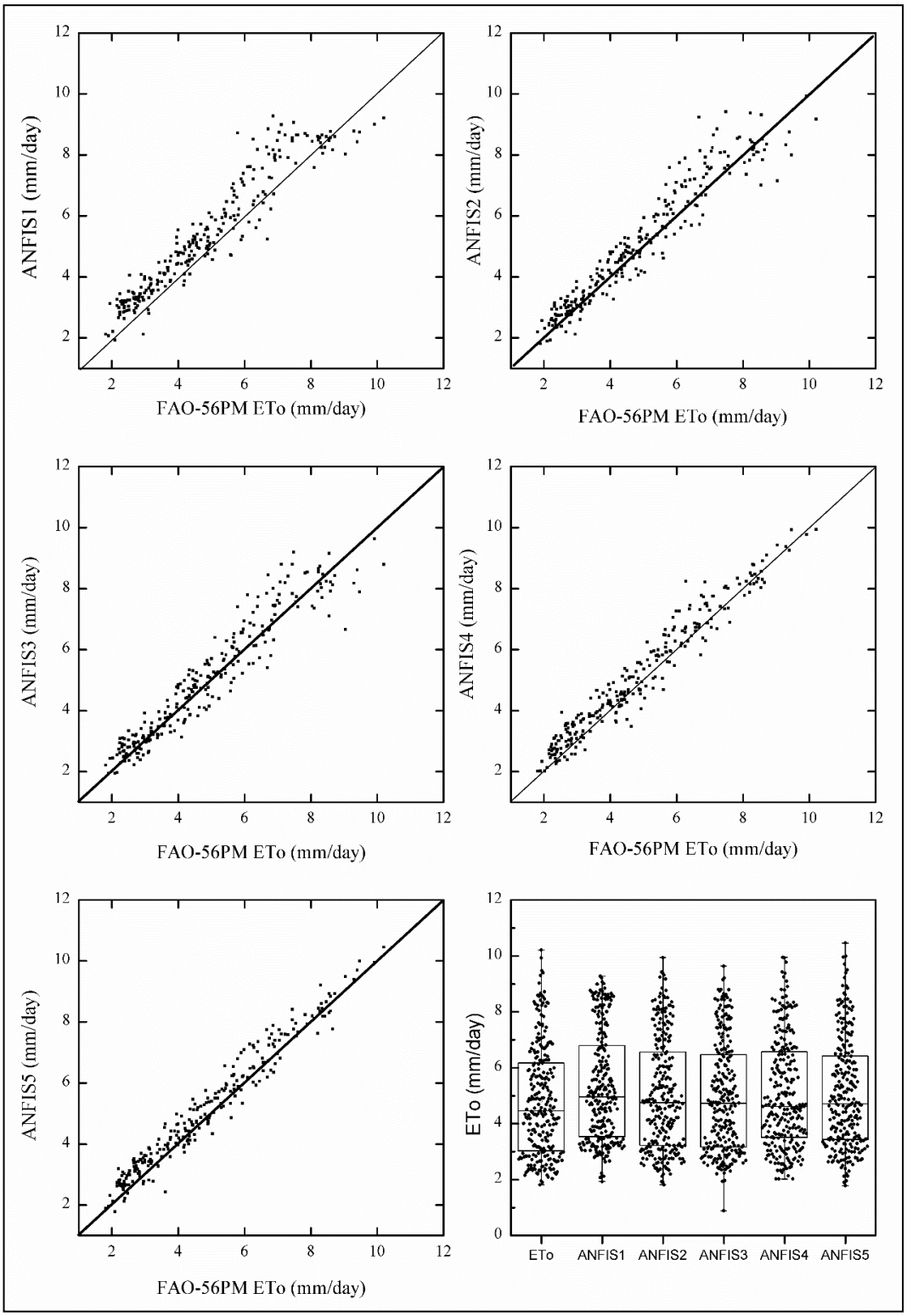

Figure 4.10 Scatter plots and box plot of ANFIS models for Jodhpur weather station.

Scatter plot and box plot for ANFIS models at Jodhpur weather station are presented in figure 4.10. The scatter plot shows that the ANFIS1 model overestimated the ETo values. The larger values are sparsely located around the 45° line. The

intrinsic data based ANFIS2 and ANFIS3 models underestimated as well as overestimated the ETo values. The results of ANFIS models are similar to the ANN models. It can be interpreted from the scatter that ANFIS4 and ANFIS5 are the most efficient ANFIS models for estimating the ETo values at Jodhpur weather station. These models overestimated the smaller ETo values, but are found to be good at estimating the greater ETo values.

4.1.4 W-ANFIS results for Jodhpur station

Use of grid partitioning was not possible while developing the W-ANFIS models. Grid partitioning generates rules by enumerating all possible combinations of membership functions using all the inputs. Use of grid partitioning even when using a moderate number of inputs may result in a large number of rules, leading to a problem referred as "curse of dimensionality". In the present study, it was decided to use subtractive clustering instead of grid partitioning for all W-ANFIS models at every weather station under consideration. The results of hybrid W-ANFIS are presented in table 4.6.

Table 4.6 Results of W-ANFIS models at Jodhpur weather station.

Model	Mother wavelet	Training RMSE (mm/d)	Testing	
			RMSE (mm/d)	NSE
W-ANFIS1	Db3 L2	0.80	0.74	0.86
W-ANFIS2	Db3 L2	0.43	0.38	0.96
W-ANFIS3	Db3 L2	0.53	0.46	0.95
W-ANFIS4	Db3 L2	0.54	0.48	0.94
W-ANFIS5	Db5 L3	0.54	0.48	0.94

The W-ANFIS2 model was found to be the best model for estimating ETo using hybrid W-ANFIS model. The W-ANFIS1 model has shown the least amount of improvement in performance (0.74 mm/day RMSE) when using wavelet preprocessed inputs. It is clear from table 4.2 and table 4.6 that using wavelet decomposed datasets, as inputs, enhanced the efficiency of both ANN and ANFIS models. However, in the case of W-ANFIS models increase in the efficiency was not appreciable when

compared to the W-ANN models. This could be because of the inability of ANFIS models to deal with the large number of inputs. It is observed that Db3 wavelet at second level of decomposition worked well for all the models except the W-ANFIS5 model. For W-ANFIS5 model Db5 wavelet at third level of decomposition has worked well. On comparing the performance of W-ANFIS4 and W-ANFIS5 model, it is observed that increasing the number of inputs did not enhance the model performance. Hence, the W-ANFIS2 model is considered as the best W-ANFIS model to estimate ETo at Jodhpur weather station.

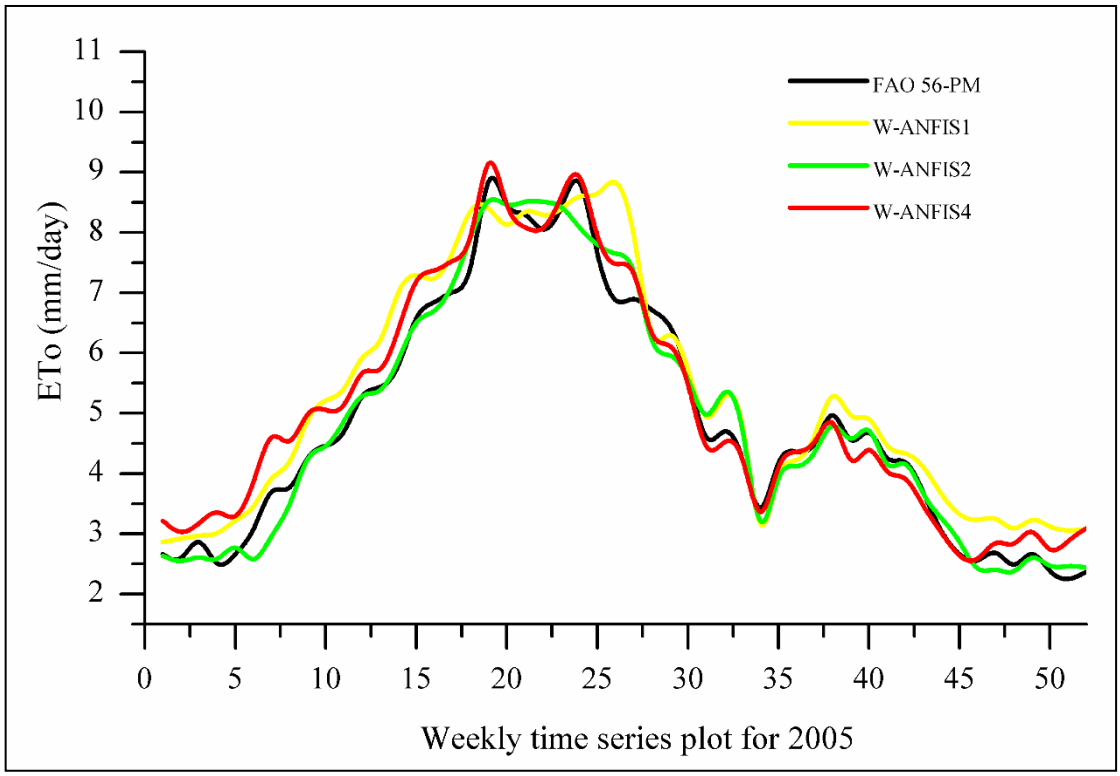

Figure 4.11 Time series plot of W-ANFIS models for testing period at Jodhpur

Figure 4.11 represents the time series plot for W-ANFIS1, W-ANFIS2 and W-ANFIS4 model. The figure makes it clear that the W-ANFIS2 model performed better than the other models. This model underestimated the peak values, but was good at estimating the smaller ETo values. W-ANFIS5 model overestimated the smaller ETo values, but was good at estimating the peak values. A significant enhancement in the performance of model using intrinsic data is observed. However, no significant improvement in the performance models using extrinsic inputs is observed.

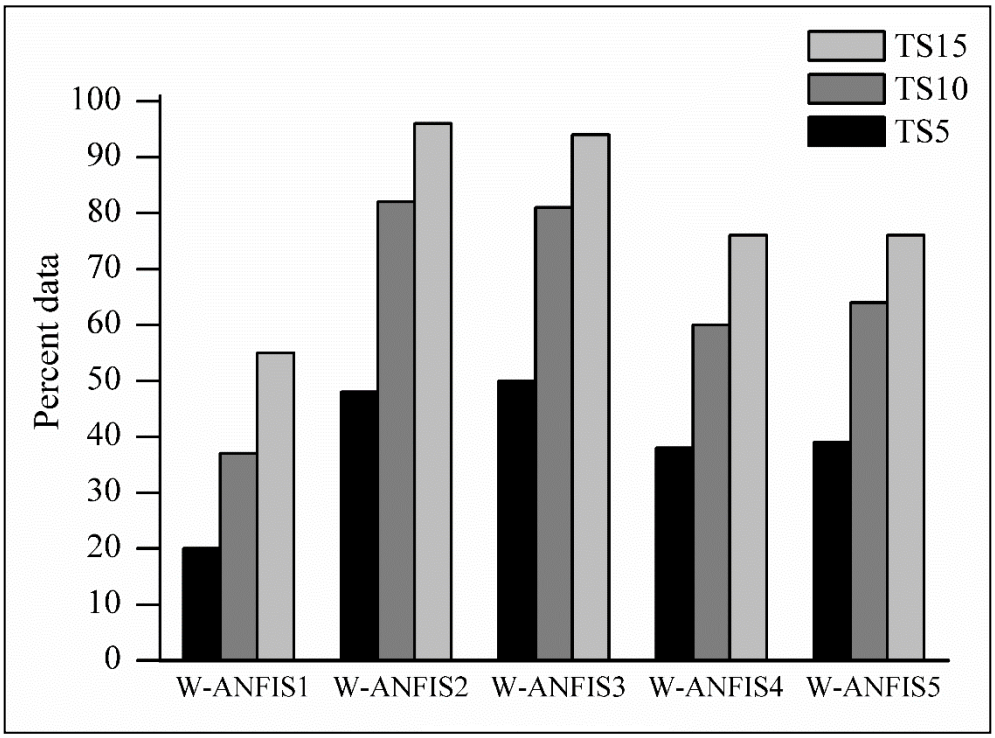

Figure 4.12 Threshold statistics for W-ANFIS models at Jodhpur weather station

Threshold statistics of the W-ANFIS models is presented in figure 4.12. The TS values for the models reveals that the performance of W-ANFIS2 and W-ANFIS3 models are similar. Additionally, it is observed that there is a significant increase in the TS5 values of W-ANFIS models when compared the ANFIS models. Further, a similarity in the performance of hybrid ANN and hybrid ANFIS models was also observed.

Scatter plots and box plots for W-ANFIS models are presented in figure 4.13. The scatter plot presents overestimation of the ETo values by the temperature based W-ANFIS1 model. Whereas, the larger ETo values are underestimated by this model. The intrinsic data based W-ANFIS2 and W-ANFIS3 models underestimated as well as overestimated the ETo values. The smaller ETo values are predicted more accurately by these two models. The W-ANFIS4 and W-ANFIS5 models overestimated the lower ETo values, but were found to be good at estimating the larger values. The box plot for the W-ANFIS models demonstrate overestimation of smaller ETo values by the W-ANFIS1 and W-ANFIS4 models. These models displayed significant underestimation of larger ETo values.

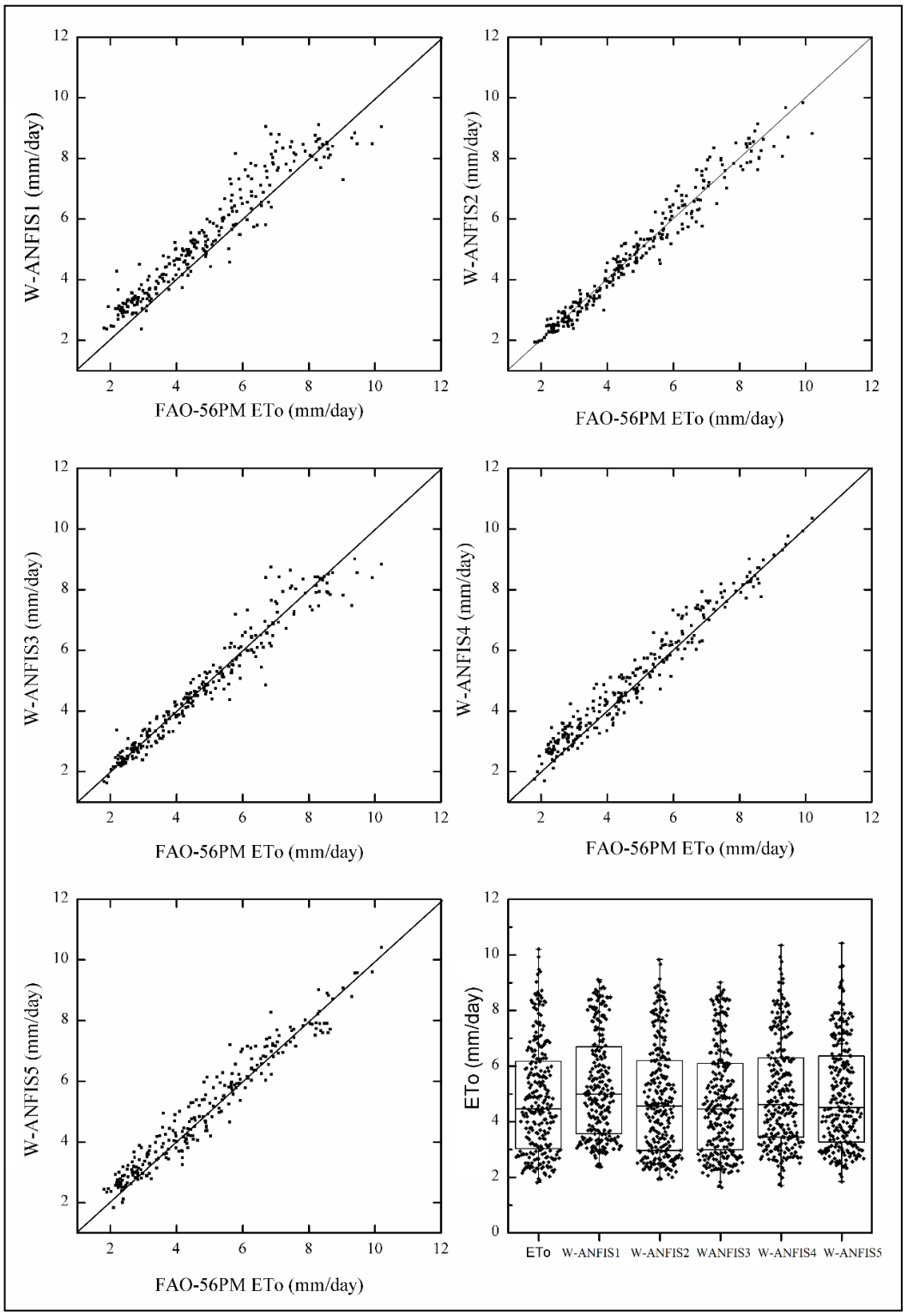

Figure 4.13 Scatter plots and box plot of W-ANFIS models for Jodhpur weather station.

4.1.5 LS-SVM results for Jodhpur station

The results for estimating weekly ETo at Jodhpur weather station using LS-SVM model are presented in table 4.7. The LS-SVM model work on the principle of structural risk minimization, which equips it with a greater generalization capacity. From the table it is clear that the performance of LS-SVM model is better than the ANN and ANFIS model. Except for the first input combination, LS-SVM has outperformed all the other ANN and ANFIS models.

Table 4.7 Results of LS-SVM models at Jodhpur weather station.

Model	Training RMSE (mm/d)	Testing	
		RMSE (mm/d)	NSE
LS-SVM1	0.79	0.77	0.85
LS-SVM2	0.60	0.59	0.91
LS-SVM3	0.54	0.55	0.92
LS-SVM4	0.48	0.48	0.94
LS-SVM5	0.48	0.46	0.94

The LS-SVM3 (0.55 mm/d RMSE) model is found to the best model for estimating ETo using intrinsic inputs. This model used temperature data along with one and two week antecedent ETo values. The LS-SVM5 (0.46 mm/d training RMSE) was found to be the best model for estimating ETo at Jodhpur weather station. The results show that use of extrinsic inputs delivered good results for estimating ETo values. A considerable difference in the RMSE values of the LS-SVM3 and LS-SVM5 model is observed, but the NSE values of the models are similar. The results confirm the fact that LS-SVM is the best model for estimating ETo. Input combination five is found to be the most efficient input combination for estimating ETo using conventional AI models (ANN, ANFIS and LS-SVM).

The time series plot of the best LS-SVM models for the testing period is presented in figure 4.14. Compared to time series plot for ANN and ANFIS models, it is observed that all the LS-SVM models performed well. The LS-SVM1 and LS-SVM3 models exhibited similar performance. These models overestimated the ETo values

for most part of the year. The LS-SVM5 model also overestimated the ETo values, but was found to be good at estimating the peaks. A slight shift (towards left for the first half of the year and towards right for the other half) in the time series of the models is observed in the time series plot. The performance of the LS-SVM5 model is considerably better than LS-SVM1 and LS-SVM3 models for twenty-fifth to thirty-fifth week. All the LS-SVM models were good at estimating the peak values when compared to the ANN and ANFIS models.

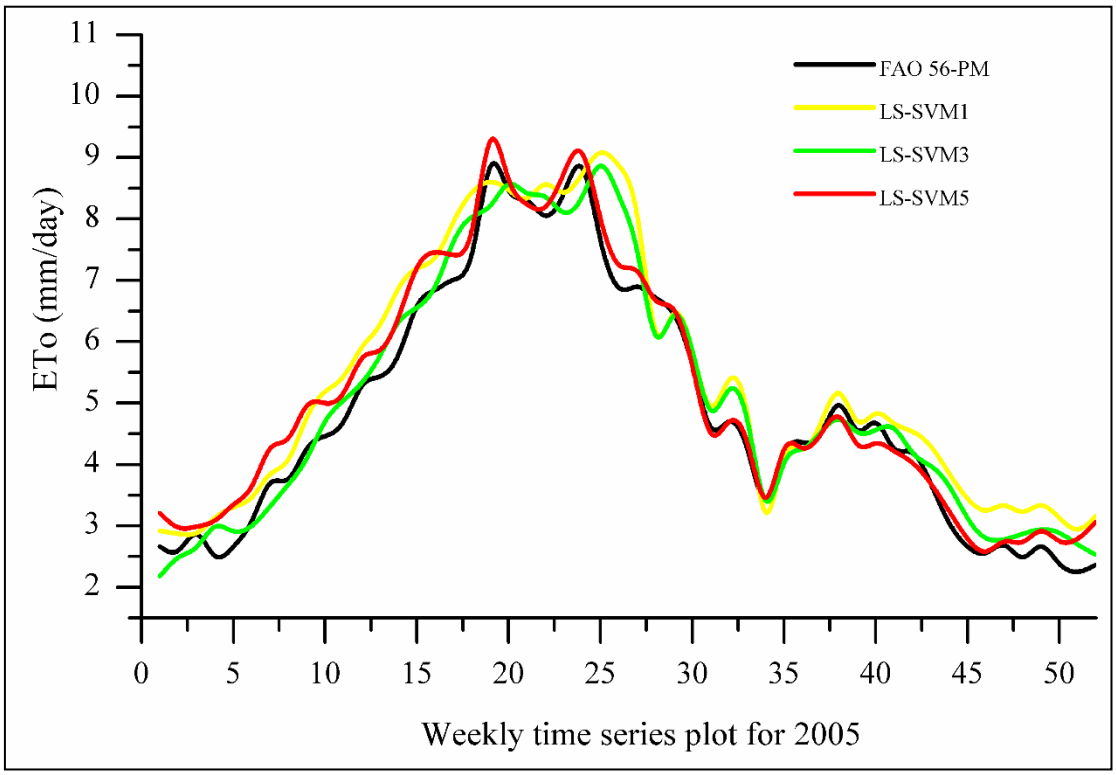

Figure 4.14 Time series plot of LS-SVM models for testing period

Threshold statistics for the LS-SVM model is presented in figure 4.15. From the RMSE results, it is clear that ANN1 model is slightly better than the ANFIS1 and LS-SVM1 model, but when compared based on NSE and TS statistics the performance of LS-SVM1 model is slightly better than the ANN1 model. The TS5 values of the LS-SVM models are more than the ANN and ANFIS models for all the combinations tested. Further, it is observed that the threshold statistics performance of the models using intrinsic as well as extrinsic inputs is almost similar.

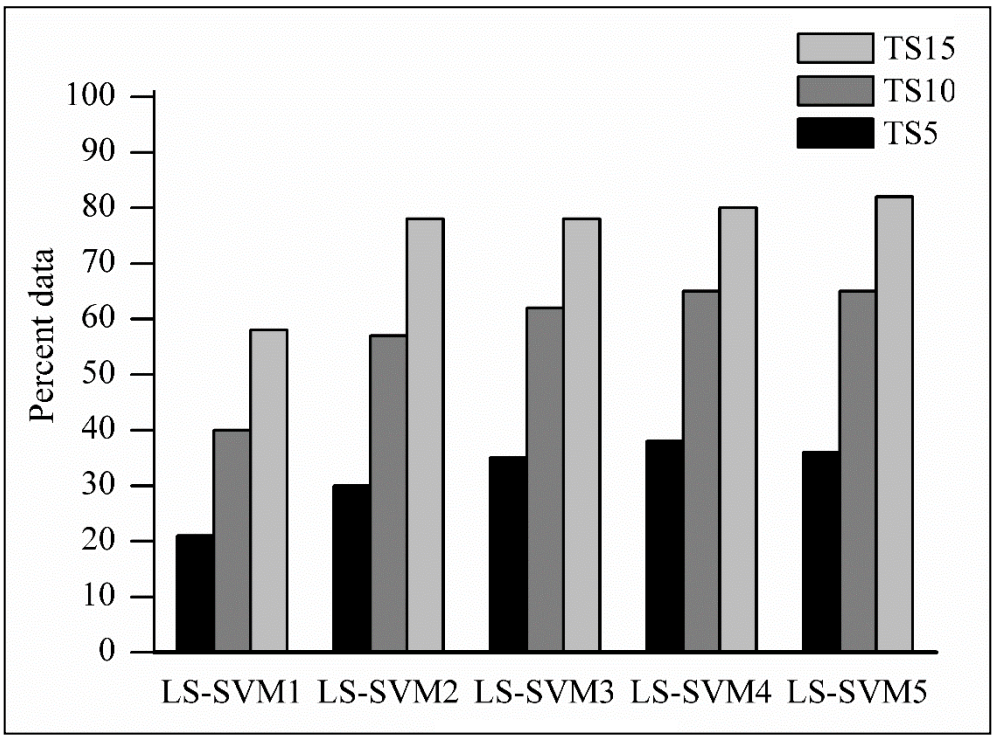

Figure 4.15 Threshold statistics for LS-SVM models at Jodhpur weather station

Figure 4.16 presents scatter plot and box plot for the LS-SVM models tested at Jodhpur station. The scatter plot highlights the superiority of the LS-SVM models. The scatter plot for the LS-SVM1 shows a better ETo estimation by the LS-SVM model compared to the ANN1 and ANFIS1 model. The LS-SVM1 model overestimated the smaller ETo values and underestimated the larger ETo values. The LS-SVM2 and LS-SVM3 model were good at estimating the smaller ETo values. The larger ETo values were both underestimated as well as overestimated by these models and the points are sparsely located around the 45° line. The LS-SVM4 and LS-SVM5 models performed alike and are found to be better than all the other models tested. A slight overestimation of all the ETo values is observed in scatter plot these models. All the other LS-SVM models presented similar spread of the data points in the box plots. Box plot for LS-SVM2 and LS-SVM3 models show overestimation of smaller ETo values and underestimation of greater ETo values.

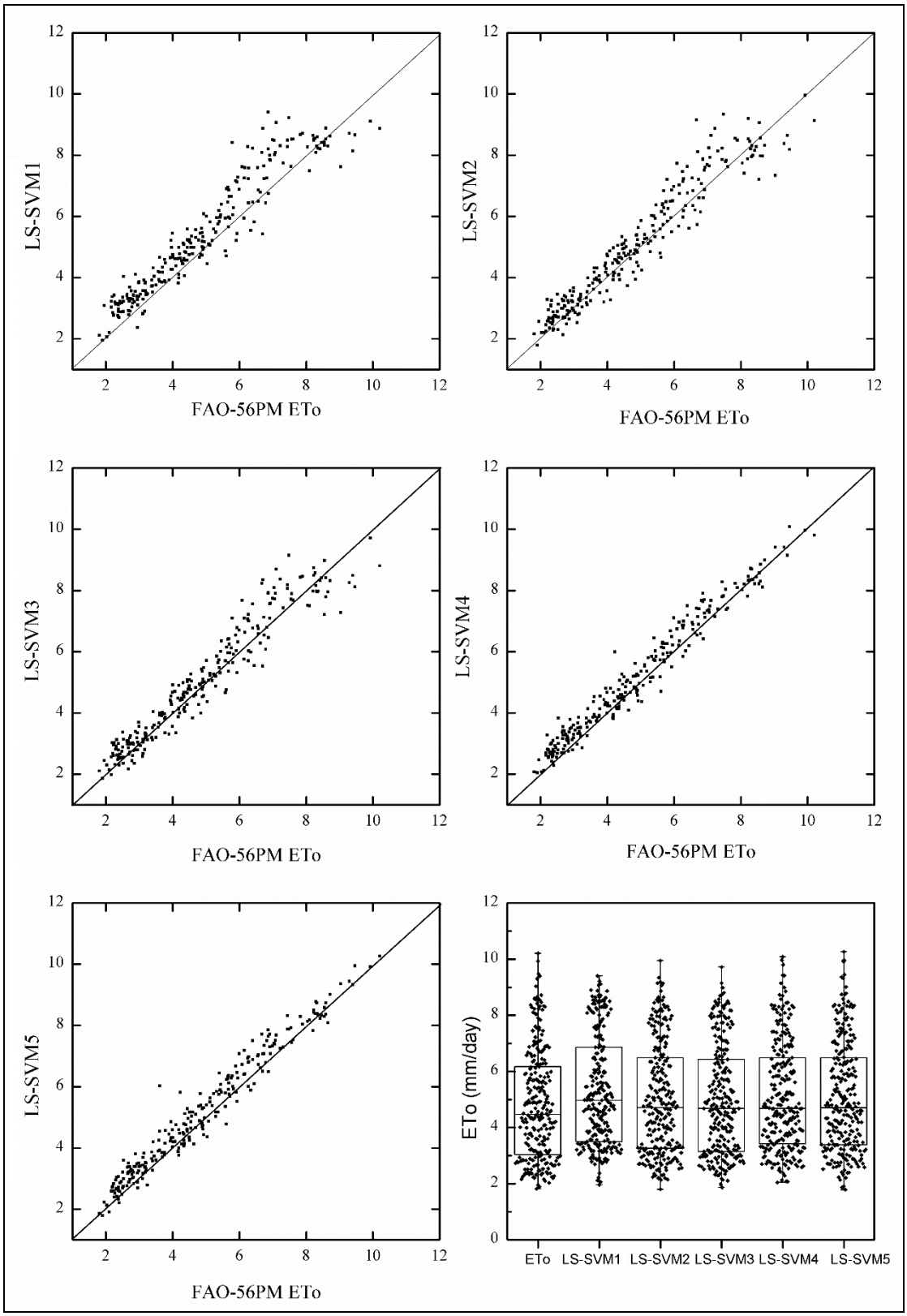

Figure 4.16 Scatter plots and box plot of LS-SVM models for Jodhpur weather station

4.1.6 W-LSSVM results for Jodhpur station

Table 4.8 presents the results of hybrid W-LSSVM model for estimating ETo at Jodhpur weather station. The results show substantial enhancement in performance of hybrid W-LSSVM models when compared to LS-SVM models.

Table 4.8 Results of W-LSSVM models at Jodhpur weather station.

Model	Mother wavelet	Training RMSE (mm/d)	Testing	
			RMSE (mm/d)	NSE
W-LSSVM1	Db3 L3	0.70	0.71	0.87
W-LSSVM2	Db3 L2	0.40	0.38	0.96
W-LSSVM3	Db3 L2	0.40	0.38	0.96
W-LSSVM4	Db5 L3	0.47	0.45	0.95
W-LSSVM5	Db5 L1	0.47	0.45	0.95

It is observed that W-ANN1 is the best model to estimate ETo using only temperature data. The W-ANN1 model performed better than the W-ANFIS1 and W-LSSVM1 model. From table 4.8 it is clear that the hybrid W-LSSVM models are the best models for estimating ETo at Jodhpur weather station. W-LSSVM3 (0.38 mm/d testing RMSE) is found to be the best model for estimating ETo at Jodhpur weather station. Performance of both W-LSSVM2 and W-LSSVM3 models is similar according to the RMSE and NSE performance statistics, but considering the TS statistics, it can be concluded that W-LSSVM3 is the best model among all the models tested at Jodhpur weather station. Similarly, the performance of W-LSSVM4 and W-LSSVM5 is alike, but considering the fact that the W-LSSVM4 model uses more number of inputs (third level of decomposition), W-LSSVM5 can be considered as the best model for estimating ETo using extrinsic data. Db3 is found to be working better with the temperature and intrinsic data based models. However, it is observed that the Db5 mother wavelet has worked better in case of extrinsic data based models. Similar results were observed in the case of W-ANN and A-ANFIS models were Db5 wavelet decomposition has worked better with W-ANN4 and W-ANFIS5 models. From the results, it is concluded that hybrid W-LSSVM models are the best

performing models for estimating weekly evapotranspiration at the Jodhpur weather station.

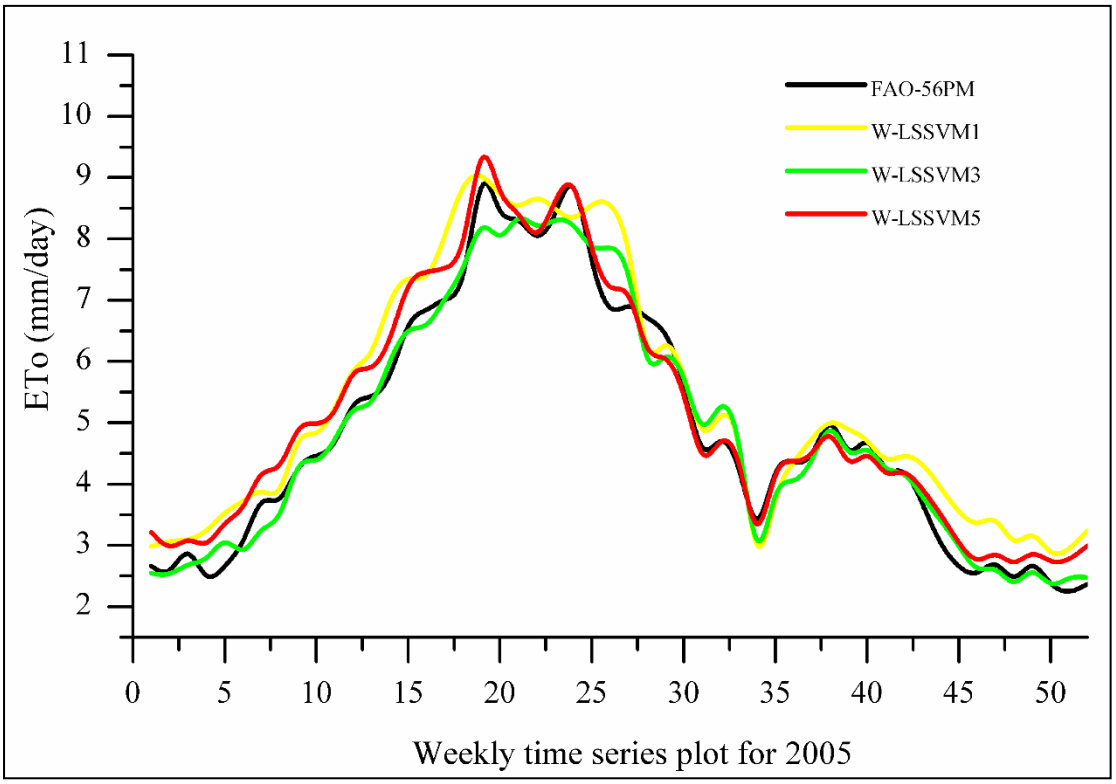

Figure 4.17 Time series plot of W-LSSVM models for testing period

Figure 4.17 presents time series plots of the W-LSSVM models for the testing period. The plot presents a considerable enhancement in the performance of W-LSSVM models when compared to the LS-SVM models. The W-LSSVM3 model has underestimated the peak ETo values, but is found to be performing well at estimating the smaller ETo values. On the other hand, the W-LSSVM5 model overestimated the smaller ETo values, but was found to be good at estimating the peak values. This result highlights the effeciency of using extrinsic inputs in estimating the peak ETo values. The temperature based W-LSSVM1 model overestimated almost all the ETo values.

The Scatterplot and box plot for the W-LSSVM models is presented in figure 4.18. The figure also shows the proficiency of hybrid W-LSSVM models in estimating the ETo values. The scatter plot for W-LSSVM1 model presents overestimation of smaller ETo values and underestimation of the peak values.

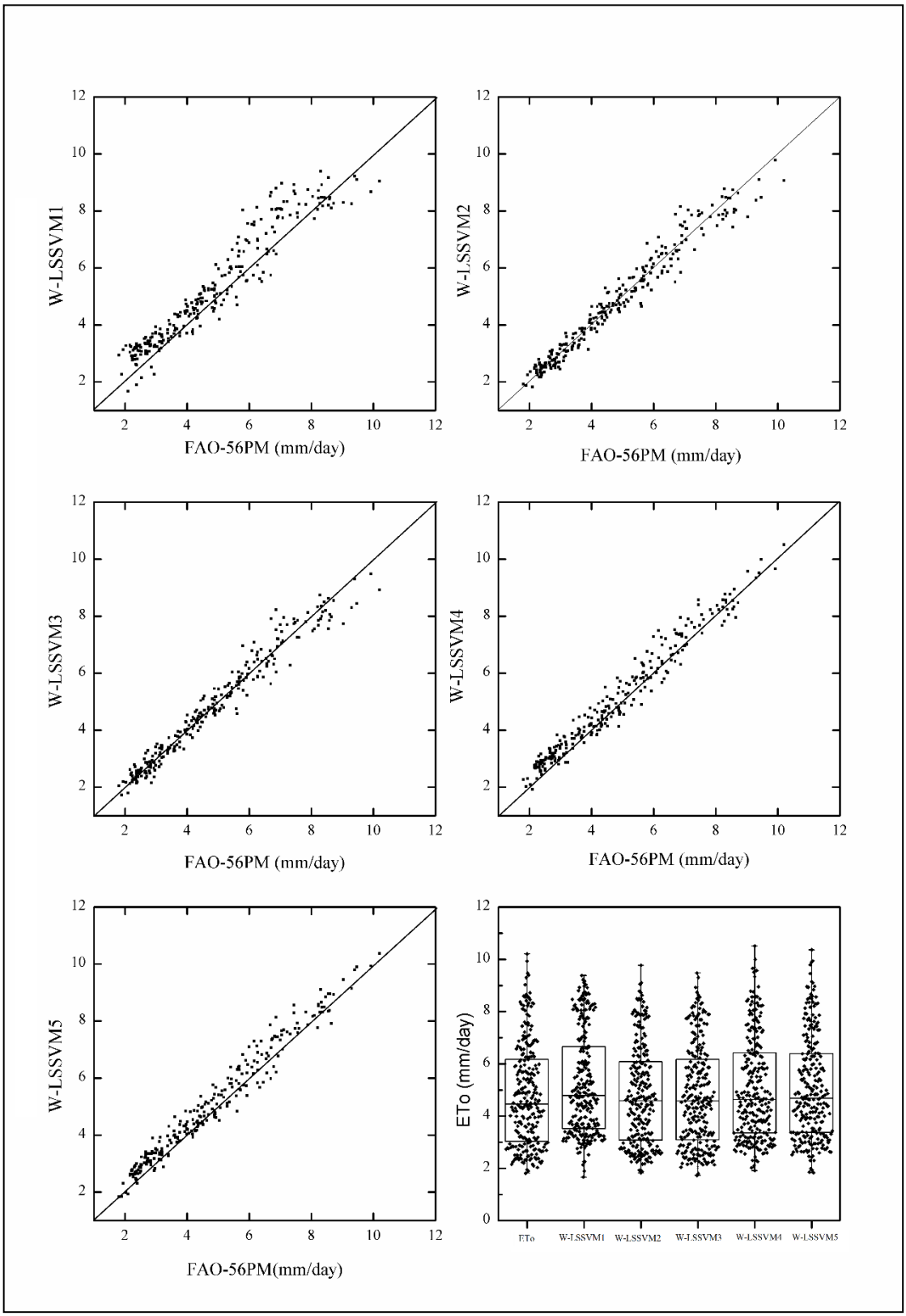

Figure 4.18 Scatter plots and box plot of W-LSSVM models for Jodhpur weather station

The W-LSSVM2 and W-LSSVM3 models are found to be performing better than the other models when compared in terms of the scatter plot. However, these models, marginally underestimate the peak values. The W-LSSVM4 and W-LSSVM5 models have overestimated the smaller ETo values, but are good at estimating the peak values when compared to the W-LSSVM2 and W-LSSVM3 models.

Figure 4.19 presents the TS values for the W-LSSVM models. It is observed that the performance of some models is similar in terms of RMSE and NSE statistics. In such cases, the threshold statistics prove to be a good option for selecting the best model.

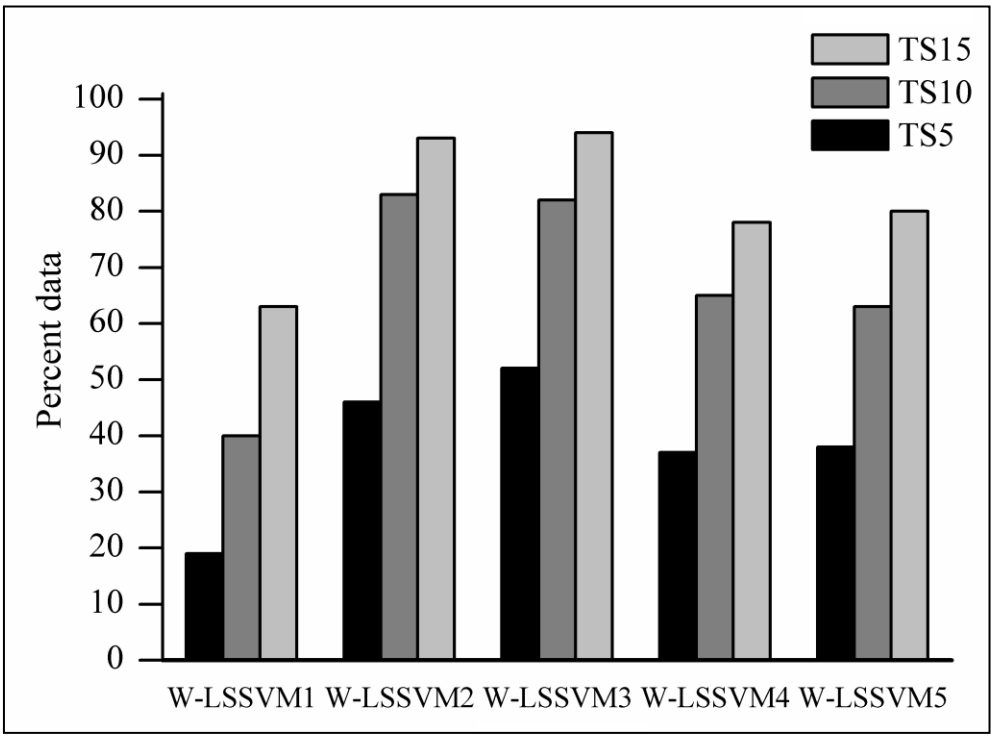

Figure 4.19 Threshold statistics for W-LSSVM models at Jodhpur weather station

The threshold statistics present the superiority of intrinsic data based models in estimating the ETo values at Jodhpur weather station. The TS statistic plot shows that the performance of W-LSSVM3 model is better than the W-LSSVM2 model. Thus, it is concluded that W-LSSVM3 is the best model for estimating the weekly ETo at Jodhpur weather station.

4.1.7 Temperature based models for Jodhpur station

Nandagiri & Kovoor (2006) compared the performance of various empirical equations over a range of different Indian climates. They found that Hargreaves equation works best for estimating evapotranspiration in arid regions of India. The Hargreaves equation is given as

$$ET_h = 0.0023\,(T_{mean}+17.8)\,(T_{max} - T_{min})^{0.5} * R_a \qquad (4.1)$$

As the input variables used by ANN1, ANFIS1 and LS-SVM1 and Hargreaves equation are same, the results of classical AI models are compared to the temperature based Hargreaves equations. At Jodhpur weather station, the Hargreaves equation yielded an RMSE of 0.90 mm/day, which is higher than all the AI models tested. This confirms the superiority of the AI model over the conventional models.

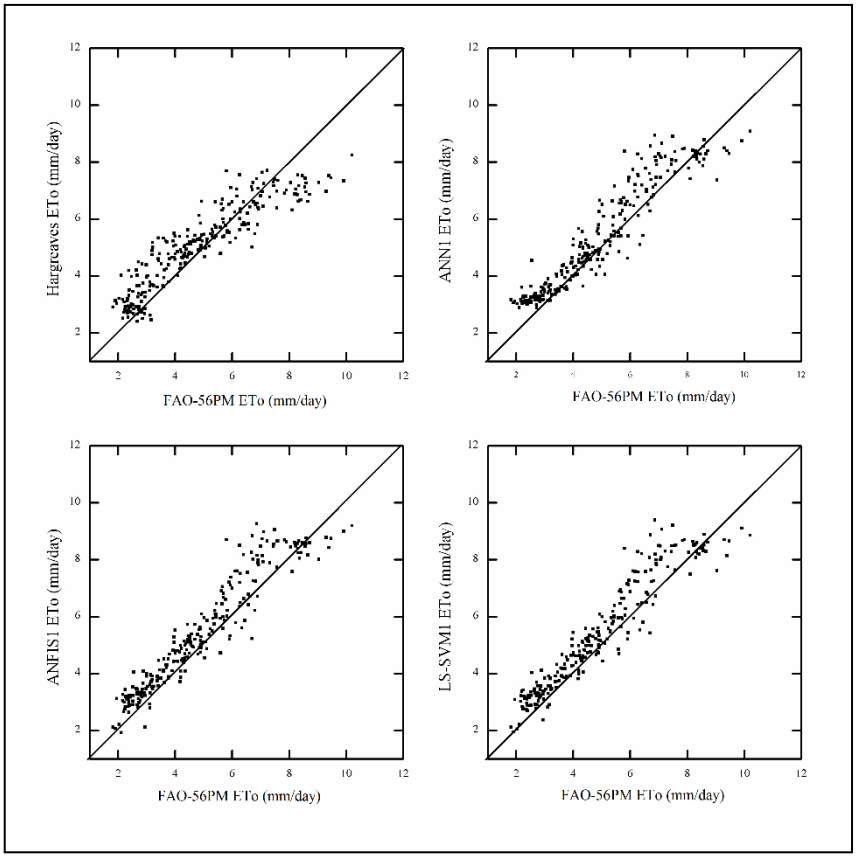

Figure 4.20 Scatter plot for temperature based models at Jodhpur station

The Scatter plots for Hargreaves model and the AI models using only temperature data for the Jodhpur station is presented in figure 4.20. On comparing these results, it

is clear that the performance of AI models is better than the conventional Hargreaves equation. It is found that the Hargreaves equation overestimates the smaller values and underestimates the larger ETo values. It is also observed in the scatter plot of Hargreaves equation that, the points are sparsely located around the 45° line. The performance of ANN1, ANFIS1, and LS-SVM1 model is more or less similar. The AI models marginally overestimated the smaller value of ETo, but the overestimation is less in case of ANN1 model. The average ETo values are both overestimated and underestimated by the AI models. The larger values of ETo are underestimated by all the AI models.

4.2 RESULTS FOR PALI STATION (ARID REGION)

4.2.1 ANN results for Pali station

As mentioned in the methodology chapter, Pali is the second weather station in arid region used for evaluating the performance of proposed models and to generalize the conclusion in arid region. The results for ANN models at the Pali weather station is presented in table 4.9. The results show that the performance of ANN models at the Pali weather station is better than the Jodhpur weather station.

Table 4.9 Results of ANN models at Pali weather station.

Model	Optimum ANN structure	Training RMSE (mm/d)	Testing				
			RMSE (mm/d)	NSE	TS5	TS10	TS15
ANN1	3-6-1	0.79	0.74	0.89	28	54	69
ANN2	4-9-1	0.71	0.62	0.92	34	63	79
ANN3	5-5-1	0.65	0.59	0.93	36	68	85
ANN4	4-8-1	0.43	0.34	0.98	51	82	94
ANN5	5-7-1	0.42	0.35	0.98	53	81	92

The results show that the ANN4 is the best model for estimating ETo at Pali weather station. The ANN4 model used four inputs (Tmax, Tmin Ra and extrinsic ETo values), eight nodes in the hidden layer and FAO-56PM ETo value as the output. Similar to the results obtained at Jodhpur weather station, the models using extrinsic data have performed well at Pali station. Performance of extrinsic data based ANN models (ANN4 and ANN5) is found to be better than the intrinsic data (ANN2 and

ANN3) based models. In terms of threshold statistics the TS15 value of ANN4 model is better than the TS15 value of ANN3 model. ANN3 model is found to be the best model for estimating ETo using intrinsic antecedent ETo data at Pali weather station. The performance of this mode is slightly better than the ANN2 model. The ANN4 model delivered an RMSE of 0.34 mm/day and NSE of 0.98. This performance is better than the best performing ANN5 model (RMSE of 0.53 and NSE 0.94) at Jodhpur station. The performance of temperature based ANN1 model at Pali weather station is also found to be slightly better than the ANN1 model at Jodhpur station.

The scatter plot and box plot for the ANN models at Jodhpur station are presented in figure 4.21. The scatter plot reveals that the ANN1 model has overestimated the smaller and average ETo values. Except for the smaller ETo value points all the other points are sparsely located around the 45° line of ANN1 model scatter plot. A similar trend is observed in the performance of ANN2 and ANN3 models. The ANN4 and ANN5 models have performed better than the other models. These models have estimated the ETo values well and the points are well distributed. These models have underestimated as well as overestimated the ETo values. The box plot also suggests overestimation of smaller ETo values by all the models except the ANN2 model. The ANN4 and ANN5 models are found to be performing better at estimating the peak ETo values. The 75 percentile line in the box plot of the ANN1, ANN2 and ANN3 models is slightly higher than that of FAO-56PM box plot. The ANN4 and ANN5 models are found to be performing well, however, the 50 percentile line of the all the models are found to be at the same level. The 25 percentile line of the box plot for all the models is at the same level and highlights the ability of AI models to efficiently estimate the smaller ETo values. The scatter plot and the box plot highlights the ability of the AI models to effectively estimate the ETo values at Pali weather station. Also, it is observed that the ETo values from another station (extrinsic data) can be successfully used to develop efficient ETo estimation AI models.

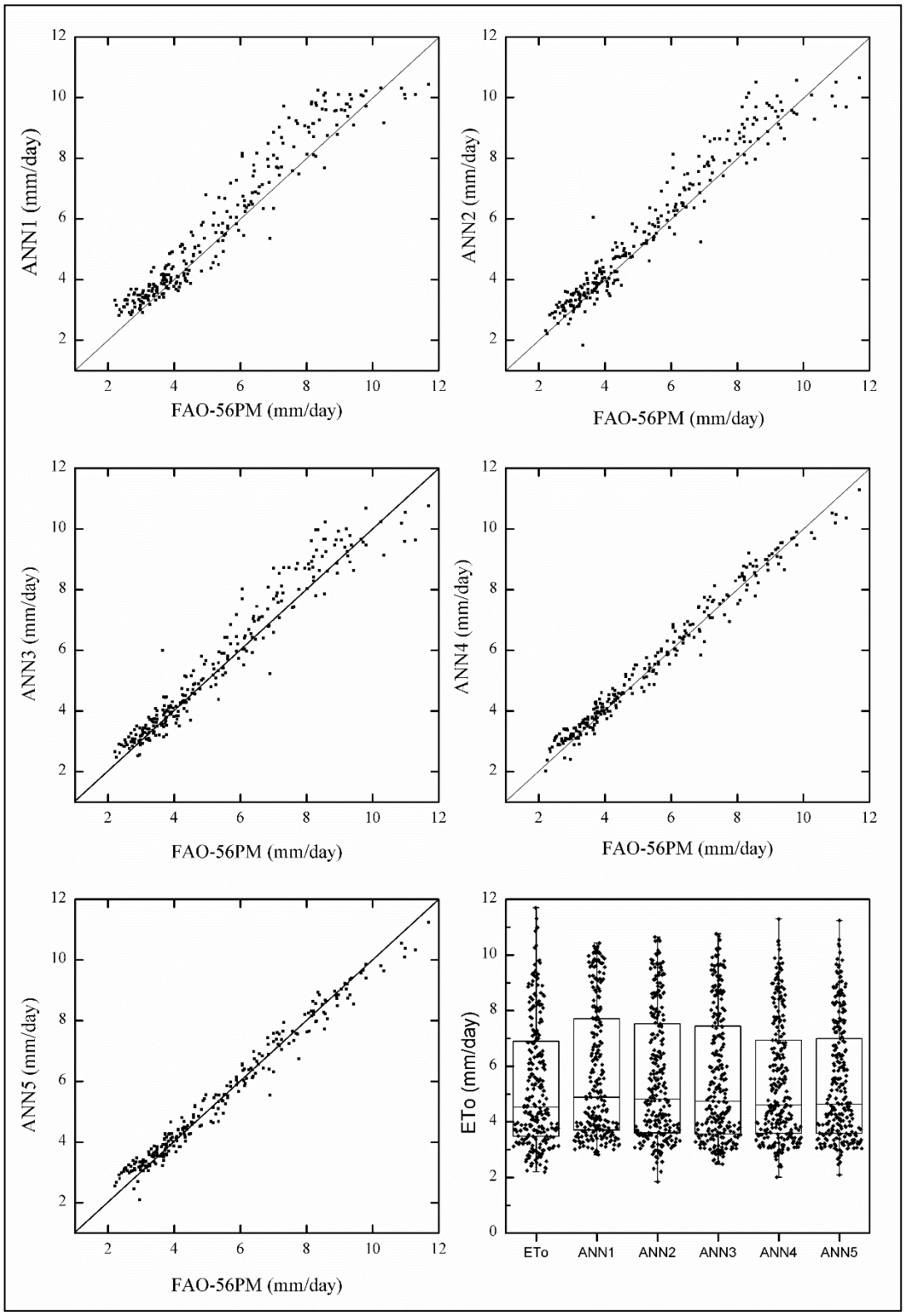

Figure 4.21 Scatter plots and box plot of ANN models for Pali weather station.

4.2.2 W-ANN results for Pali station

The results of W-ANN models are presented in table 4.10. Use of wavelet transform for input preprocessing has enhanced the performance of W-ANN models. However, an appreciable increase in the performance of W-ANN4 and W-ANN5 models was not observed. Further, it is observed that the Db3 wavelet mother wavelet at second level of decomposition has worked well in all the models. This result is in line with the results observed at Jodhpur station where, Db3 mother wavelet has worked well for almost all the models.

Table 4.10 Results of W-ANN models at Pali weather station.

Model	Mother wavelet	Optimum ANN structure	Training RMSE (mm/d)	Testing				
				RMSE (mm/d)	NSE	TS5	TS10	TS15
W-ANN1	Db5 L2	7-11-1	0.68	0.65	0.92	33	54	69
W-ANN2	Db3 L2	10-11-1	0.43	0.39	0.97	51	82	94
W-ANN3	Db3 L2	13-14-1	0.47	0.42	0.97	52	83	93
W-ANN4	Db3 L2	10-16-1	0.37	0.32	0.98	57	84	93
W-ANN5	Db3 L2	13-17-1	0.42	0.34	0.98	53	81	92

The performance of W-ANN1 model at Pali station is found to be better than the ANN1 model. Compared to Jodhpur station the temperature based ANN1 model has performed better at Pali station. However, it is observed that the performance of W-ANN1 model at Jodhpur station is better than the W-ANN1 model at Pali station. A Similar trend is also observed in the performance of intrinsic data based models. The result makes it clear that extrinsic data based W-ANN3 (testing RMSE= 0.32 mm/day) model has performed better than all the W-ANN models at Pali weather station. This model architecture comprised of ten input nodes, sixteen hidden nodes and FAO-56PM ETo values as the output. Unlike the results at Jodhpur station where intrinsic data based hybrid models have performed well, at Pali weather station the extrinsic data based models have performed better than the other models. The threshold statistics also indicate good results for the hybrid models where the TS5 value of all the models is more than 50.

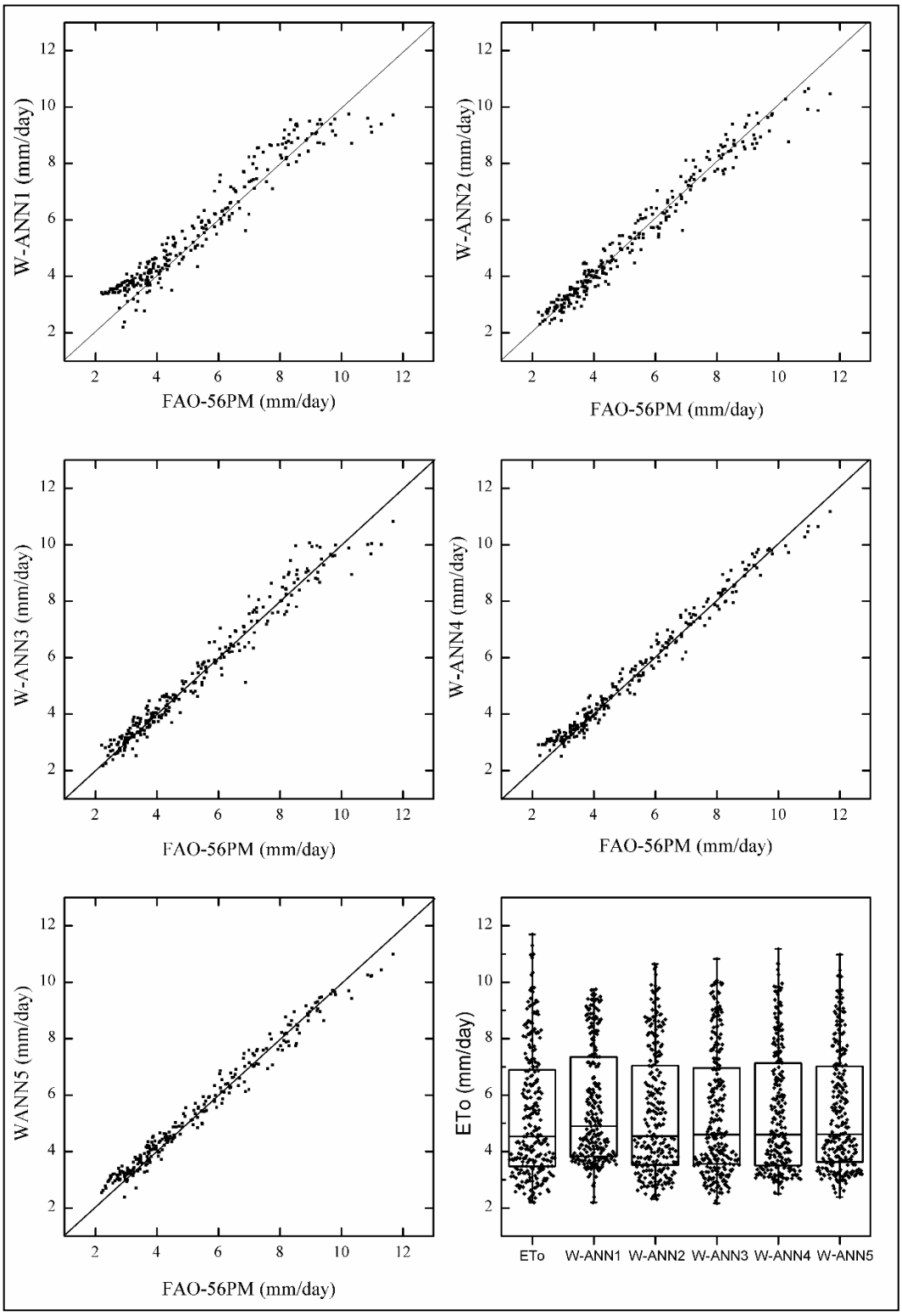

Figure 4.22 Scatter plots and box plot of W-ANN models for Pali weather station.

The scatter plot for the W-ANN models at Pali station are presented in figure 4.22. The scatter plot presents overestimation of smaller and underestimation of larger ETo values by the W-ANN1 model. The points are sparsely located around the 45° line. This behavior was also observed for all the temperature-based models tested earlier at Jodhpur station. The intrinsic data based W-ANN2 and W-ANN3 models are good at estimating the smaller values, but the greater values are largely underestimated. Undoubtedly, the W-ANN4 and W-ANN5 models have performed better than the other models. The smaller ETo values are marginally overestimated by these models. The greater ETo values are underestimated by these models, but to a smaller extent compared to the intrinsic data based models.

4.2.3 ANFIS results for Pali station

Similar to the study carried out at Jodhpur weather station, ANFIS models were also tested at Pali station. The results of ANFIS models using different input combinations are presented in table 4.11.

Table 4.11 Results of ANFIS models at Pali weather station.

Model	Membership Function	Training RMSE (mm/d)	Testing				
			RMSE (mm/d)	NSE	TS5	TS10	TS15
ANFIS1	Trapezoidal	0.81	0.78	0.88	28	54	69
ANFIS2	Gaussian	0.67	0.62	0.92	34	65	81
ANFIS3	Gaussian	0.62	0.59	0.93	36	65	82
ANFIS4	Gaussian	0.42	0.35	0.98	51	82	94
ANFIS5	Gaussian	0.43	0.37	0.97	54	85	94

The performance of all the ANFIS models at Pali weather station is better than the ANFIS models tested at Jodhpur station. The ANFIS2 model has a lower RMSE value, but when compared in terms of NSE statistics the ANFIS2 model at Pali station has performed better than the ANFIS2 model at Jodhpur station. Further, it is observed that the performance of extrinsic data based models is better than the intrinsic data based model. The RMSE of ANFIS4 model (0.35 mm/day) is almost half of the ANFIS2 model (0.62 mm/day).

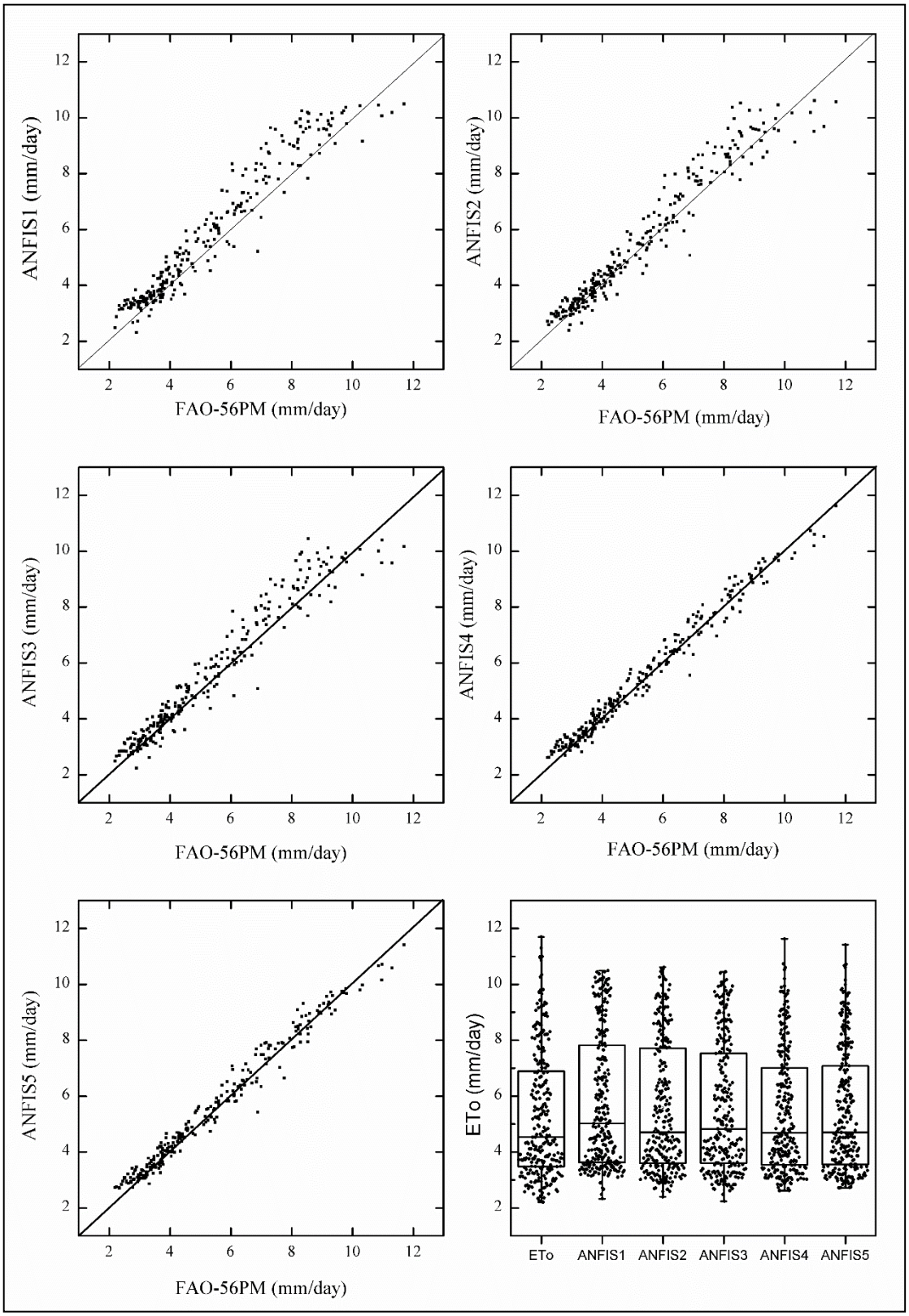

Figure 4.23 Scatter plots and box plot of ANFIS models for Pali weather station.

ANFIS4 model is the best ANFIS model for estimating ETo at Pali station. This model used three numbers of Gaussian membership function and delivered an RMSE of 0.35 mm/day. The threshold statistics of this model also highlight the superiority of this model. The TS5 value of ANFIS4 model represents that around fifty percent of data points estimated have less than five percent absolute relative error.

The scatter plot and box plot for the ANFIS models are presented in figure 4.23. The temperature based ANFIS1 model has mostly overestimated the ETo values. However, this model underestimated the peak values. The intrinsic data based ANFIS2 and ANFIS3 models were better at estimating smaller ETo values, but did not perform well in estimating greater values. The extrinsic data based ANFIS4 and ANFIS5 model slightly overestimated the smaller ETo values, but were good at estimating the peak values. The box plot also suggests that the ANFIS2 and ANFIS3 model were good at estimating the smaller ETo values while the ANFIS4 and ANFIS5 model were good at estimating peak values.

4.2.4 W-ANFIS results for Pali station

The results for W-ANFIS models are discussed in this section. For developing W-ANFIS models for Pali section too, subtractive clustering was used instead of the grid search method. The results in terms of RMSE, NSE and threshold statistics are presented in table 4.12.

Table 4.12 Results of W-ANFIS models at Pali weather station.

Model	Mother wavelet	Training	Testing				
		RMSE (mm/d)	RMSE (mm/d)	NSE	TS5	TS10	TS15
W-ANFIS1	Db5 L1	0.79	0.75	0.89	22	46	68
W-ANFIS2	Db3 L2	0.45	0.40	0.97	54	80	93
W-ANFIS3	Db3 L2	0.48	0.45	0.96	51	80	91
W-ANFIS4	Db3 L1	0.38	0.36	0.97	50	82	91
W-ANFIS5	Db3 L2	0.40	0.36	0.97	50	81	91

The table reveals an enhancement in the performance of ANFIS models on using wavelet decomposed input data. Except for the extrinsic data based models, a substantial enhancement in the performance of temperature and intrinsic data based models is observed. For most of the models, decomposition by Db3 mother wavelet has performed well. The performance of temperature based W-ANFIS1 models (RMSE 0.75 mm/day) is found to be slightly better than the W-ANN1 model (RMSE 0.65 mm/day). Also, the enhancement in the performance of this model is very less when compared to the performance of ANFIS1 model of Pali station. It is observed that in case of W-ANFIS1 models the Db5 wavelet transform at first level of decomposition has performed better. Use of wavelet transform has enhanced the performance of W-ANFIS2 and W-ANFIS3 models when compared to the respective ANFIS models. The performance of W-ANFIS4 and W-ANFIS5 model is almost same. However, considering the lesser number of inputs used by the W-ANFIS4 models, it can be concluded that W-ANFIS4 is the best hybrid W-ANFIS model for estimating ETo at Pali weather station.

Scatter plots and box plots of W-ANFIS models for Pali station are presented in figure 4.24. Like ANFIS1 model the W-ANFIS1 model also overestimates the ETo values, but the performance of this model is slightly better. The intrinsic data based W-ANFIS2 and W-ANFIS3 models performed well at estimating the larger ETo values when compared to ANFIS2 and ANFIS3 models. This highlights the applicability of using wavelet transform for enhancing the performance of ANFIS models. The performance of W-ANFIS4 and W-ANFIS5 is found to be alike and best among all the W-ANFIS models tested at Pali station. These models slightly overestimated the very small ETo values, but are good at estimating the greater values. The box plot shows that the ANFIS2 and ANFIS3 models overestimated the ETo values, whereas the hybrid W-ANFIS2 and W-ANFIS3 models using wavelet transformed data inputs have performed better than the conventional ANFIS models. The box plot shows underestimation of greater ETo values by W-ANFIS3 model when compared to the box plot of other models. The box plot for the W-ANFIS4 model shows a very good resemblance to the box plot of the FAO-56PM ETo. Hence, this model can be considered as the best W-ANFIS model for estimating ETo at Pali station.

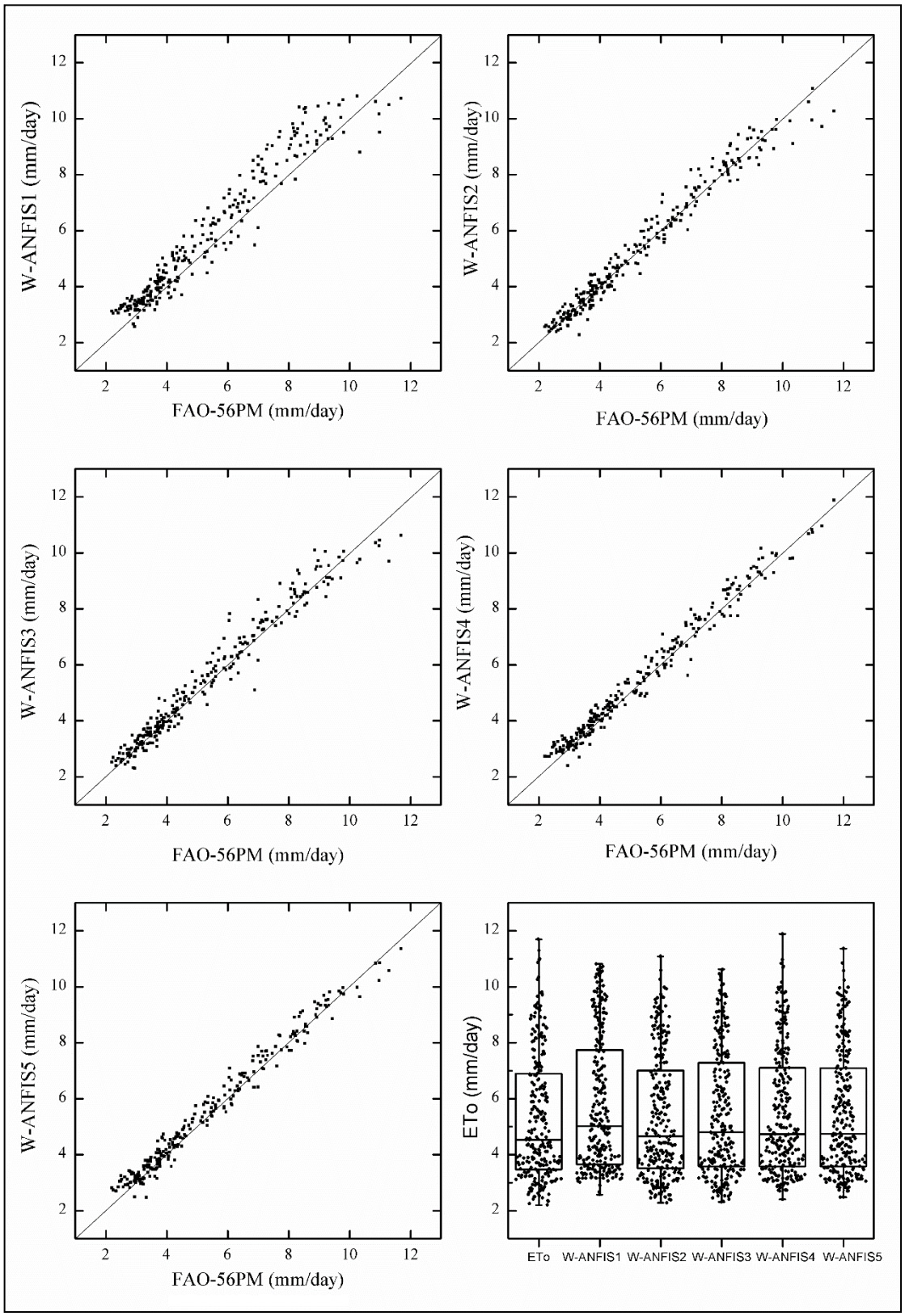

Figure 4.24 Scatter plots and box plot of W-ANFIS models for Pali weather station.

4.2.5 LS-SVM results for Pali station

The LS-SVM models is found to be the best AI model for estimating ETo at the Jodhpur weather station. The results for LS-SVM models at Pali weather station are discussed in this section. Table 4.13 presents the RMSE, NSE and threshold statistics for the LS-SVM models tested at Pali weather station. The results reveal that, except for the temperature-based model, performance of LS-SVM models is better than all the other AI models tested at this station. The intrinsic data based LS-SVM model has performed better than the ANN and ANFIS models. The results suggest that the performance of both the LS-SVM4 and LS-SVM5 models is similar. However, considering the lesser number of inputs used by the LS-SVM4 model, this model can be considered as the best LS-SVM model to estimate ETo at Pali weather station.

Table 4.13 Results of LS-SVM models at Pali weather station.

Model	Training RMSE (mm/d)	Testing				
		RMSE (mm/d)	NSE	TS5	TS10	TS15
LS-SVM1	0.78	0.73	0.89	25	50	69
LS-SVM2	0.62	0.58	0.93	38	65	83
LS-SVM3	0.60	0.56	0.94	40	68	85
LS-SVM4	0.38	0.33	0.98	55	86	93
LS-SVM5	0.37	0.33	0.98	55	85	94

Scatter plots for all the LS-SVM models tested at the Pali station are presented in figure 4.25. The scatter plot and box plot suggests that the performance of all the LS-SVM model is better than the ANN and ANFIS models. The LS-SVM1 model overestimated the ETo values. The LS-SVM2 and LS-SVM3 models performed better at estimating the smaller values of ETo but slightly overestimated the greater values. Similar performance is also observed in case of intrinsic inputs based ANN and ANFIS models. The performance of LS-SVM4 and LS-SVM5 models tested at Pali station is found to better than other LS-SVM models tested at Jodhour station.

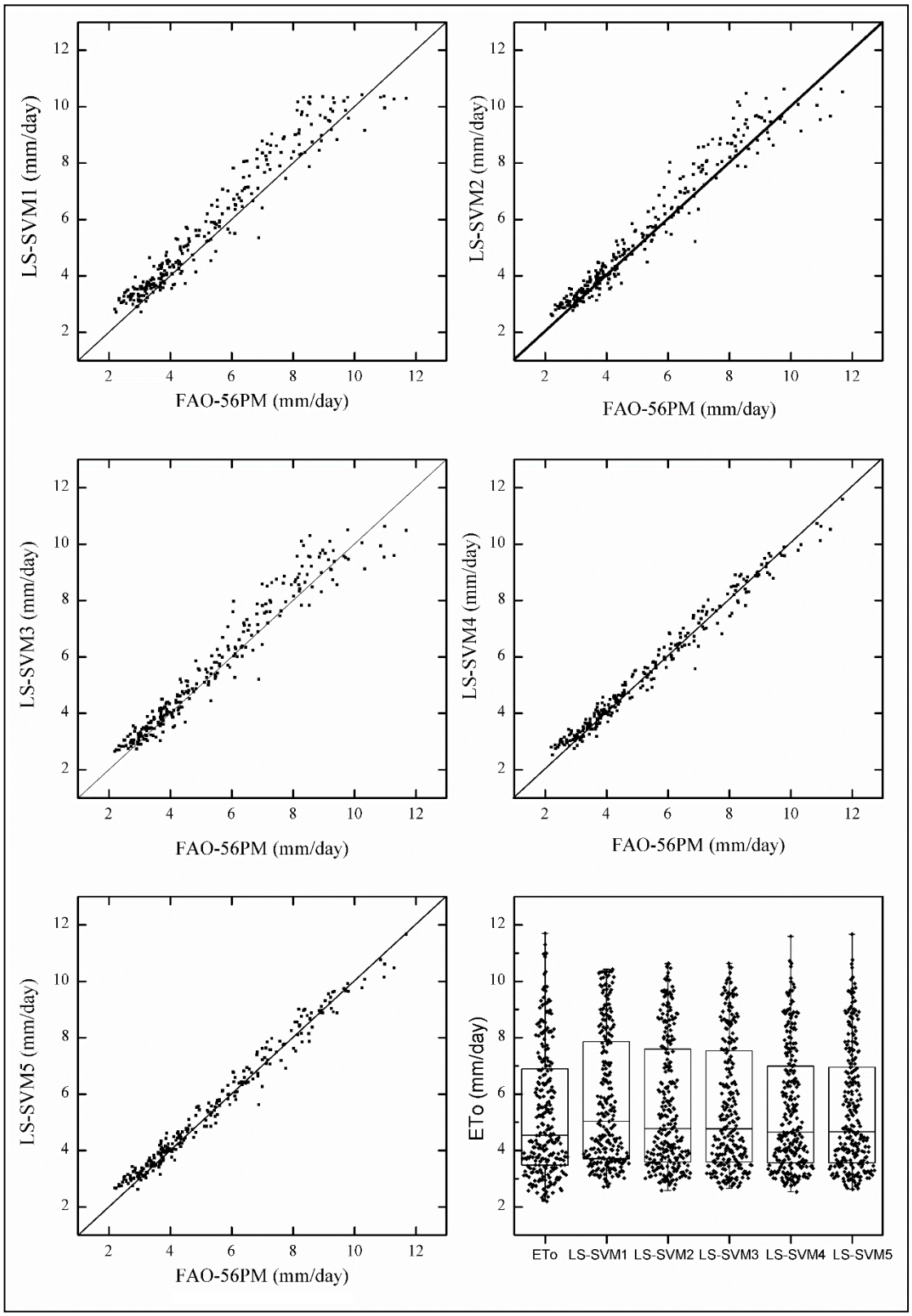

Figure 4.25 Scatter plots and box plot of LS-SVM models for Pali weather station.

4.2.6 W-LSSVM results for Pali station

The results for W-LSSVM model tested at Pali station are presented in table 4.14. Except for the temperature based model, the hybrid W-LSSVM models have performed better than all the other models tested at Pali station. From the W-ANN results, it is also observed that the performance of W-ANN1 model is better than the W-ANFIS1 and W-LSSVM1 model.

Table 4.14 Results of LS-SVM models at Pali weather station.

Model	Mother wavelet	Training RMSE (mm/d)	Testing				
			RMSE (mm/d)	NSE	TS5	TS10	TS15
W-LSSVM1	Db3 L3	0.74	0.71	0.90	22	50	69
W-LSSVM2	Db3 L2	0.42	0.39	0.97	54	85	96
W-LSSVM3	Db3 L2	0.48	0.42	0.96	58	83	96
W-LSSVM4	Db5 L3	0.35	0.32	0.98	54	85	95
W-LSSVM5	Db3 L2	0.36	0.33	0.98	54	87	94

The table shows that W-LSSVM4 is the best hybrid model for estimating ETo at Pali weather station. The model used inputs decomposed by Db5 mother wavelet at second level of decomposition. It is seen that the enhancement in the performance of W-LSSVM4 model when compared to the LS-SVM4 model is very small. Both the models delivered same NSE of 0.98. The threshold statistics also indicated similar performance by both the models. Further, it is observed that out of all the models tested, W-LSSVM4 is the most efficient model for estimating ETo at Pali weather station. This model used temperature data along with the extrinsic ETo values as inputs.

Figure 4.26 presents scatter plots and box plots for the W-LSSVM models. The scatter plot for W-LSSVM1 model shows overestimation of all the ETo values. The intrinsic data based W-LSSVM2 and W-LSSVM3 models performed better than the extrinsic data based W-LSSVM4 and W-LSSVM5 models. It can also be observed that the intrinsic data based models were poor at estimating the larger ETo values. These models underestimated as well as overestimated the ETo values. The extrinsic

data based models underestimated the smaller ETo values, but were good at estimating the larger values.

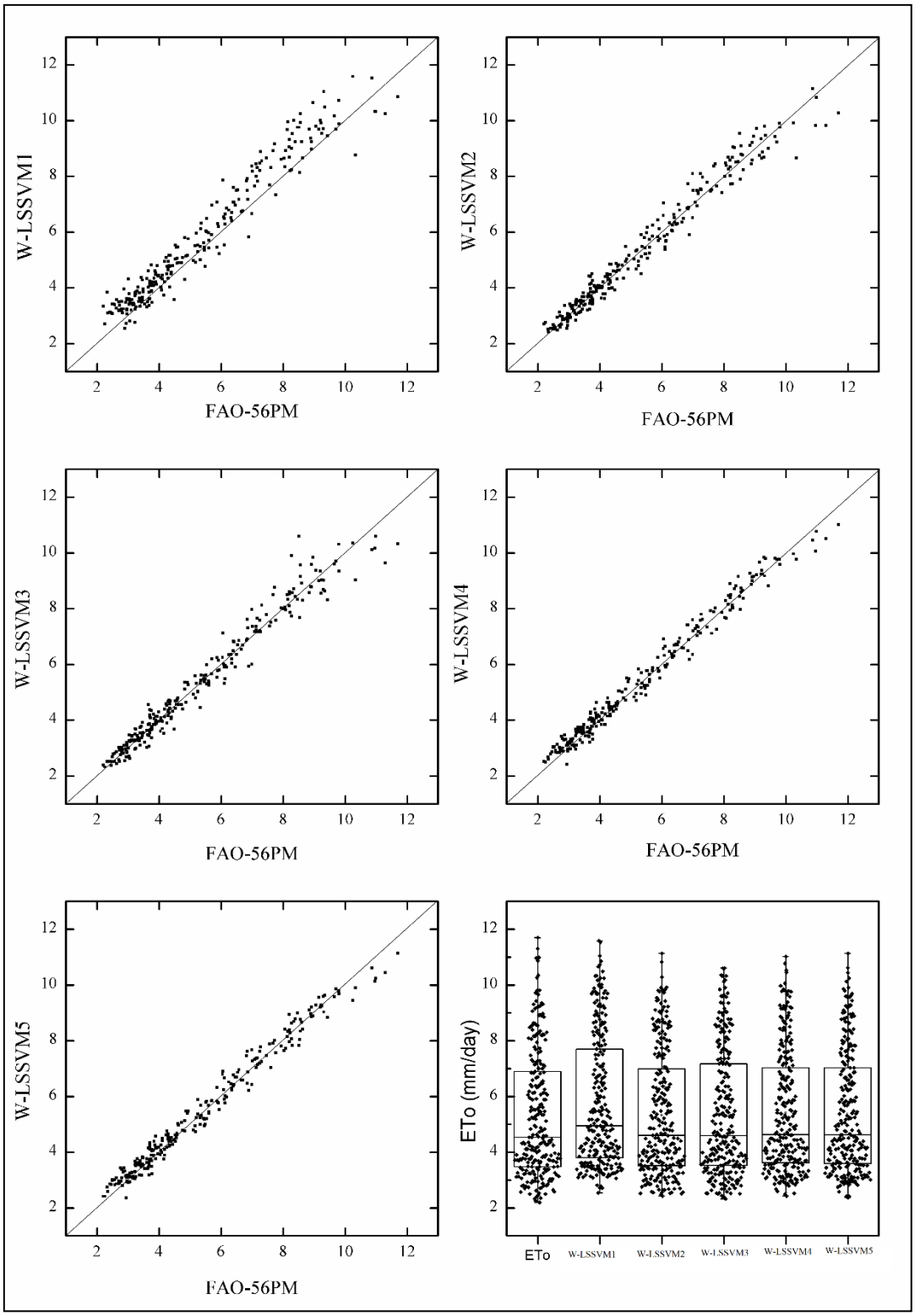

Figure 4.26 Scatter plots and box plot of W-LSSVM models for Pali weather station.

4.2.7 Temperature based models for Pali station.

On comparing the performance of temperature based Hargreaves, ANN1, ANFIS1 and LS-SVM1 based models, it is observed that the performance of Hargreaves model is poor (RMSE of 0.99 mm/day) compared to all the AI models. The result reveals the superiority of AI models over the Hargreaves equation. Figure 4.27 presents the scatter plots of the temperature based models. The scatter plots clearly highlight the efficiency of the AI models. The AI models slightly overestimated the smaller ETo values. The Hargreaves model underestimated the greater values ETo. The underestimation was very high compared to the AI models. The AI models are good at estimating the larger ETo values and the performance of LS-SVM1 models is good when compared to the ANN1 and ANFIS1 model. It is observed that data points with greater ETo values are sparsely distributed around the 45° line.

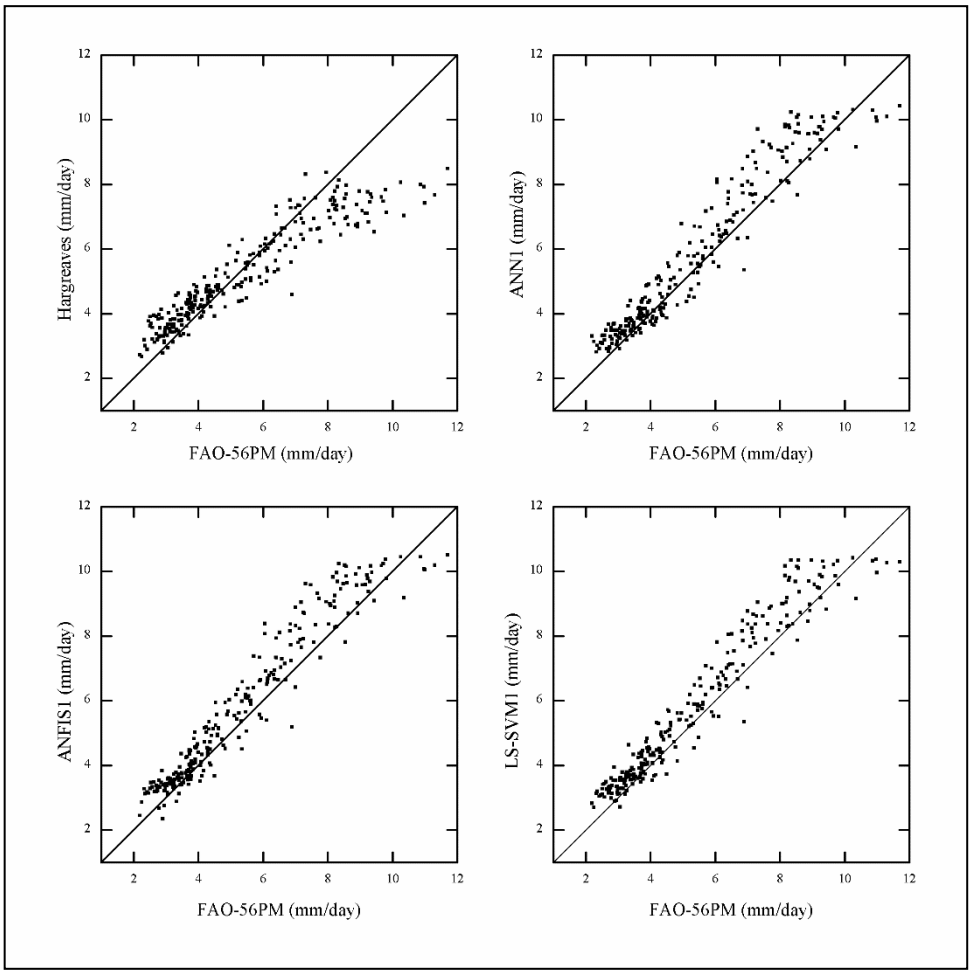

Figure 4.27 Scatter plot for temperature based models at Pali weather station

4.3 RESULTS FOR HYDERABAD STATION (SEMI-ARID REGION)

As stated in the methodology, the performance of proposed hybrid AI models for estimating daily ETo in semi-arid region is also analyzed in this study. The results for Hyderabad station are discussed in this section.

4.3.1 ANN results for Hyderabad station

The performance of ANN models for estimating ETo at Hyderabad station are presented in table 4.15. The results reveal that the performance of ANN models in semi-arid region is inferior to the performance of ANN models in arid region. This may be due to the inefficiency of ANN to model ETo using the given input variables or due to the input data properties like high coefficient of variation.

Table 4.15 Results of ANN models at Hyderabad weather station.

Model	Optimum ANN structure	Training RMSE (mm/d)	Testing				
			RMSE (mm/d)	NSE	TS5	TS10	TS15
ANN1	3-5-1	1.07	0.92	0.71	26	54	68
ANN2	4-7-1	0.96	0.87	0.74	29	51	72
ANN3	5-8-1	0.98	0.89	0.72	30	52	72
ANN4	4-9-1	1.23	1.04	0.62	27	47	62
ANN5	5-9-1	1.21	1.13	0.56	26	44	63

The temperature based ANN1 model delivered a testing RMSE of 0.92 mm/day and NSE of 0.71. This result is found to be poorer than the performance of temperature based ANN models in arid regions. Similar trend is observed in the performance of other ANN models tested for the Hyderabad station. The performance of intrinsic inputs based ANN2 and ANN3 model is found to be better than the extrinsic inputs based ANN4 and ANN5 model. The temperature based ANN1 model has performed better than ANN4 and ANN5 models. This reveals the inability of extrinsic inputs to model ETo at the selected weather stations. Display of poor performance by extrinsic inputs based models may be due to the large distance between stations selected for the study. The scatter plot and box plot for the ANN models is presented in figure 4.28. The scatter plot and box plot also reveal that ANN2 is the best model for estimating ETo at Hyderabad weather station. It is further observed that this model did not perform well in modeling higher ETo values.

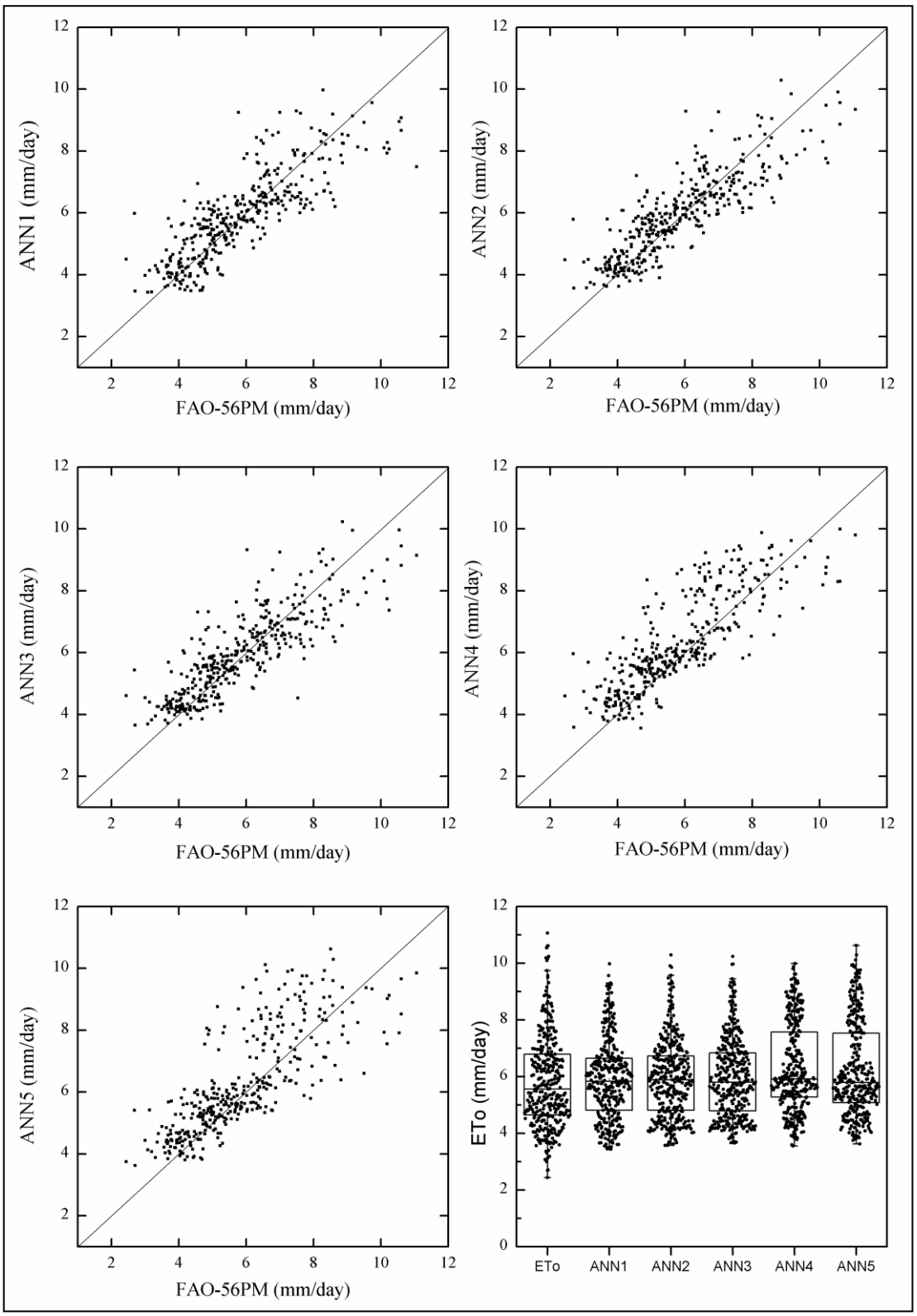

Figure 4.28 Scatter plots and box plot of ANN models for Hyderabad weather station.

4.3.2 W-ANN results for Hyderabad station

The results for hybrid W-ANN models are presented in this section. Use of wavelet decomposed input variables have shown an enhancement in the performance of AI models at arid region. However, in case of semi-arid region, use of wavelet decomposed inputs did not show a significant enhancement in the performance. The results for W-ANN models are presented in table 4.16.

Table 4.16 Results of W-ANN models at Hyderabad weather station.

Model	Mother wavelet	Optimum ANN structure	Training RMSE (mm/d)	Testing				
				RMSE (mm/d)	NSE	TS5	TS10	TS15
W-ANN1	Db5 L2	5-8-1	1.04	0.90	0.72	30	52	70
W-ANN2	Db3 L2	10-14-1	0.76	0.66	0.85	41	68	83
W-ANN3	Db3 L2	13-16-1	0.54	0.48	0.92	59	82	92
W-ANN4	Db3 L2	10-17-1	1.10	1.09	0.59	29	52	66
W-ANN5	Db3 L2	9-13-1	1.09	1.09	0.59	27	47	63

Use of wavelet decomposed inputs has helped in improving the efficiency of the intrinsic data based W-ANN2 and W-ANN3 models. The result reveals that W-ANN3 model (testing RMSE of 0.48 mm/day) is the best W-ANN model for estimating ETo at Hyderabad weather station. The W-ANN3 model has also performed well in terms of NSE and threshold statistics. This model used thirteen inputs, sixteen nodes in hidden layer and FAO-56PM ETo as the output. For most of the models tested, the Db3 mother wavelet at second level of decomposition has performed well. Similar to the observations for ANN models, results for W-ANN models also point out the inability of extrinsic input based models for estimating ETo in semi-arid regions.

The scatter plot and box plot for the W-ANN models are presented in Figure 4.29. The result reveals poor performance by the models in estimating the higher ETo values. All the data points are sparsely located around the 45° line. The W-ANN2 and W-ANN3 models performed well overall, but were not good at estimating the higher ETo values. The box plot suggests overestimation of ETo values by all the models. It is observed that the performance of extrinsic data based models is similar to the temperature based W-ANN1 model.

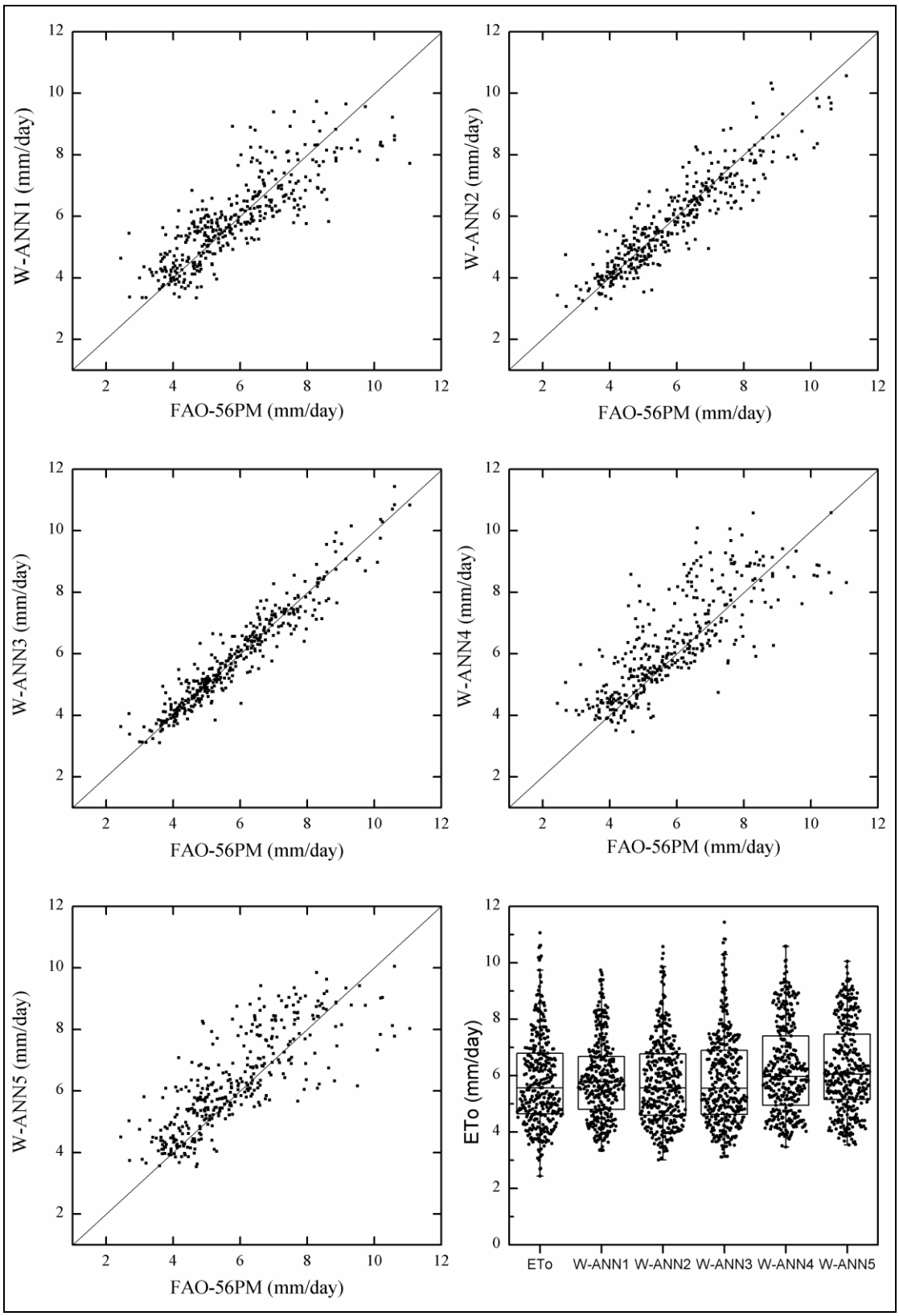

Figure 4.29 Scatter plots and box plot of W-ANN models for Hyderabad weather station.

4.3.3 ANFIS results for Hyderabad station

The results for ANFIS models are presented in table 4.17. The results suggest similar performance by ANN and ANFIS models.

Table 4.17 Results of ANFIS models at Hyderabad weather station.

Model	Membership function	Training RMSE (mm/d)	Testing				
			RMSE (mm/d)	NSE	TS5	TS10	TS15
ANFIS1	Gbell	1.03	0.93	0.70	31	51	68
ANFIS2	Gbell	0.97	0.87	0.74	29	51	72
ANFIS3	Gbell	1.10	0.93	0.70	28	51	71
ANFIS4	Gbell	1.24	1.01	0.65	30	50	65
ANFIS5	Gbell	1.28	1.17	0.52	27	50	70

The temperature based ANN1 model performed slightly better than the ANFIS1 model. ANFIS2 is the best ANFIS model for estimating ETo at Hyderabad station. It is observed that use of extrinsic data deteriorated the performance of AI model. The performance of ANN4 and ANN5 models is found to be inferior than the temperature based ANN1 model. It is also observed that the Gbell membership function has performed well in all the ANFIS models. Further, it is observed that increasing the number of inputs (in case of ANFIS3 and ANFIS5 models) has deteriorated the performance of ANFIS models.

The scatter plots and box plots for the ANFIS models are presented in figure 4.30. It is observed that the models did not perform well in estimating ETo of Hyderabad station. The ANN1 model overestimated as well as underestimated the ETo values. The ANN2 and ANN3 models performed well at estimating smaller ETo values, but the larger values were overestimated as well as underestimated. The extrinsic data based ANN4 and ANN5 model overestimated the ETo values. The box plots show overestimation of smaller values by all the models. The ANFIS4 and ANFIS5 model shows data points above the seventy five percentile line which are not observed in the box plot for ETo values estimated by FAO-56PM method. The box plot for ANFIS5 model shows presence of outliers in the estimated values.

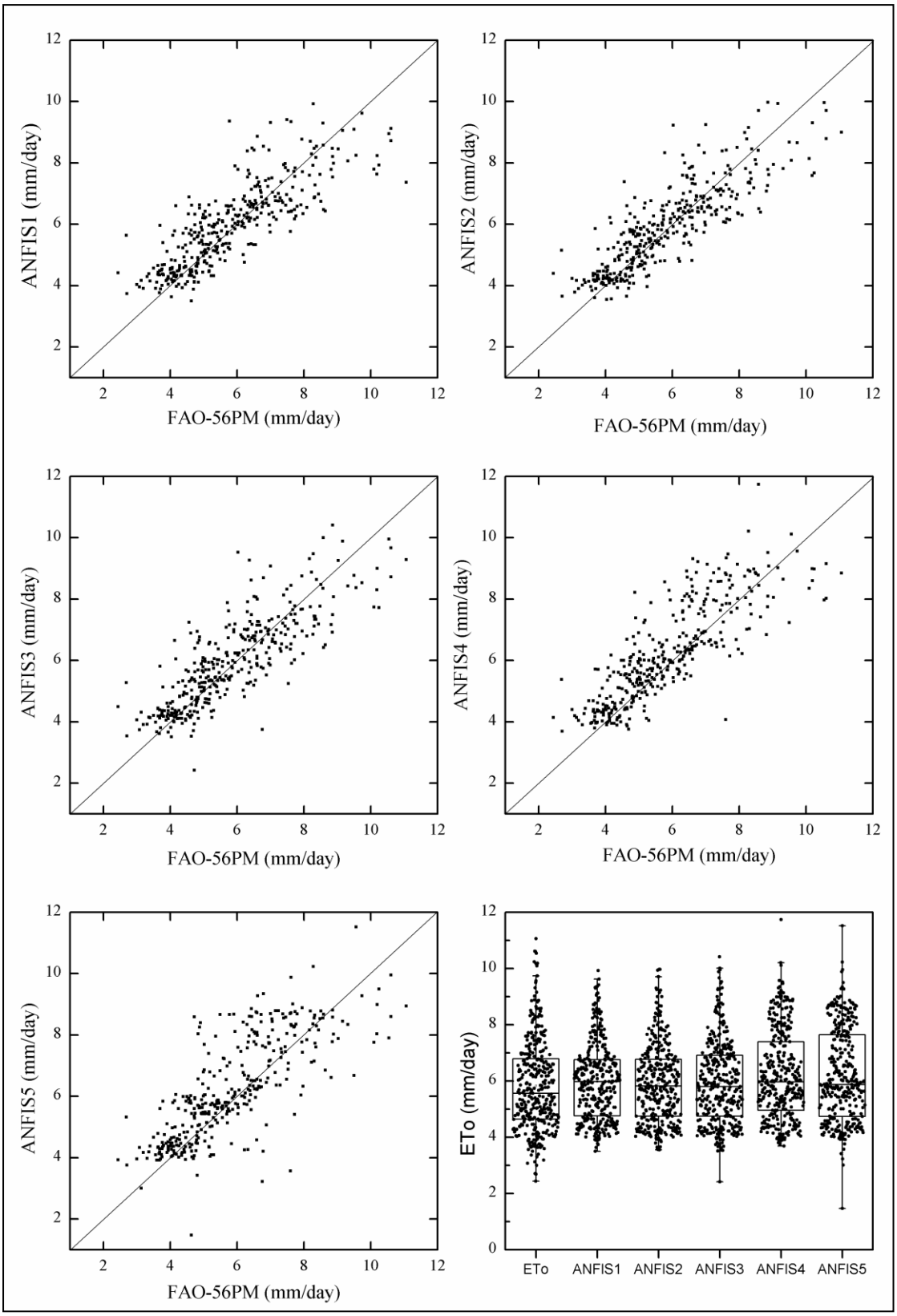

Figure 4.30 Scatter plots and box plot of ANFIS models for Hyderabad weather station.

4.3.4 W-ANFIS results for Hyderabad station

The results for hybrid W-ANFIS models are discussed in this section. The results for these models are presented in table 4.18. An enhancement in the performance of W-ANFIS2 and W-ANFIS3 models is observed over the ANFIS2 and ANFIS3 models. For all the other models tested, use of wavelet inputs did not contribute towards the performance of the models.

Table 4.18 Results of W-ANFIS models at Hyderabad weather station.

Model	Mother wavelet	Training RMSE (mm/d)	Testing			
			RMSE (mm/d)	NSE	TS5	TS10	TS15
W-ANFIS1	Db5 L1	1.16	0.92	0.70	27	53	68
W-ANFIS2	Db3 L3	0.73	0.66	0.85	41	71	84
W-ANFIS3	Db3 L3	0.58	0.46	0.93	59	80	93
W-ANFIS4	Db3 L1	1.05	1.03	0.63	28	46	60
W-ANFIS5	Db5 L1	1.23	1.06	0.61	27	46	59

The W-ANFIS1 model performed better than the ANFIS1 model in terms of RMSE statistics, but when compared in terms of threshold statistics the ANFIS1 has model performed better. It is seen that, Db3 and Db5 mother wavelets worked better for all the W-ANFIS models tested. The W-ANFIS3 model has performed better than all the other W-ANFIS models tested. Extrinsic data based W-ANFIS4 delivered testing RMSE of 0.46 mm/day and TS15 value of ninety three.

Scatter plots and box plots for the W-ANFIS models are presented in figure 4.31. The scatter plot reveals good performance by W-ANFIS2 and W-ANFIS3 models. These models performed better at estimating smaller ETo values. The other models overestimated the smaller ETo values and overestimated as well as underestimated larger ETo values. The larger values of W-ANFIS1, W-ANFIS4 and W-ANFIS5 models are sparsely located around the 45° line. The box plot also reveals overestimation of ETo values by the extrinsic data models. It is clear from the scatter plots and box plots that the W-ANFIS3 is the best hybrid W-ANFIS model for estimating ETo at Hyderabad station.

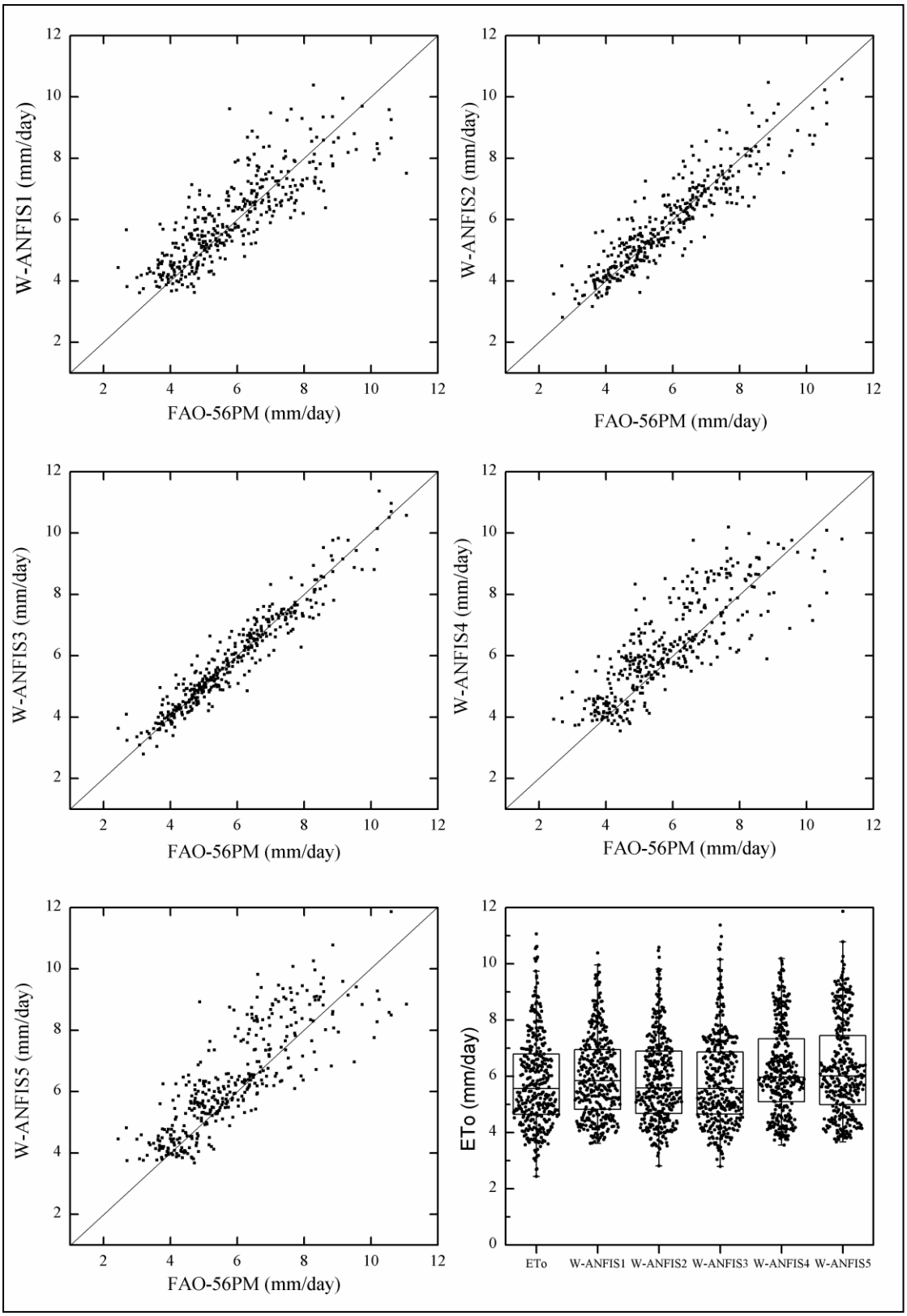

Figure 4.31 Scatter plots and box plot of W-ANFIS models for Hyderabad weather station.

4.3.5 LS-SVM results for Hyderabad station

The results for models tested in arid region reveal that LS-SVM are the best AI models for estimating ETo. The results for LS-SVM models at Hyderabad station are discussed in this section. The result reveals that the LS-SVM is best AI models for estimating ETo at Hyderabad station. The results for the models tested are presented in table 4.19.

Table 4.19 Results of LS-SVM models at Hyderabad weather station.

Model	Training RMSE (mm/d)	Testing				
		RMSE (mm/d)	NSE	TS5	TS10	TS15
LS-SVM1	1.03	0.93	0.70	28	51	69
LS-SVM2	0.96	0.86	0.74	30	52	73
LS-SVM3	0.96	0.87	0.74	30	51	73
LS-SVM4	1.06	0.99	0.66	27	53	67
LS-SVM5	1.12	1.04	0.62	29	49	66

At Hyderabad station, it is observed that the performance of ANN, ANFIS and LS-SVM models are identical. LS-SVM6 is the best LS-SVM model for estimating ETo at Hyderabad weather station. In addition, this model performed better than all the other ANN, ANFIS and LS-SVM models. Further, it is seen that the temperature based LS-SVM1 model performed better than the extrinsic data based LS-SVM4 and LS-SVM5 model. This result highlights the inability of extrinsic inputs in modeling the ETo process.

The Scatter plots and box plots for the LS-SVM models are presented in Figure 4.32. The LS-SVM1 model did not perform well and the data points are sparsely located around the 45° line. The LS-SVM2 and LS-SVM3 models were good at estimating the smaller ETo values, but did not perform well at estimating the larger ETo values. The extrinsic data based LS-SVM4 and LS-SVM5 model overestimated the ETo values at Hyderabad station. The box plot indicated overestimation of smaller ETo values by all the LS-SVM models. The box plot reveals overestimation of ETo values by the LS-SVM4 and LS-SVM5 models.

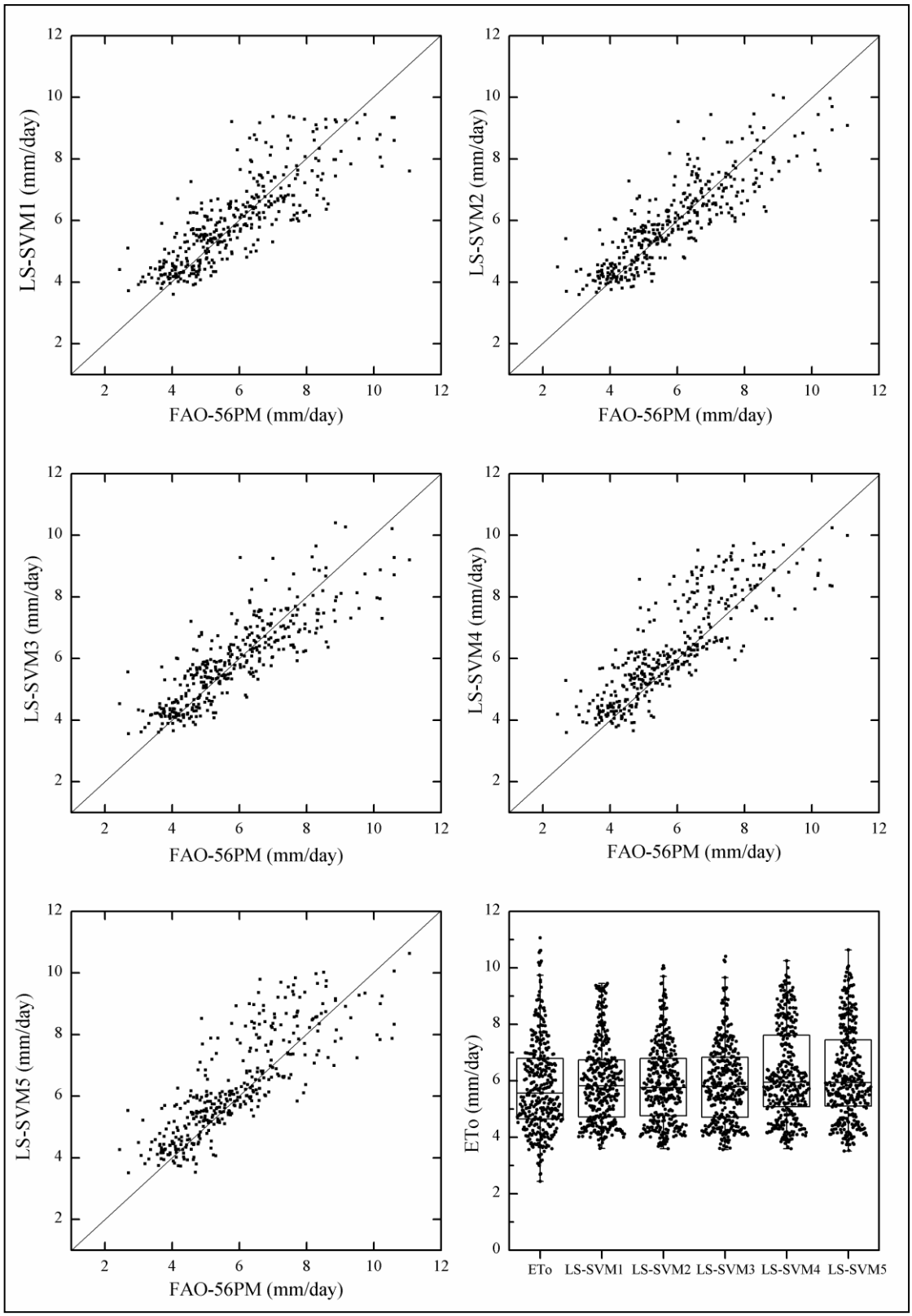

Figure 4.32 Scatter plots and box plot of LS-SVM models for Hyderabad weather station.

4.3.6 W-LSSVM results for Hyderabad station

W-LSSVM is found to be the best hybrid model for the estimating ETo at Jodhpur and Pali weather station. The results for W-LSSVM models for Hyderabad weather station are presented in table 4.20. The table suggests that there the is no enhancement in the performance of some models on using wavelet decomposed data as inputs.

Table 4.20 Results of W-LSSVM models at Hyderabad weather station.

Model	Mother wavelet	Training RMSE (mm/d)	Testing				
			RMSE (mm/d)	NSE	TS5	TS10	TS15
W-LSSVM1	Db3 L3	0.98	0.92	0.71	25	52	70
W-LSSVM2	Db3 L2	0.74	0.65	0.85	41	69	85
W-LSSVM3	Db3 L2	0.56	0.43	0.93	60	84	93
W-LSSVM4	Db5 L3	1.12	1.03	0.63	28	50	65
W-LSSVM5	Db3 L2	1.13	1.04	0.62	27	48	65

It is clear from the table that W-LSSVM3 model with RMSE of 0.43 mm/day is the best hybrid model for estimating ETo at Hyderabad weather station. This model delivered an NSE of 0.93 and TS15 value of ninety-three. It is observed that except for the W-LSSVM4 model, Db3 at second level of decomposition has performed well for all the other models. It is observed that the performance of W-LSSVM1 model is better than the extrinsic data based W-LSSVM4 and W-LSSVM5 model.

Scatter plot and box plot for the W-LSSVM models for Hyderabad weather station are presented in figure 4.33. The scatter plot presents a good performance by the W-LSSVM2 and W-LSSVM3 model. The box plot makes it clear that the temperature and extrinsic data based models overestimated the ETo values. The performance of W-LSSVM3 is best amongst all the models tested at Hyderabad station. The results make it clear that W-LSSVM is the best model for estimating ETo at the Hyderabad weather station. Additionally, it is observed that the intrinsic data based AI models have performed well. Unlike the results obtained for arid region, the models using extrinsic data have failed to deliver good performance at Hyderabad weather station.

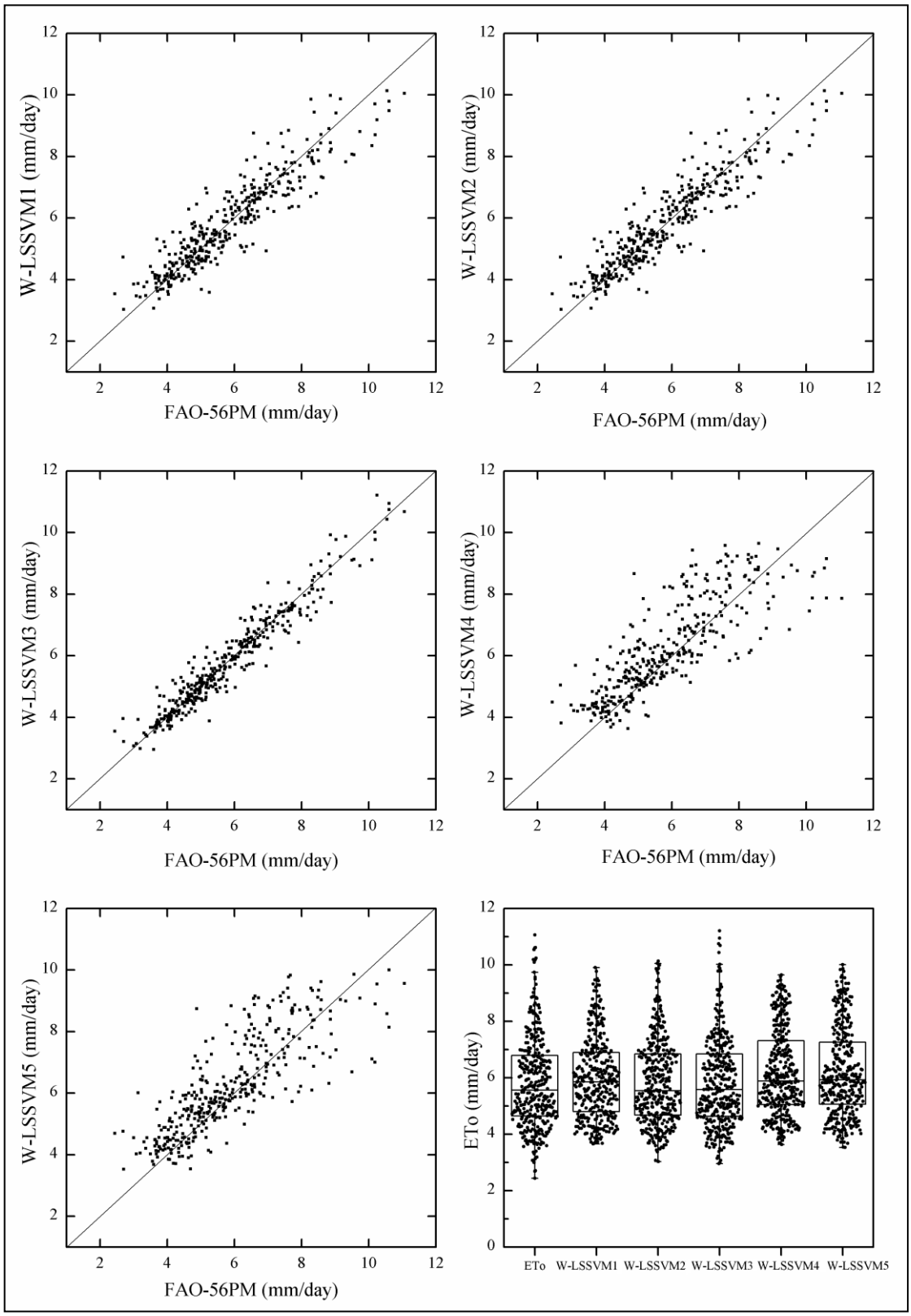

Figure 4.33 Scatter plots and box plot of W-LSSVM models for Hyderabad weather station.

4.3.7 Temperature based models for Hyderabad station

The performance of different temperature based equations for estimating daily ETo at Hyderabad station is compared in this section. The Hargreaves equation yielded an RMSE of 1.08 mm/day for the Hyderabad weather station. It is clear that all the AI models performed better than the Hargreaves equation. Scatter plots of all the temperature based models are presented in figure 4.34. It is clear from the figure that the Hargreaves equation underestimated the ETo values at the Hyderabad station. The AI models performed better at estimating the smaller ETo. However, the larger ETo values are sparsely located around the 45° line suggesting a poor performance by all the temperature based models.

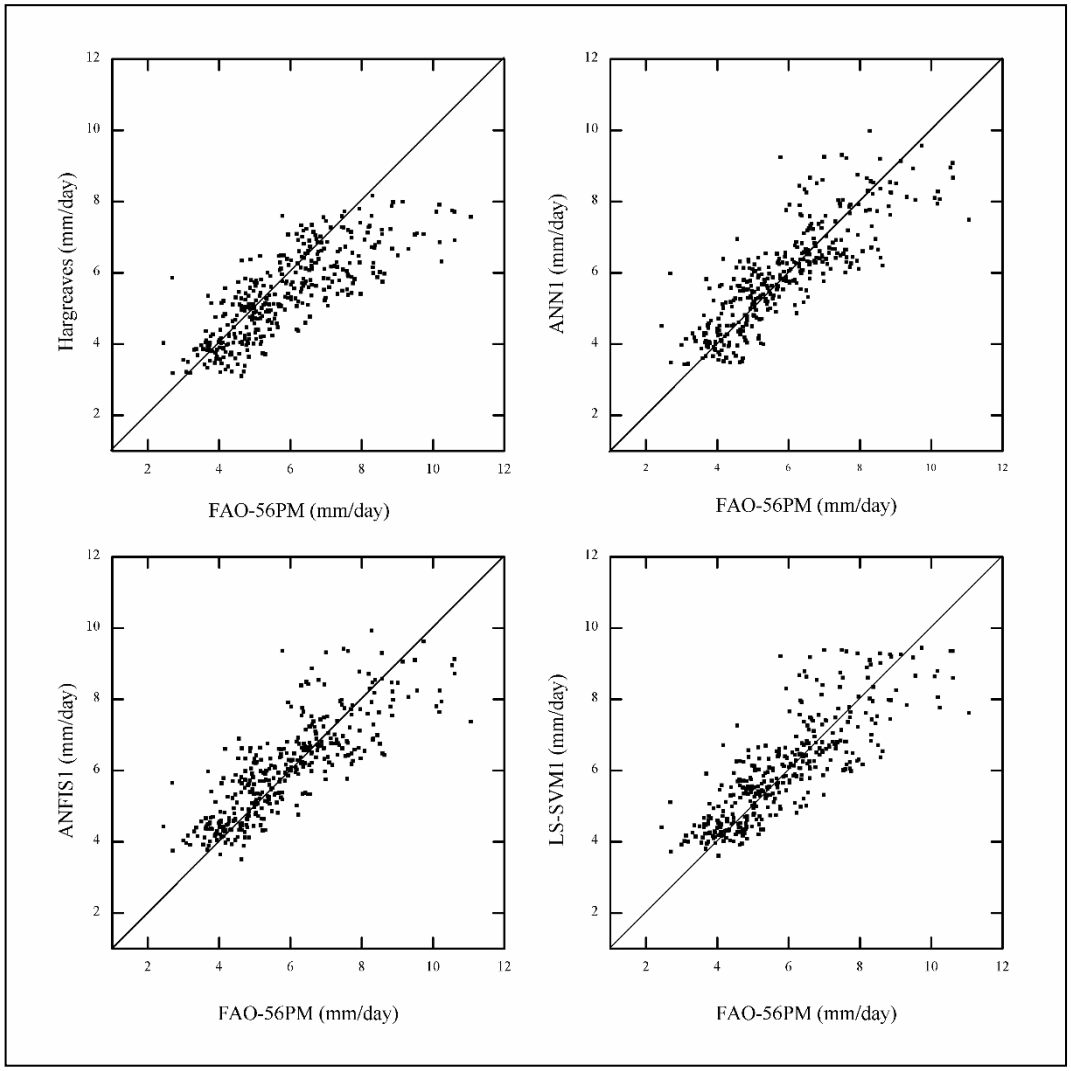

Figure 4.34 Scatter plot for temperature based models at Hyderabad station

4.4 RESULTS FOR KURNOOL STATION (SEMI-ARID REGION)

Kurnool weather station situated in the semi-arid region of India is the fourth case study used to access the applicability of the proposed models. The performance of proposed models are presented in this section and the results are discussed.

4.4.1 ANN results for Kurnool station

Results for ANN models tested at Kurnool station are discussed in this section. The results reveal that the models tested at Kurnool station displayed poor performance when compared to the performance of models in arid region. The results of various ANN models are presented in table 4.21.

Table 4.21 Results of ANN models at Kurnool weather station.

Model	Optimum ANN structure	Training RMSE (mm/d)	Testing				
			RMSE (mm/d)	NSE	TS5	TS10	TS15
ANN1	3-6-1	1.16	1.04	0.58	17	33	51
ANN2	4-9-1	0.89	0.71	0.80	25	51	74
ANN3	5-5-1	0.83	0.79	0.76	26	49	71
ANN4	4-8-1	1.15	1.00	0.61	17	35	54
ANN5	5-7-1	1.18	1.11	0.52	18	34	49

It is clear from the table that ANN1 model displayed poor performance at Kurnool station than the Hyderabad station. This model delivered testing RMSE of 1.04 mm/day and NSE of 0.58. It is observed that ANN2 (with nine nodes in hidden layer) is the best ANN model to estimate ETo at Kurnool station. This model used temperature data along with the antecedent ETo values from the same weather station. The extrinsic data based models (ANN4 and ANN5) performed similar to the temperature based models. This highlights the inability of using extrinsic data for modeling ETo in semi-arid region.

The scatter plot for the ANN models are presented in figure 4.35. The scatter plot suggests underestimation of ETo values by all the models. The performance of ANN2 model is better than all the other models tested. This model performed well at estimating the smaller ETo values.

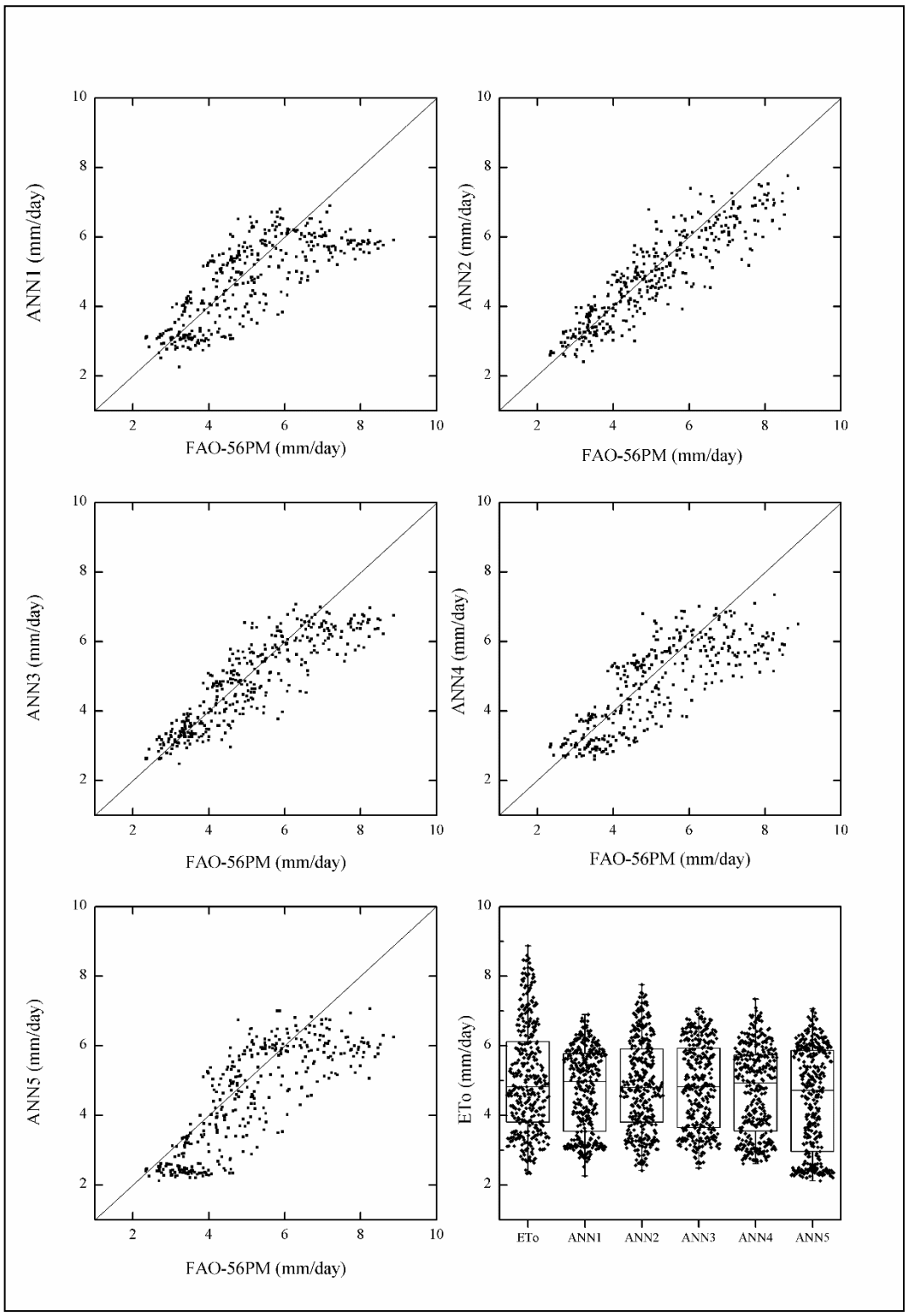

Figure 4.35 Scatter plots and box plot of ANN models for Kurnool weather station.

4.4.2 W-ANN results for Kurnool station

The results for W-ANN models tested for Kurnool weather station are discussed in this section. The results for the W-ANN models are presented in table 4.22. Similar to the results for Hyderabad station, it is observed that the use of wavelet transformed has not led to any significant enhancement in the performance of temperature based and extrinsic data based models.

Table 4.22 Results of W-ANN models at Kurnool weather station.

Model	Mother wavelet	Optimum ANN structure	Training RMSE (mm/d)	Testing				
				RMSE (mm/d)	NSE	TS5	TS10	TS15
W-ANN1	Db5 L3	9-12-1	1.03	1.08	0.55	15	28	48
W-ANN2	Db3 L3	13-15-1	0.49	0.43	0.93	52	83	94
W-ANN3	Db5 L2	13-13-1	0.41	0.33	0.96	62	90	98
W-ANN4	Db5 L1	7-10-1	1.03	0.96	0.64	21	37	59
W-ANN5	Db3 L2	13-18-1	1.05	0.98	0.63	21	39	58

The W-ANN2 and W-ANN3 models have performed better than the ANN2 and ANN3 models. The table reveals that, only the W-ANN2 and W-ANN3 models have shown improvement in performance. The W-ANN3 model with 13 nodes in hidden layer is the best W-ANN model to estimate ETo at Kurnool weather station. It is observed that, out of all the mother wavelets tested, the Db3 and Db5 mother wavelets have performed better. The W-ANN3 model delivered an RMSE of 0.33 mm/day and NSE of 0.96.

Scatter plot and box plot for the W-ANN models are presented in figure 4.36. The scatter plot suggests that the temperature based W-ANN1 and extrinsic data based W-ANN4 and W-ANN5 models have underestimated the ETo values. It is further observed that these models are comparatively good at estimating smaller ETo values. The W-ANN2 and W-ANN3 models have performed better than all the other models tested. Out of all the models tested, W-ANN3 is found to be the best model for estimating ETo at Kurnool weather station. It is observed that this model underestimate as well as overestimate the ETo values, but the data points are well scattered around the 45° line.

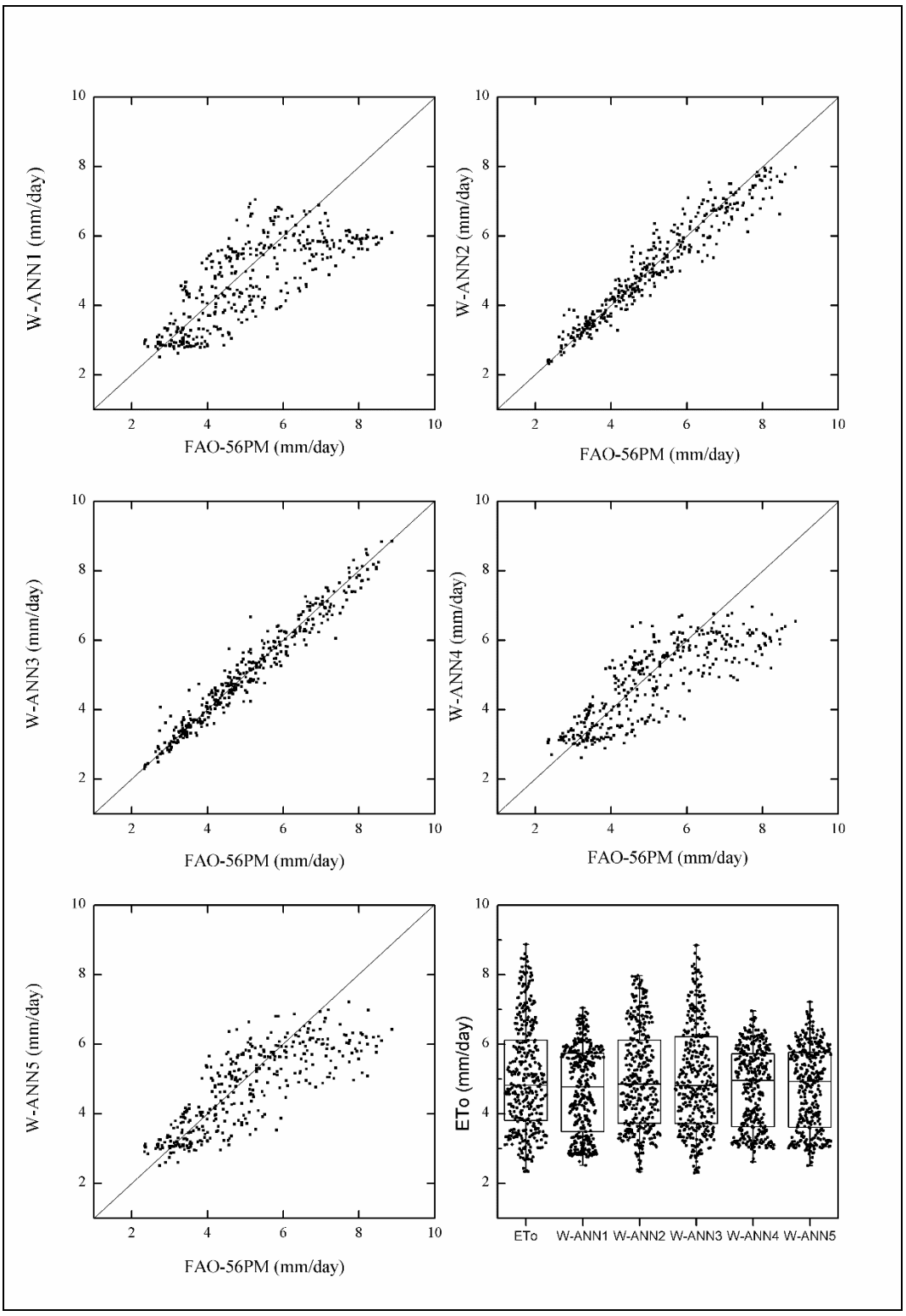

Figure 4.36 Scatter plots and box plot of W-ANN models for Kurnool weather station.

4.4.3 ANFIS results for Kurnool station

Results for ANFIS models tested at Kurnool station are discussed in this section. The result of the ANFIS models are presented in table 4.23.

Table 4.23 Results of ANFIS models at Kurnool weather station.

Model	Membership function	Training RMSE (mm/d)	Testing				
			RMSE (mm/d)	NSE	TS5	TS10	TS15
ANFIS1	Gbell	1.14	1.00	0.61	19	35	53
ANFIS2	Gbell	0.74	0.68	0.82	26	54	74
ANFIS3	Gbell	0.86	0.78	0.76	25	54	73
ANFIS4	Gbell	1.13	0.97	0.63	20	39	55
ANFIS5	Gbell	0.98	0.99	0.62	21	38	54

It is clear from the table that ANFIS models have performed better than the ANN models. The ANFIS2 model (testing RMSE of 0.68 mm/day) is the best ANFIS model to estimate ETo at the Kurnool weather station. The ANFIS4 model performed slightly better than the temperature based ANFIS1 model. Unlike the results in arid regions, the models using extrinsic ETo data inputs have not performed well in semi-arid regions. Gbell membership function has performed better for all the ANFIS models tested at Kurnool station.

The scatter plots and box plots for ANFIS models are presented in figure 4.37. All the models underestimate the ETo values. High amount of underestimation is observed in the larger ETo values. ANFIS1 model has underestimated the higher ETo values. The ANFIS2 model is comparatively better than all the other models tested. This model is good at estimating the smaller ETo values compared to the other models. The box plots for the models shows good performance by the ANN2 model. The box plot for ANFIS3 model shows presence of outliers in the estimated values.

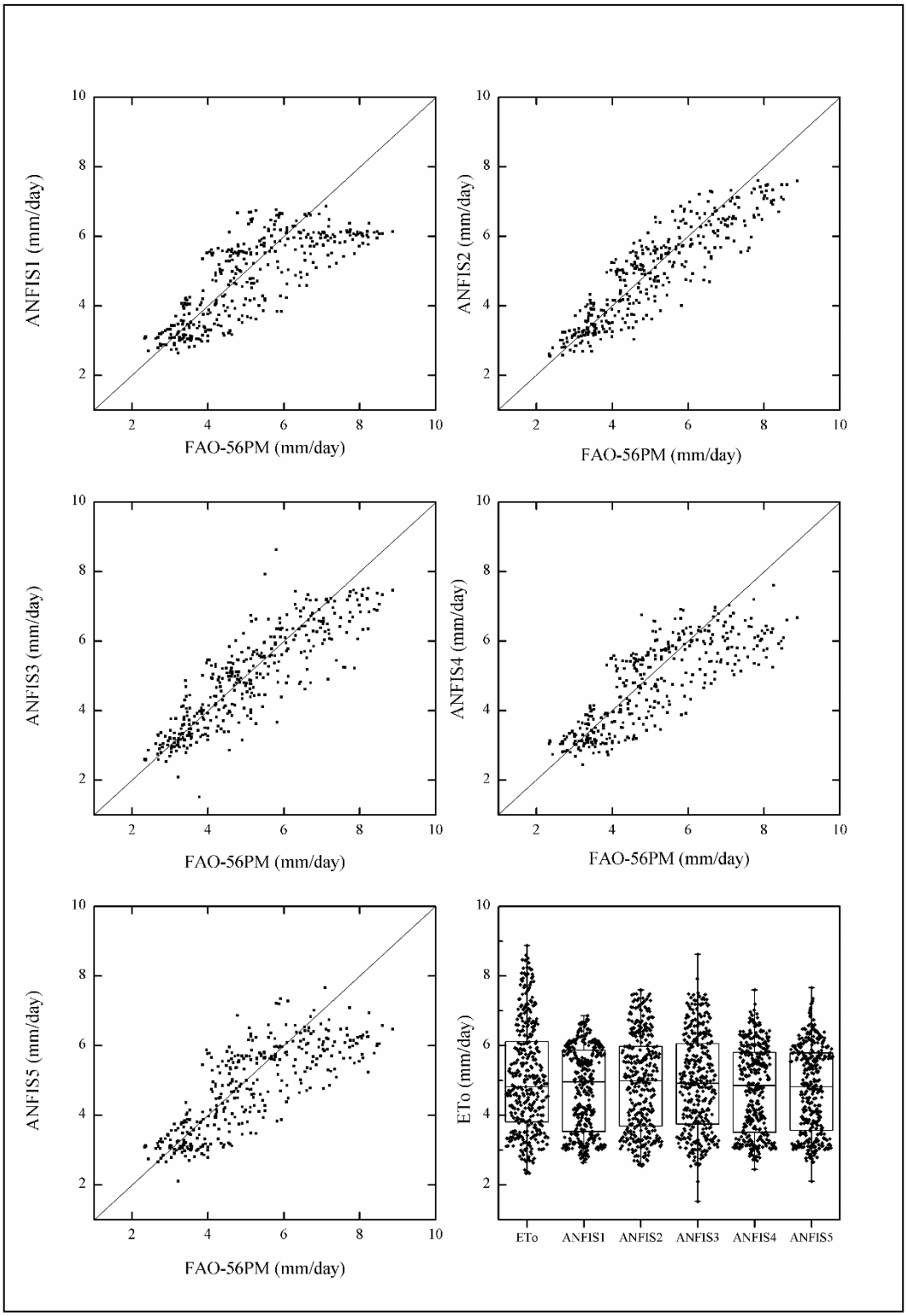

Figure 4.37 Scatter plots and box plot of ANFIS models for Kurnool weather station.

4.4.4 W-ANFIS results for Kurnool station

The results for W-ANFIS models at Kurnool weather station are discussed in this chapter. Table 4.24 presents the results for various W-ANFIS models tested at Kurnool weather station. Similar to the results obtained from W-ANN models it is observed that only intrinsic data based W-ANFIS models have shown enhancement in performance.

Table 4.24 Results of W-ANFIS models at Kurnool weather station.

Model	Mother wavelet	Training RMSE (mm/d)	Testing				
			RMSE (mm/d)	NSE	TS5	TS10	TS15
W-ANFIS1	Db5 L1	1.06	0.98	0.62	16	31	53
W-ANFIS2	Db5 L3	0.51	0.46	0.92	49	78	91
W-ANFIS3	Db3 L3	0.44	0.36	0.95	58	87	96
W-ANFIS4	Db3 L2	1.08	1.00	0.61	20	39	56
W-ANFIS5	Db5 L1	1.15	0.98	0.63	23	40	57

From the table it is observed that there is no significant enhancement in the performance of temperature based W-ANFIS model. Similar to the temperature based models the extrinsic ETo data based W-ANFIS4 and W-ANFIS5 also did not show any enhancement in the performance. The W-ANFIS3 model with training RMSE of 0.36 mm/day is found to be the best W-ANFIS model for estimating ETo at Kurnool station. This model delivered NSE of 0.92 and TS15 value of ninety-six. It can also be observed that the W-ANN3 model has performed slightly better than this model.

Scatter plot and box plot for W-ANFIS models are presented in figure 4.38. Similar to the results obtained from W-ANN models, the A-ANFIS1, W-ANFIS4 and W-ANFIS5 models did not perform well in estimating ETo values of Kurnool weather station. However, the W-ANFIS2 and W-ANFIS3 models displayed a good performance. The W-ANFIS2 model slightly underestimated the larger ETo values. The scatter plot shows that W-ANFIS3 is the best W-ANFIS model to estimate ETo at Kurnool weather station. Box plot for W-ANFIS3 models shows presence of some outliers, as some larger values are overestimated by the model.

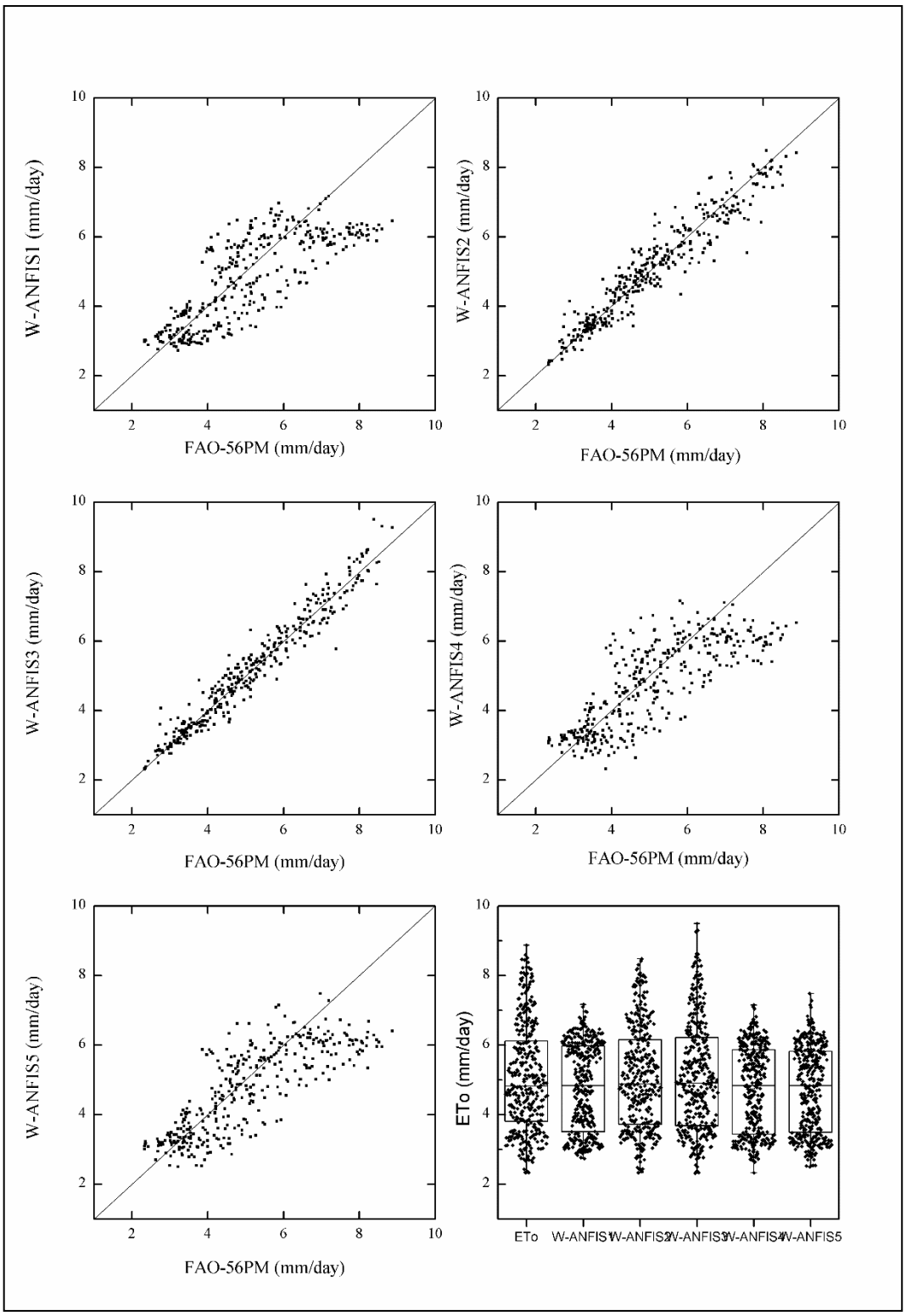

Figure 4.38 Scatter plots and box plot of W-ANFIS models for Kurnool weather station.

4.4.5 LS-SVM results for Kurnool station

The results for LS-SVM models tested for Kurnool weather station are discussed in this section. Table 4.25 presents the results for various LS-SVM models tested for Kurnool weather station.

Table 4.25 Results of LS-SVM models at Kurnool weather station.

Model	Training RMSE (mm/d)	Testing				
		RMSE (mm/d)	NSE	TS5	TS10	TS15
LS-SVM1	1.12	1.08	0.55	15	28	48
LS-SVM2	0.98	0.78	0.76	26	49	69
LS-SVM3	0.86	0.72	0.80	29	54	76
LS-SVM4	1.12	1.07	0.55	17	34	52
LS-SVM5	1.20	1.05	0.57	18	35	54

The results reveal that the LS-SVM3 is the best LS-SVM models for estimating ETo at Kurnool weather station. The LS-SVM3 model delivered an RMSE of 0.72 mm/day and NSE of 0.80. At the Hyderabad station, the LS-SVM model has performed well amongst all the AI models tested. Whereas, for the Kurnool weather station the ANFIS3 model has performed better than all the other AI models tested. Similar to the ANN and ANFIS models the LS-SVM1, LS-SVM4 and LS-SVM5 models have not performed well. It is observed that the performance of extrinsic data based models is similar to the temperature based LS-SVM1 model.

The Scatter plot and box plot for the LS-SVM models are presented in figure 4.39. It is clear from the figure that all the LS-SVM models have underestimated the larger values of ETo. Compared to other models the LS-SVM2 and LS-SVM3 models have performed well at estimating the smaller ETo values. The box also suggests underestimation of larger ETo by the LS-SVM models.

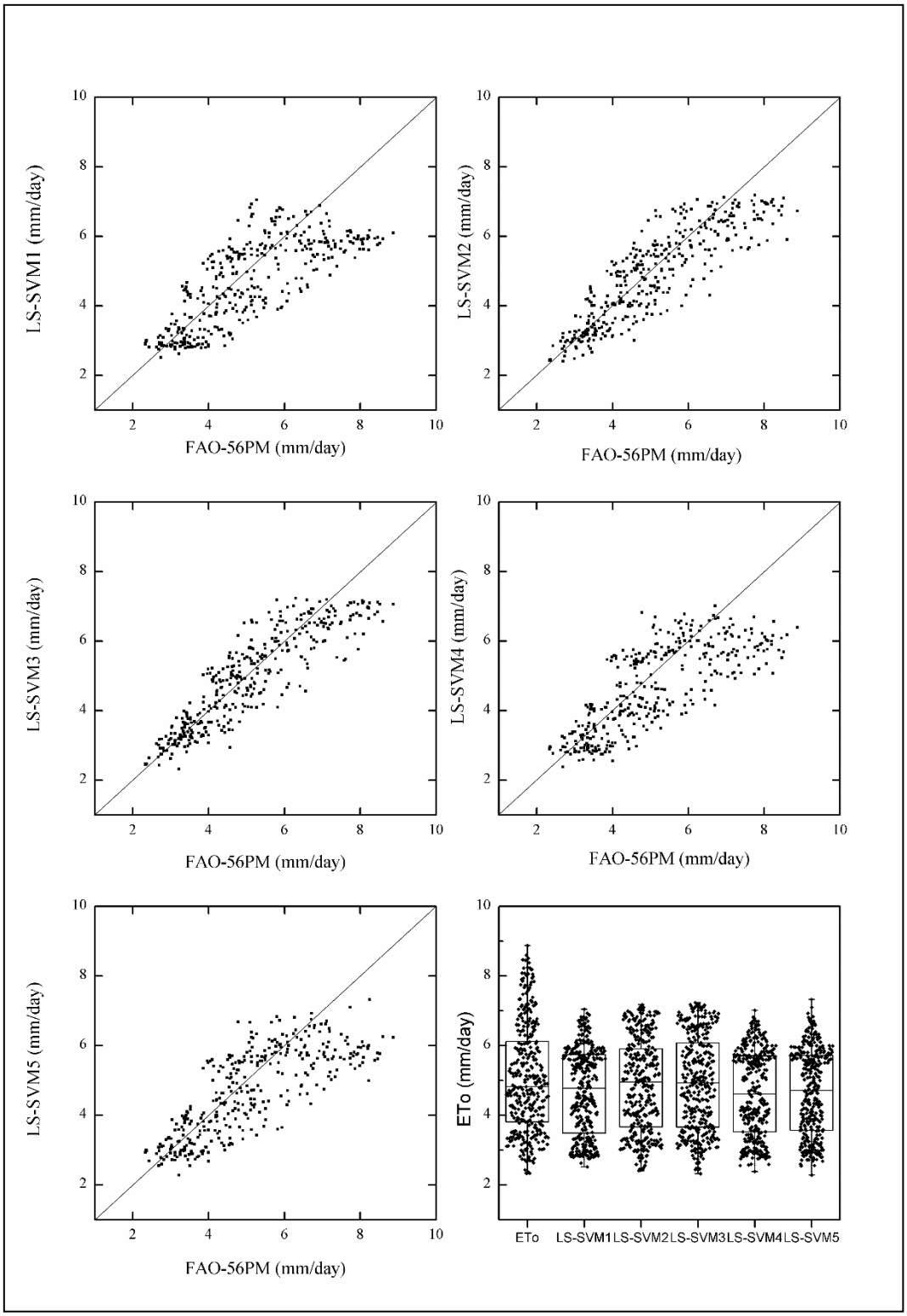

Figure 4.39 Scatter plots and box plot of LS-SVM models for Kurnool weather station.

4.4.6 W-LSSVM results for Kurnool station

W-LSSVM is found to be the best model for estimating ETo at all the stations considered in this study. The results for W-LSSVM models tested for Kurnool weather station are discussed in this section. The results for various W-LSSVM models are presented in table 4.26.

Table 4.26 Results of W-LSSVM models at Kurnool weather station.

Model	Mother wavelet	Training RMSE (mm/d)	Testing				
			RMSE (mm/d)	NSE	TS5	TS10	TS15
W-LSSVM1	Db3 L3	1.01	0.98	0.63	20	39	55
W-LSSVM2	Db5 L2	0.44	0.37	0.95	58	84	92
W-LSSVM3	Db3 L2	0.38	0.31	0.97	71	92	97
W-LSSVM4	Db5 L2	1.02	0.95	0.93	23	42	62
W-LSSVM5	Db5 L2	0.98	0.94	0.64	21	38	57

The table makes it clear that for Kurnool station also, W-LSSVM is the best model for estimating daily ETo. The results reveal that the W-LSSVM3 with an RMSE of 0.31 mm/day and NSE of 0.97 is the best model for estimating ETo at Kurnool station. This model has also performed well in terms of threshold statistics with TS15 value of ninety-seven. Further, it is observed that the extrinsic data based W-LSSVM4 and W-LSSVM5 models have not performed well. However, when compared to the LS-SVM models, a slight enhancement in the performance of these models is observed.

The scatter plot and box plot for the W-LSSVM models tested at Kurnool weather station are presented in figure 4.40. The scatter plot and box plot revel a performance similar to the earlier tested W-ANN and W-ANFIS models. The W-LSSVM1 model underestimated the larger ETo values. Also the extrinsic data based W-LSSVM4 and W-LSSVM5 models display a similar performance. The W-LSSVM2 model slightly underestimated the smaller ETo values. The W-LSSVM3 model is found to be the best model for estimating ETo at Kurnool weather station. The box plot for W-LSSVM3 model is similar to the box plot for FAO-56PM ETo values. From the results it is concluded that the W-LSSVM3 is the best model for estimating daily ETo at Kurnool weather station.

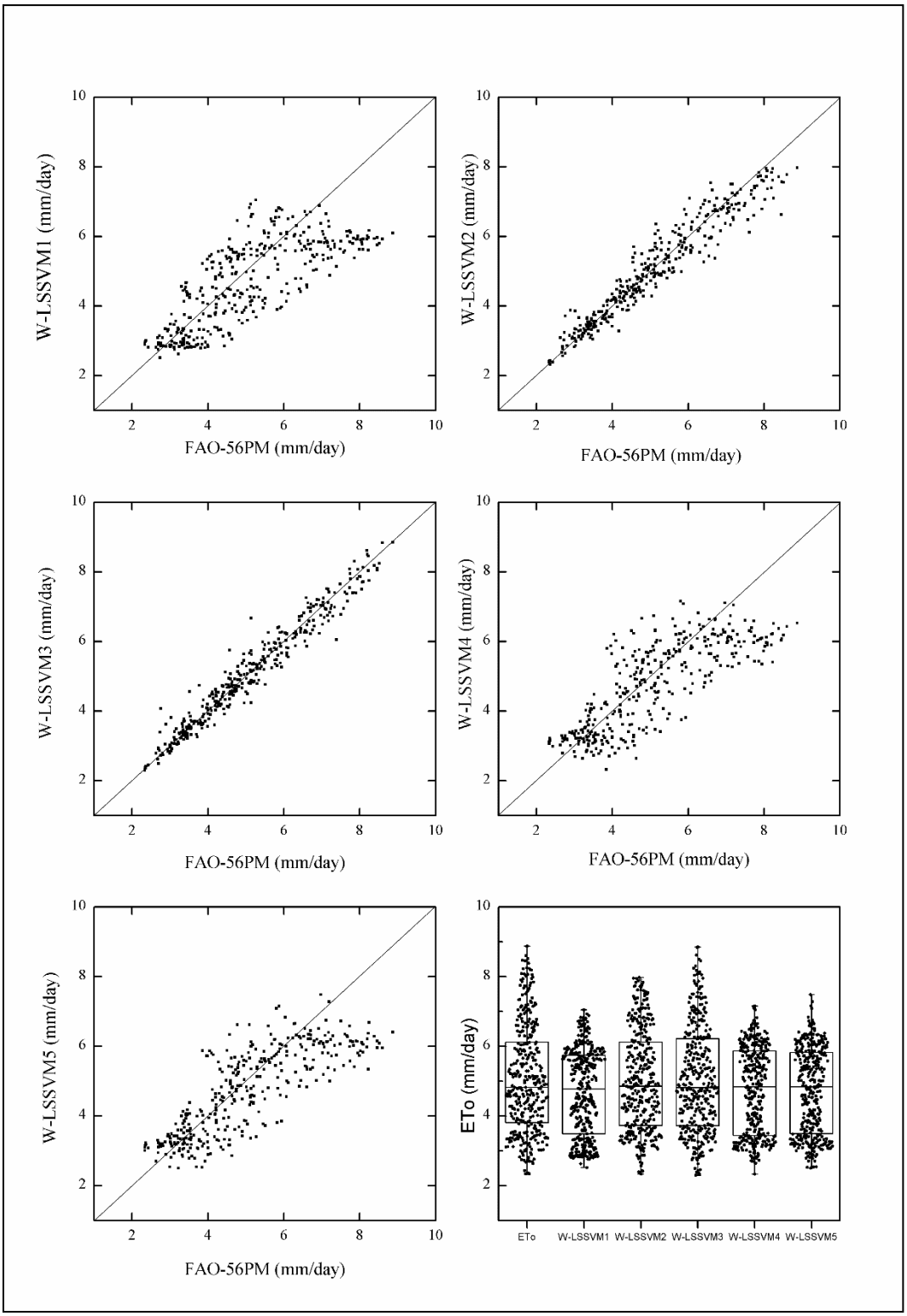

Figure 4.40 Scatter plots and box plot of W-LSSVM models for Kurnool weather station.

4.4.7 Temperature based models for Kurnool station

The performance of different temperature based equations for estimating daily ETo at Kurnool station is compared in this section. The Hargreaves equation yielded an RMSE of 1.37 mm/day for the Kurnool weather station. It is clear that all the AI models performed better than the Hargreaves equation. Scatter plots of all the models are presented in figure 4.41. It is clear from the figure that the Hargreaves equation underestimated the ETo values at the Kurnool station. The AI models performed better at estimating the smaller ETo. However, the larger ETo values are sparsely located around the 45° line suggesting a poor performance by all the temperature based models.

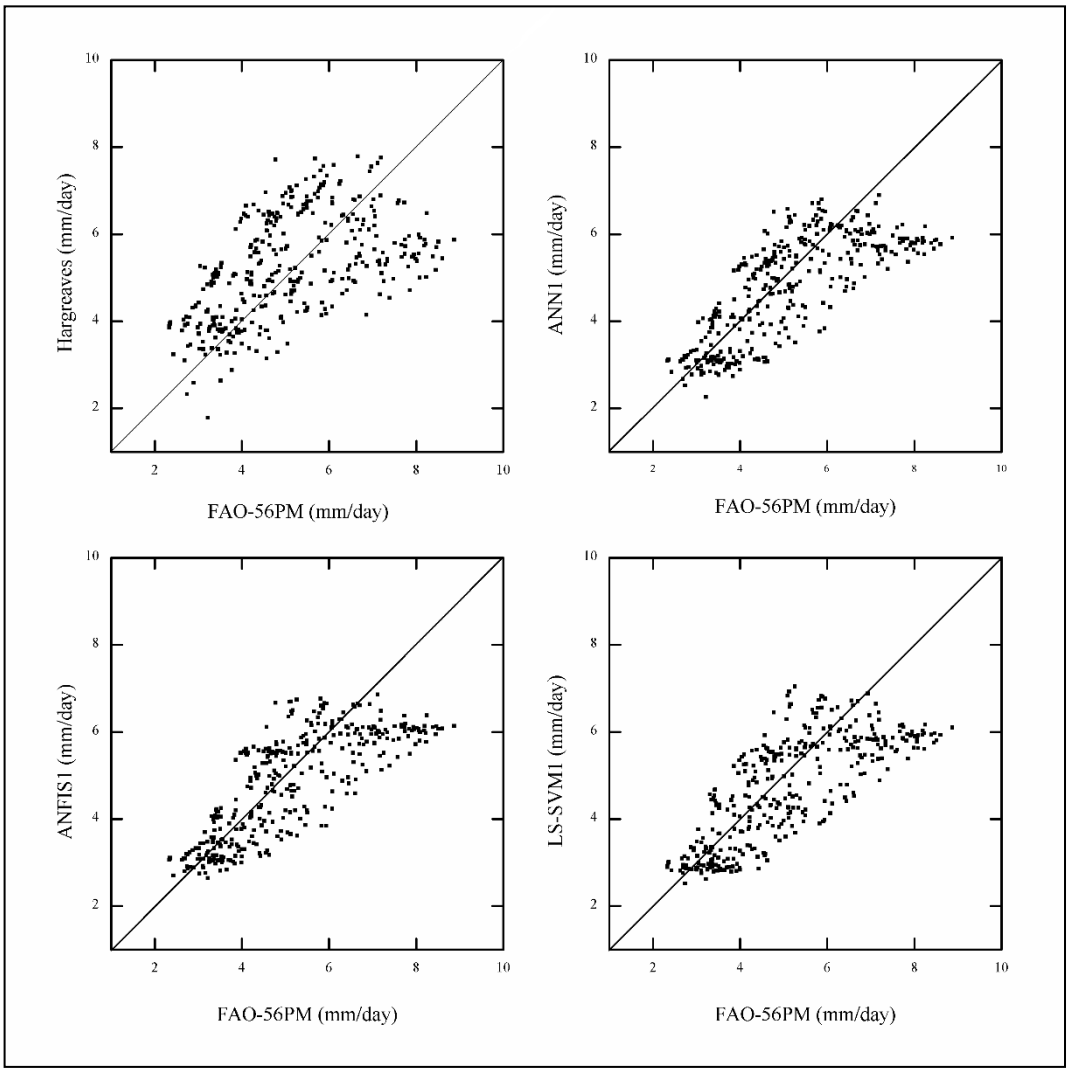

Figure 4.41 Scatter plot for temperature based models at Kurnool station

CHAPTER 5

CONCLUSIONS

5.1 SUMMARY

This study attempts to develop various hybrid models such as Wavelet-ANN, Wavelet-ANFIS and Wavelet-LSSVM models for estimating ETo in arid (Jodhpur and Pali weather station) and semi-arid (Hyderabad and Kurnool) regions of India. Hybrid models were developed by pre-processing the raw datasets of input variables with discrete wavelet transform and presenting the decomposed subseries to ANN, ANFIS and LS-SVM models where FAO-56PM ETo is the output. The proposed models can be used for real field application in data scarce/ limited data scenario for managing irrigation systems. The performance of the proposed models was evaluated using RMSE, NSE and TS statistics. Scatter plots were used to evaluate the accuracies of the models and box plots were used to analyze the spread of the data points estimated by the models.

5.2 CONCLUSIONS

1. Factor analysis can be successfully used for selecting the most influencing input parameters in the process of evapotranspiration. It was found that temperature plays the most important role in the process of evapotranspiration process at arid and semi-arid region and can be used as the sole input under limited data availability scenario.
2. Overall performance of LS-SVM model was better than ANN and ANFIS models in both arid and semi-arid region.
    a. LS-SVM5 model using extrinsic data inputs was found to be the best model for estimating ETo at Jodhpur and Pali weather station.
    b. In semi-arid region (Hyderabad and Kurnool weather station) performance of all the models using intrinsic antecedent ETo values was similar.
3. Use of wavelet decomposed datasets has significantly influenced the performance of AI models.
    a. Compared to classical AI models, an enhancement in the performance of hybrid AI models was observed in the arid region. The W-LSSVM2 model performed

well in Jodhpur station, while the W-LSSVM4 performed better at the Pali weather station.

b. For semi-arid region, use of wavelet decomposed inputs did not show an appreciable enhancement in the performance of hybrid AI models. The W-LSSVM3 model using intrinsic antecedent ETo values as inputs was found to be the best model for estimating ETo at Hyderabad and Kurnool weather station.

4. Selection of proper mother wavelet plays a significant role in performance of hybrid wavelet-AI models. Out of all the Daubechies mother wavelets tested, the performance of Db3 and Db5 mother wavelet was found better.
5. The temperature based AI and hybrid AI models have performed better than the conventional Hargreaves equation. ANN1 and W-ANN1 models have performed better than all the other temperature based models tested in arid and semi-arid regions.
6. Use of extrinsic inputs proved to be useful only in the arid regions. In semi-arid region, the models using intrinsic antecedent ETo values have performed well. In semi-arid regions, use of wavelet decomposed extrinsic data has deteriorate the performance of some hybrid models.

5.3 CONTRIBUTION FROM THE THESIS

1 In this study, an attempt is made to study the performance of hybrid wavelet-AI models for estimating reference evapotranspiration. It is observed that use of wavelet decomposed inputs significantly influenced the performance of classical AI models.

2 On comparing the performance of AI and hybrid AI models in arid and semi-arid regions it is observed that, the performance of models is better at modeling weekly ETo in arid region.

3 Use of extrinsic inputs has proved to be helpful in enhancing the performance of proposed models in certain circumstances (nearby places) only.

5.4 LIMITATION OF THE STUDY

1. This study is confined to two stations in arid region and two stations in semi-arid region which partially represents the generalized ETo characteristics of the region.

2. Performance of only ANN, ANFIS and LS-SVM method with wavelet transform is evaluated in this study.

5.5 FUTURE SCOPE OF THE STUDY

1. Use of datasets from more stations can be further used to confirm the results in more conclusive way.
2. Performance of other AI methods hybridized with wavelet transform can be evaluated in future studies.

REFERENCES

Abudu, S., Bawazir, A. S., and King, J. P. (2010). "Infilling Missing Daily Evapotranspiration Data Using Neural Networks." *Journal of Irrigation and Drainage Engineering*, *136*(5), 317–325.

Abyaneh, H. Z., Nia, A. M., Varkeshi, M. B., Marofi, S., and Kisi, O. (2011). "Performance Evaluation of ANN and ANFIS Models for Estimating Garlic Crop Evapotranspiration." *Journal of Irrigation and Drainage Engineering*, *137*(5), 280–286.

Adamowski, J., Fung Chan, H., Prasher, S. O., Ozga-Zielinski, B., and Sliusarieva, A. (2012). "Comparison of multiple linear and nonlinear regression, autoregressive integrated moving average, artificial neural network, and wavelet artificial neural network methods for urban water demand forecasting in Montreal, Canada." *Water Resources Research*, *48*(1), W01528.

Aksoy, H., Guven, A., Aytek, A., Yuce, M. I., and Unal, N. E. (2007). "Discussion of "Generalized regression neural networks for evapotranspiration modelling." *Hydrological Sciences Journal*, *52*(4), 825–831.

Allen, R., Pereira, L., Raes, D., and Smith, M. (1998). "Crop evapotranspiration-Guidelines for computing crop water requirements-FAO Irrigation and drainage paper 56." *Food and Agriculture Organization of the United Nations, Rome.*

Aytek, A. (2009). "Co-active neurofuzzy inference system for evapotranspiration modeling." *Soft Computing*, *13*(7), 691–700.

Aytek, A., Guven, A., Yuce, M. I., and Aksoy, H. (2008). "An explicit neural network formulation for evapotranspiration." *Hydrological Sciences Journal*, *53*(4), 893–904.

Campisi-Pinto, S., Adamowski, J., and Oron, G. (2012). "Forecasting Urban Water Demand Via Wavelet-Denoising and Neural Network Models. Case Study: City of Syracuse, Italy." *Water Resources Management*, *26*(12), 3539–3558.

Chauhan, S., and Shrivastava, R. K. (2009). "Estimating Reference Evapotranspiration From Limited Climatic Data Using Artificial Neural Networks." *ISH Journal of Hydraulic Engineering*, *15*(1), 34–44.

Cobaner, M. (2011). "Evapotranspiration estimation by two different neuro-fuzzy

inference systems." *Journal of Hydrology, 398*(3-4), 292–302.

Daubechies, I. (1990). "The wavelet transform, time-frequency localization and signal analysis." *IEEE Transactions on Information Theory, 36*(5), 961–1005.

Deka, P. C., and Prahlada, R. (2012). "Discrete wavelet neural network approach in significant wave height forecasting for multistep lead time." *Ocean Engineering, 43*(4), 32–42.

Doorenbos, J., and Pruitt, W. O. (1977). "Crop water requirements. FAO Irrigation and drainage Paper No. 24." *Food and Agriculture Organization of the United Nations, Rome.*, 15–29.

Falamarzi, Y., Palizdan, N., Huang, Y. F., and Lee, T. S. (2014). "Estimating evapotranspiration from temperature and wind speed data using artificial and wavelet neural networks (WNNs)." *Agricultural Water Management, 140*, 26–36.

Feng, Y., Cui, N., Zhao, L., Hu, X., and Gong, D. (2016). "Comparison of ELM, GANN, WNN and empirical models for estimating reference evapotranspiration in humid region of Southwest China." *Journal of Hydrology, 536*, 376–383.

Gocić, M., Motamedi, S., Shamshirband, S., Petković, D., Ch, S., Hashim, R., and Arif, M. (2015). "Soft computing approaches for forecasting reference evapotranspiration." *Computers and Electronics in Agriculture, 113*, 164–173.

Goyal, M. K., Bharti, B., Quilty, J., Adamowski, J., and Pandey, A. (2014). "Modeling of daily pan evaporation in sub tropical climates using ANN, LS-SVR, Fuzzy Logic, and ANFIS." *Expert Systems with Applications, 41*(11), 5267–5276.

Izadifar, Z. (2010). "Modeling and Analysis of Actual Evapotranspiration Using Data Driven and Wavelet Techniques." MSc*Thesis*, University of Saskatchewan, Saskatoon, Canada.

Jang, J.-S. R. J. (1993). ANFIS: "Adaptive-network-based fuzzy inference system." *IEEE Transactions on Systems, Man, and Cybernetics, 23*(3), 665–685.

Jhajharia, D., Kumar, R., Dabral, P. P., Singh, V. P., Choudhary, R. R., and Dinpashoh, Y. (2015). "Reference evapotranspiration under changing climate over the Thar Desert in India." *Meteorological Applications, 22*(3), 425–435.

Karimaldini, F., and Shui, L. (2012). "Daily evapotranspiration modeling from limited

weather data by using neuro-fuzzy computing technique." *Journal of Irrigation and …*, *138*(1), 21–34.

Khan, M. S., and Coulibaly, P. (2006). "Application of Support Vector Machine in Lake Water Level Prediction." *Journal of Hydrologic Engineering*, *11*(3), 199–205.

Kim, S., and Kim, H. S. (2008). "Neural networks and genetic algorithm approach for nonlinear evaporation and evapotranspiration modeling." *Journal of Hydrology*, *351*(3-4), 299–317.

Kisi, O. (2006). "Generalized regression neural networks for evapotranspiration modelling." *Hydrological Sciences Journal*, *51*(6), 1092–1105.

Kisi, O. (2010). "Fuzzy Genetic Approach for Modeling Reference Evapotranspiration." *Journal of Irrigation and…*, 136(3) 175–183.

Kisi, O. (2012). "Least squares support vector machine for modeling daily reference evapotranspiration." *Irrigation Science*, *31*(4), 611–619.

Kisi, O., and Cengiz, T. M. (2013). "Fuzzy Genetic Approach for Estimating Reference Evapotranspiration of Turkey: Mediterranean Region." *Water Resources Management*, *27*(10), 3541–3553.

Kisi, O., and Cimen, M. (2011). "A wavelet-support vector machine conjunction model for monthly streamflow forecasting." *Journal of Hydrology*, *399*(1-2), 132–140.

Kisi, O., and Cimen, M. (2012). "Precipitation forecasting by using wavelet-support vector machine conjunction model." *Engineering Applications of Artificial Intelligence*, *25*(4), 783–792.

Kisi, O., and Cimen, M. (2009). "Evapotranspiration modelling using support vector machine." *Hydrological Sciences Journal*, *54*(5), 918–928.

Kisi, Ö., and Ozturk, O. (2007). "Adaptive Neurofuzzy Computing Technique for Evapotranspiration Estimation." *Journal of Irrigation and Drainage Engineering*, *133*(4), 368–379.

Kisi, O., Sanikhani, H., Zounemat-Kermani, M., and Niazi, F. (2015). "Long-term monthly evapotranspiration modeling by several data-driven methods without climatic data." *Computers and Electronics in Agriculture*, *115*, 66–77.

Kostinakis, K., Xystrakis, F., Theodoropoulos, K., Stathis, D., Eleftheriadou, E., and

Matzarakis, A. (2011). "Estimation of Reference Potential Evapotranspiration with Focus on Vegetation Science—the EmPEst Software." *Journal of Irrigation and Drainage Engineering*, *137*(9), 616–619.

Kumar, M., Bandyopadhyay, A., Raghuwanshi, N. S., and Singh, R. (2008). "Comparative study of conventional and artificial neural network-based ETo estimation models." *Irrigation Science*, *26*(6), 531–545.

Lopez-Urrea, R., Martín de Santa Olalla, F., Fabeiro, C., and Moratalla, a. (2006). "Testing evapotranspiration equations using lysimeter observations in a semiarid climate." *Agricultural Water Management*, *85*(1-2), 15–26.

Mallat, S. G. (1989). "A theory for multiresolution signal decomposition: the wavelet representation." *IEEE Transactions on Pattern Analysis and Machine Intelligence*, *11*(7), 674–693.

Martí, P., Royuela, A., Manzano, J., and Palau-Salvador, G. (2010). "Generalization of ANN Models through Data Supplanting." *Journal of Irrigation and Drainage Engineering*, *136*(3), 161–174.

Martinez, C. J., and Thepadia, M. (2010). "Estimating Reference Evapotranspiration with Minimum Data in Florida." *Journal of Irrigation and Drainage Engineering*, *136*(7), 494–501.

Mellit, A., Pavan, A. M., and Benghanem, M. (2013). "Least squares support vector machine for short-term prediction of meteorological time series." *Theoretical and Applied Climatology*, *111*(1-2), 297–307.

Moosavi, V., Vafakhah, M., Shirmohammadi, B., and Behnia, N. (2013). "A Wavelet-ANFIS Hybrid Model for Groundwater Level Forecasting for Different Prediction Periods." *Water Resources Management*, *27*(5), 1301–1321.

Nandagiri, L., and Kovoor, G. M. (2006). "Performance Evaluation of Reference Evapotranspiration Equations across a Range of Indian Climates." *Journal of Irrigation and Drainage Engineering*, *132*(3), 238–249.

Nayak, P. C., Venkatesh, B., Krishna, B., and Jain, S. K. (2013). "Rainfall-runoff modeling using conceptual, data driven, and wavelet based computing approach." *Journal of Hydrology*, *493*, 57–67.

Oki, T., and Kanae, S. (2006). "Global Hydrological Cycles and World Water Resources." *Science*, *313*(5790), 1068–1072.

Ozkan, C., Kisi, O., and Akay, B. (2011). "Neural networks with artificial bee colony algorithm for modeling daily reference evapotranspiration." *Irrigation Science*, *29*(6), 431–441.

Partal, T., and Cigizoglu, H. K. (2008). "Estimation and forecasting of daily suspended sediment data using wavelet–neural networks." *Journal of Hydrology*, *358*(3-4), 317–331.

Petković, D., Gocic, M., Trajkovic, S., Shamshirband, S., Motamedi, S., Hashim, R., and Bonakdari, H. (2015). "Determination of the most influential weather parameters on reference evapotranspiration by adaptive neuro-fuzzy methodology." *Computers and Electronics in Agriculture*, *114*, 277–284.

Priestley, C. H. B., and Taylor, R. J. (1972). "On the assessment of surface heat flux and evaporation using largescale parameters." *Monthly Weather Review*, *100*(2), 81–92.

Raghavendra, S., and Deka, P. C. (2014). "Support vector machine applications in the field of hydrology: A review." *Applied Soft Computing Journal*, *19*, 372–386.

Rahimi Khoob, A. (2007). "Comparative study of Hargreaves's and artificial neural network's methodologies in estimating reference evapotranspiration in a semiarid environment." *Irrigation Science*, *26*(3), 253–259.

Rahimikhoob, A. (2010). "Estimation of evapotranspiration based on only air temperature data using artificial neural networks for a subtropical climate in Iran." *Theoretical and Applied Climatology*, *101*(1-2), 83–91.

Rojas, J. P., and Sheffield, R. E. (2013). "Evaluation of Daily Reference Evapotranspiration Methods as Compared with the ASCE-EWRI Penman-Monteith Equation Using Limited Weather Data in Northeast Louisiana." *Journal of Irrigation and Drainage Engineering*, *139*(4), 285–292.

Shamshirband, S., Amirmojahedi, M., Gocić, M., Akib, S., Petković, D., Piri, J., and Trajkovic, S. (2016). "Estimation of Reference Evapotranspiration Using Neural Networks and Cuckoo Search Algorithm." *Journal of Irrigation and Drainage Engineering*, *142*(2), 04015044.

Shiri, J., Nazemi, A. H., Sadraddini, A. A., Landeras, G., Kisi, O., Fakheri Fard, A., and Marti, P. (2014a). "Comparison of heuristic and empirical approaches for estimating reference evapotranspiration from limited inputs in Iran." *Computers*

and Electronics in Agriculture, *108*, 230–241.

Shiri, J., Nazemi, A. H., Sadraddini, A. A., Landeras, G., Kisi, O., Fard, A. F., and Marti, P. (2013). "Global cross-station assessment of neuro-fuzzy models for estimating daily reference evapotranspiration." *Journal of Hydrology*, *480*, 46–57.

Shiri, J., Sadraddini, A. A., Nazemi, A. H., Marti, P., Fakheri Fard, A., Kisi, O. and Landeras, G. (2015). "Independent testing for assessing the calibration of the Hargreaves–Samani equation: New heuristic alternatives for Iran." *Computers and Electronics in Agriculture*, *117*, 70–80.

Shiri, J., Kim, S., and Kisi, O. (2014b). "Estimation of daily dew point temperature using genetic programming and neural networks approaches." *Hydrology Research, 45(2),165-181*

Shirmohammadi, B., Moradi, H., Moosavi, V., Semiromi, M. T., and Zeinali, A. (2013). "Forecasting of meteorological drought using Wavelet-ANFIS hybrid model for different time steps (case study: Southeastern part of east Azerbaijan province, Iran)." *Natural Hazards*, *69*(1), 389–402.

Snyder, R. L. (1992). "Equation for Evaporation Pan to Evapotranspiration Conversions." *Journal of Irrigation and Drainage Engineering*, *118*(6), 977–980.

Stefánsson, A., Končar, N., and Jones, A. (1997). "A note on the gamma test." *Neural Computing and Applications*, *5*(3), 131–133.

Sudheer, K. P., Gosain, A. K., and Ramasastri, K. S. (2003). "Estimating Actual Evapotranspiration from Limited Climatic Data Using Neural Computing Technique." *Journal of Irrigation and Drainage Engineering*, *129*(3), 214–218.

Sungwon, K., and Hung, S. K. (2011). "Nonlinear evapotranspiration modelling using MLP-NNM and SVM-NNM approach." Evapotranspiration, Labedzki, L., ed InTech.

Suryanarayana, C., Sudheer, C., Mahammood, V., and Panigrahi, B. K. (2014). "An integrated wavelet-support vector machine for groundwater level prediction in Visakhapatnam, India." *Neurocomputing*, *145*, 324–335.

Suykens, J., and Vandewalle, J. (1999). "Least squares support vector machine classifiers." *Neural Processing Letters*, *9*(3), 293–300.

Tabari, H., and Hosseinzadeh Talaee, P. (2012). "Multilayer perceptron for reference evapotranspiration estimation in a semiarid region." *Neural Computing and Applications*, *23*(2), 341–348.

Tabari, H., Kisi, O., Ezani, A., and Hosseinzadeh Talaee, P. (2012). "SVM, ANFIS, regression and climate based models for reference evapotranspiration modeling using limited climatic data in a semi-arid highland environment." *Journal of Hydrology*, *444-445*, 78–89.

Tabari, H., Martinez, C., Ezani, A., and Hosseinzadeh Talaee, P. (2013). "Applicability of support vector machines and adaptive neurofuzzy inference system for modeling potato crop evapotranspiration." *Irrigation Science*, *31*(4), 575–588.

Thornthwaite, C. W. (1948). "An approach toward a rational classification of climate." *Geographical Review*, *38*, 55–94.

Turc, L. (1961). "Estimation of irrigation water requirements, potential evapotranspiration: A simple climatic formula evolved up to date." *Annals of Agronomy*, *12*, 13–14.

Vapnik, V. (1995). "The Nature of Statistical Learning Theory." *Springer Verlag*, New York, USA.

Wang, W. G., and Luo, Y. F. (2008). "Wavelet network model for Reference Crop Evapotranspiration forecasting." *Proc., Int. Con. on Wavelet Analysis and Pattern Recognition*, 2 751–755.

Wang, Z., Wu, P., Zhao, X., Cao, X., and Gao, Y. (2013). "GANN models for reference evapotranspiration estimation developed with weather data from different climatic regions." *Theoretical and Applied Climatology*, *116*(3-4), 481–489.

Wei, S., Yang, H., Song, J., Abbaspour, K., and Xu, Z. (2013). "A wavelet-neural network hybrid modelling approach for estimating and predicting river monthly flows." *Hydrological Sciences Journal*, *58*(2), 374–389.

Wen, X., Si, J., He, Z., Wu, J., Shao, H., and Yu, H. (2015). "Support-Vector-Machine-Based Models for Modeling Daily Reference Evapotranspiration With Limited Climatic Data in Extreme Arid Regions." *Water Resources Management*, *29*(9), 3195–3209.

Xystrakis, F., and Matzarakis, A. (2011). "Evaluation of 13 Empirical Reference Potential Evapotranspiration Equations on the Island of Crete in Southern Greece." *Journal of Irrigation and Drainage Engineering*, *137*(4), 211–222.

Zanetti, S. S., Sousa, E. F., Oliveira, V. P., Almeida, F. T., and Bernardo, S. (2007). "Estimating Evapotranspiration Using Artificial Neural Network and Minimum Climatological Data." *Journal of Irrigation and Drainage Engineering*, *133*(2), 83–89.

Zhang, Y., Liu, C., Tang, Y., and Yang, Y. (2007). "Trends in pan evaporation and reference and actual evapotranspiration across the Tibetan Plateau." *Journal of Geophysical Research*, *112*(D12), D12110.

LIST OF PUBLICATIONS

International Journal

- Amit Prakash Patil and Paresh Chandra Deka, (2015) "Performance evaluation of hybrid Wavelet-ANN and Wavelet-ANFIS models for estimating evapotranspiration in arid regions of India." **Neural Computing and Applications (Springer).** DOI: 10.1007/s00521-015-2055-0
- Amit Prakash Patil and Paresh Chandra Deka, (2016) "An extreme learning machine approach for modeling evapotranspiration using extrinsic inputs." **Computers and Electronics in Agriculture (Elsevier).** Vol. 121 pp. 385-392 DOI: 10.1016/j.compag.2016.01.016

International Conference

- Amit Prakash Patil and Paresh Chandra Deka, "Performance evaluation of various artificial intelligence models for estimating evapotranspiration under limited data scenario." International conference on emerging trends in engineering, held at NITTE 2014.
- Amit Prakash Patil and Paresh Chandra Deka, "Performance evaluation of extreme learning machine for modeling evapotranspiration in arid regions." International conference on hydraulics, water resources and river engineering (HYDRO-2015), held at IIT Roorkee 2015

BIO-DATA

Name:	Mr. Patil Amit Prakash
D.O.B:	10-06-1987
Address:	'Nandadeep' Ashtavinayak Colony Vidyanagar Karad, Dist: Satara Maharashtra India. 415124 Telephone: +91 9420697681
Email:	*amitpatil.nitk@gmail.com*
Qualification:	M. Tech
Area of Specialization:	Soft computing Applications in hydrology